# A MODEL
# FOR THE FLOW OF BLOOD
# IN CAPILLARIES

# A MODEL
# FOR THE FLOW OF BLOOD
# IN CAPILLARIES

By

ARMEANE MURZBAN CHOKSI, B.Sc. (HONS.)

A MAJOR STUDY REPORT

Submitted to the Faculty of Graduate Studies

in Partial Fulfilment of the Requirements

for the Degree

Master of Engineering

McMaster University

(October) 1969

MASTER OF ENGINEERING (1969)
(Chemical Engineering)

McMASTER UNIVERSITY
Hamilton, Ontario.

TITLE: A Model For the Flow of Blood in Capillaries

AUTHOR: Armeane Murzban Choksi, B.Sc. (HONS.)
(University of Edinburgh)

SUPERVISOR: Dr. J. Vlachopoulos

NUMBER OF PAGES: vii, 126

## ACKNOWLEDGEMENTS

The author wishes to express his gratitude to Dr. J. Vlachopoulos for his constant guidance and advice throughout this project.

He also wishes to thank Messrs. J. Yamanis and S. Katotakis for their assistance in this investigation.

Gratitude is also due to the Department of Chemical Engineering, McMaster University, for its financial support to the author.

## ABSTRACT

A new constitutive equation has been developed for the flow of blood through capillaries. Pressure drop and volume flow data of Haynes and Burton and Merrill et al. have been utilized in this development for a range of radii from 57.04 micra to 747.4 micra, and a hematocrit range of 8.8% to 82.5%. A comparison has been made with the Casson equation used by Merrill and Pelletier and the advantage of this new equation over the Casson equation has been verified. The usual assumption of no-slip-at-the-wall has been verified to be valid up to a hematocrit level of 39.3%.

TABLE OF CONTENTS

# 1. INTRODUCTION

## 1.1 The Flow of Blood Through Capillaries

The circulatory system of the human body, in simplified mechanical terms, may be considered to be two reciprocating pumps in series, i.e., the heart, connected to a network of branching elastic conduits, viz. blood vessels. The fluid circulating through this system, blood, is a complex suspension of formed elements, ions and proteins in salt water. This network of blood vessels divides from relatively few large ones into many small ones, with the internal diameter of the individual vessel changing from approximately 2.5 cms. to 10 micra. The smallest of these vessels is known as the capillary. Any given cell of the body tissue is no further than 25 to 50 micra from a given capillary (1).

The mechanical function of the heart, the distributing arteries and the collecting veins is to conduct blood to and from the capillaries, for it is in the capillaries that the molecular exchange between blood and the surrounding cells takes place. It is in the capillaries also that the red cells receive maximum exposure to the surrounding tissue in order to facilitate oxygen diffusion. Here in the capillaries blood serves its life-giving function.

Blood flow through a capillary is intermittent. Sometimes the flow is too rapid for the individual discrimination

of the red cell. At slower flows, or in slow motion photographic studies of flow (2), the cells have been observed to twist, turn and deform readily. Red cells are frequently seen stacked together though not stuck together, in long columns, like a row of coins. Occasionally, long lengths of capillaries, completely free of red cells, may be observed.

In spite of such complex two-phase phenomena which occur in the capillaries, from the fluid-mechanical aspect of the situation, all capillaries have one important factor in common - this is the low Reynolds number flow due to their small diameter. Also, the fluid in the capillaries is bounded externally by the capillary wall and internally by the moving highly elastic disc-like red cells. Hence, blood flow in capillaries is basically the flow of a fluid carrying disc-like bodies, whose diameters are large compared to the tube radius, at low Reynolds number.

## 1.2 The Nature of Capillary Vessels and Blood in Man

### 1.2.1 Capillaries

The capillary vessels in man are cylindrical tubes formed by a network of interlocking cells called endothelium. True capillaries contain no muscular elements and show no tendency to contract or dilate spontaneously (1). The small vessels which supply the capillaries are called the arterioles and have nearly the same internal diameter. The arterioles

contain smooth muscle elements and are capable of changing caliber. At the arteriolar-capillary junctions there exist valves called precapillary sphincters, which can control the capillary flow by opening and closing. This sphincter action is believed to be controlled by the metabolic demands of the surrounding tissue (1, 3).

1.2.2 Blood

Whole blood is a suspension of formed elements in a colloidal solution of proteins in saline. The formed elements known as red cells (erythrocytes), white cells (leukocytes, granulocytes), and platelets (thrombocytes), constitute some 40% to 48% by volume of whole blood. This concentration is known as the hematocrit level of blood. The red cell in man is a very flexible biconcave disc, approximately 8.5 micra in diameter. The thickness of the red cell at its centre is approximately 1 micron and its thickness at its rim about 2.4 micra (4). The red cells outnumber the white cells and platelets by approximately 5000:1 and 12:1 respectively. Compared to the red and white cells, the platelets, with a maximum diameter of 0.5 micra are insignificant in size. Red cell populations in humans are very uniform in diameter and all mammalian red cells are approximately of the same diameter (5). The density of the red cell is about 5 to 6% greater than that of the surrounding fluid.

The fluid constituent of whole blood is called plasma.

It is a saline solution of large protein molecules, the most prominent of which are albumin, globulin, and fibrinogen. These molecules have maximum dimensions in the range of 0.01 to 0.05 micra. Although its mechanical properties are still under investigation, plasma is widely accepted as a Newtonian fluid (6). Whole blood, though, is a non-Newtonian fluid with a finite, but very small yield stress (7, 8).

## 2. GENERAL LITERATURE SURVEY

### 2.1 Hemorheology and Hemodynamics

The name hemorheology was originally suggested by Professor Copley in 1952 to cover not only the deformation and flow of blood and its components but also "the rheological properties of vessel structure with which blood comes into direct contact." In 1960, however, Professor Copley and Dr. Scott Blair suggested a further division into hemorheology (concerned with the reactions of blood to shearing and other stresses) and hemodynamics, dealing with the flow of blood "in relation to shapes of vessels, velocities, pressure effects etc." Hemorheology is now used to describe the inherent stress/strain characteristics of blood, which would be independent of the apparatus in which they are measured and of the subsequent procedure by which the characteristics are derived. The term hemodynamics is used to describe the behaviour of blood which is moving in a circumscribed space or adjacent to a wall interface or other discontinuity. It involves a knowledge not only of the rheological properties of blood, but also of the physical, chemical and probably biological characteristics of the restraining surface or discontinuity and of the flow pattern of the blood.

## 2.2 The Viscosity of Blood

Measurements on a cone-and-plate viscometer have shown that fresh human plasma is slightly non-Newtonian (9, 11), the apparent viscosity falling with increasing rate of shear to an asymptotic constant value. This is due to the presence of the large protein molecules of albumin, globulin, and fibrinogen. The additions of reagents which inhibit coagulation of the fibrinogen influence the rheological behaviour, so that herapin reduces slightly the general level of viscosity of the plasma (10 - 13), and reduces its non-Newtonian behaviour. Evidence of adding oxalate or citrate to plasmas is conflicting: in some cases it reduces the general level of viscosity still further and makes it Newtonian (10, 14, 15); in others, it raises the level above that given by herapin and increases non-Newtonian behaviour (12, 13).

The viscosity of fresh plasma, at high rates of shear where non-Newtonian behaviour can be neglected, is about 0.012 - 0.016 P and its density is about 1.035 g/ml. The shear rate above which it behaves as a Newtonian fluid is 100 - 120 $sec^{-1}$ (10). There is no evidence to indicate whether the rheological or physical properties vary appreciably from mammal to mammal and at the moment it must be assumed that such variations are small.

If the fresh plasma is allowed to clot, the fibrinogen is converted to fibrin and the fluid remaining after the clot

has formed, is termed the serum; it is also non-Newtonian to approximately the same degree as the plasma (16). For the serum a shear rate of some 250 $sec^{-1}$ must be exceeded at a capillary-tube wall in order to obtain Newtonian behaviour.

Whole blood is considerably more non-Newtonian than plasma or serum and this property has been well recognized for many years (17, 18), i.e., its viscosity depends on the flow rate (or rate of shear) and tube size as well as the hematocrit. Thus, the rheological behaviour of blood resembles that of certain colloidal suspensions rather than ordinary liquids such as water or glycerine (19). However, it would appear that under normal conditions, in most branches of the circulatory system, these non-Newtonian properties are not of great importance, and blood can often be considered to be Newtonian. For example, in the large arteries, Taylor in 1959, found that the oscillatory flow is largely unaffected by the shear dependent viscosity of blood; an error of 2% is introduced in the calculations of the flow from the pressure gradient by assuming a constant coefficient of viscosity (19). An important exception to this generalization is in the capillaries where "plug flow" occurs, since the cell and vessel diameters are nearly equal.

Most measurements have been made in capillary tube instruments, where the diameter of the tube may have some influence on the results obtained, but work using cone-and-plate (9, 13) and rotating cylinder (20) viscometers where the

measured viscosity should be substantially independent of concentration changes occurring during shear, have given generally confirmatory results. (A very small yield stress of about 0.15 dyn/cm.$^2$ is exhibited by blood so that the behaviour can be classified as Bingham.) When the rate of shear exceeds approximately 50 sec$^{-1}$ the influence of the yield stress on the total stress is so small that Newtonian behaviour can be assumed.

There is some indication that in a capillary-tube instrument the shear rate required to give Newtonian behaviour may increase with decreasing tube diameter (17). Assuming parabolic velocity distribution in the tube, the rate of shear at the wall at which Newtonian behaviour is attained is shown in the table below for various investigators. This condition is achieved asymptotically, and could be slightly affected by a velocity-dependent radial distribution of cells if this occurs in the viscometer tube, but the figures given below are correct in their order of magnitude if not in absolute values.

In a capillary-tube instrument the rate of shear varies from a maximum at the wall to zero along the axis. Thus, the shear rate at the wall is considerably greated than the minimum at which plasma, serum, or blood becomes Newtonian, if the bulk of the fluid is to behave as a Newtonian fluid. In a cone-and-plate or rotating cylinder viscometer, the rate of shear is reasonably constant throughout the sample,

| INVESTIGATOR | INSTRUMENT | MAMMAL | SUSPENDING FLUID | ANTI-COAGULANT | RATE AT WHICH NON-NEWTONIAN BEHAVIOUR DISAPPEARS |
|---|---|---|---|---|---|
| | | | | | $Sec^{-1}$ |
| Merrill & Wells (10) | Cone-and-Plate | Human | Plasma | None | 100 |
| Cokelet et al (20) | Rot. Cyl. | Human | Plasma | Citrate | 50 |
| Brundage (14) | Rot. Cyl. | Cat Rabbit | Plasma | Oxalate | 50 |
| Bayliss (22) | Cap. Tube | Dog | Serum | - | 450* |
| Müller (21) | Cap. Tube | Bovine | Serum | - | 300* |
| Coulter and Pappenheimer (22) | Cap. Tube | Bovine | | | 280* |

* At the tube wall

and the minimum shear rate necessary to produce Newtonian behaviour is less than the rate of shear at the wall of a capillary instrument corresponding to the same mean shearing condition in the sample.

Some experimenters, such as L.C. Cerney et al. (11), R.H. Haynes et al. (23), have resuspended red cells in citrate/dextrin (A.C.D. solution which is Newtonian (23). Non-Newtonian behaviour was observed until a certain rate of shear was exceeded at the capillary-tube viscometer wall. On sampling red cells in saliva containing 3.5% of albumin, complete dispersion of the cell was achieved and the yield stress disappeared reducing (but not eliminating) the non-Newtonian behaviour (20).

It has been suggested (30) that the measured fall in apparent viscosity with increasing rate of shear is associated with the breaking up of chains of erythrocytes, rouleaux or clumps which can be present at low rates of flow (31). Similar characteristics have been observed for suspensions of particles which have a tendency to adhere or flocculate (32). At low rates of shear floccules impede the flow and increase the effective concentration of particles by retaining fluid in their interstices. This increases the viscosity of the suspension so that, as the rate of flow is increased and the floccules are destroyed, the viscosity decreases, its limiting value being reached when all the particles are dispersed. It is well known that erythrocytes cohere when left undisturbed

in serum or plasma (31), and it has been suggested that the presence of these clumps or rouleaux cause the observed high viscosity at low rates of shear. As the flow rate is increased the clumps progressively break up to that the viscosity falls to an asymptotic value. It has been shown that if red cells are suspended in a fluid which is chosen to ensure their complete dispersion, the yield stress disappears and there is a smaller fall in apparent viscosity with increasing rate of shear.

Evidence for this theory can be found in the results of Coultier and Pappenheimer (22a) who measured the electrical resistance of blood at different rates of shear. They found that both the measured viscosity and the electrical resistance attained steady values which were almost identical, corresponding to a rate of shear at the wall of approximately 280 $sec^{-1}$. When the flow reached turbulence, the hydrodynamic resistance increased, but the electrical resistance remained constant. The authors attributed the initial fall in electrical resistance to an orientation of red cells, parallel to the tube axis, as the rate of flow was increased. To explain why it did not rise again when turbulence was reached they found it necessary to propose that the cells did not take part in the turbulent motion and maintained their orientation parallel to the tube axis.

It is suggested that the high electrical resistance measured at low rates of shear was due to the longer path for the electrical current through the structured blood. After

the clumps had been destroyed by the increasing rate of shear, the electrical resistance of the dispersed cells would not be affected by random movements of the individual cells irrespective of whether they were exposed to streamline or turbulent flow conditions.

A theory of blood viscosity for which some doubt has been expressed is the Farhaeus-Lindqvist effect. Farhaeus and Lindqvist (24) were the first to study the effect of the radius of the tube used in the measurements of the apparent viscosity of blood. They found that the apparent viscosity at high flow rates is reduced in tubes of radius less than 0.2 mm. However, the theories that have been proposed to account for this effect are phenomenological in character, and, are based on qualitative models designed to approximate the effect of the particles in suspension. There appear to be only two such theories that can be used in the analysis of the Farhaeus-Lindqvist effect; one is based on the existence, in steady flow, of a marginal zone at the tube wall which is presumed to have a lower viscosity than the rest of the fluid. Taylor (25) has made direct optical studies of a marginal zone that is, on the average, particle-free, and whose existence could be explained on the basis of the axial accumulation of the red cells (26, 27). The other theory is based on the existence of unsheared laminae in the fluid which arise from the presence of particles of finite size - there seems to be little doubt now that the red cells do possess sufficient rigidity to

resist the local shearing stress and thereby give rise to finite unsheared laminae in steady flow.

On the work performed by Haynes (27) applied to his own data and to those of Kümin, in light of the latter theory, he found that the thickness of the unsheared laminae varied between 3.5 micra at 10% hematocrit and 34 micra at 80%. In view of the former theory, the effect could have been caused by a cell-free marginal zone adjacent to the tube wall, which would be 6 micra thick at 10% hematocrit and 1.5 at 80%. He also suggests that the Farhaeus-Lindqvist effect may be reversed as the flow rate approaches zero (i.e., the apparent viscosity rises in small tubes). Though his evidence is not conclusive he explains such a reversal on the basis of the establishment of the marginal zone by axial accumulation at vanishing shear rates, the marginal zone would not be present and the red cells would be in intimate contact with the tube wall. This added friction between the cells and walls would contribute relatively more to the apparent viscosity in small tubes than in larger ones.

Cerney, Cook and Walker (11) however, have expressed some doubt on the existence of this Farhaeus-Lindqvist effect. They have used the data of Haynes as well as those of Kumin and maintain that within the bounds of experimental error, they do not find the existence of the Farhaeus-Lindqvist effect. Merrill et al (29) have also found that at a given wall shear stress, the limiting apparent viscosities at high flow rates

are independent of tube radius over a range of 0.013 to 0.085 cms.

## 2.3 The Effect of Hematocrit Level and Temperature on the Rheological Properties of Blood

### 2.3.1 The variation of viscosity with hematocrit level

The variation in viscosity with hematocrit level has often been measured (11, 17, 21, 22, 23, 24, 27). At shear rates sufficiently large for non-Newtonian behaviour to be neglected, an equation of the form shown below has been found satisfactory up to an hematocrit level of 30% (17, 30).

$$\mu_r = \mu_o/(1 - KH)$$

where $\mu_r$ = asymptotic viscosity of the blood at high rate of shear

$\mu_o$ = asymptotic viscosity of the suspending fluid at high rate of shear

H = hematocrit level

K = constant

The values for K seem to vary between 1.5 and 2.5 (11, 17, 21, 24). There seems to be a general agreement that the value of K is slightly less than 2.5 as is shown elsewhere for soft flexible bodies (35, 36). The effect of coagulation of the cells is to increase the value of K due to the increased hydrodynamic volume of the coagulates caused by fluid trapped

between them.

There is a progressive deviation of the above equation for hematocrit levels exceeding 30% due to the non-Newtonian behaviour of the cells which is absent below the 30% level.

Haynes (17) maintains that no concentration power series discussed in the literature provides a good fit for blood, but that it follows an exponential relation which is only invalid for hematocrits less than 10%. As shown below it is:

$$\mu_a(H) = \mu_s e^{X(R)H}$$

where $\mu_a$ = apparent asymptotic viscosity in a tube of large radius

$\mu_s$ = viscosity of the suspending fluid

H = hematocrit level

X = exponential constant depending on tube radius

The relation has been given a phenomenological interpretation by Richardson (37) in which it is assumed that as the particle concentration increases, the fractional decrease in mean particle separation is proportional to the fractional increase in apparent viscosity.

2.3.2 The variation of viscosity with temperature

This may be represented by an empirical relation (11):

$$\mu = Be^{+E/RT}$$

where $\mu$ = viscosity at temperature T

R = gas constant

B = constant of proportionality dependent only on the shear rate and the nature of the suspension, but not on temperature

E = energy necessary to start the fluid in motion, also known as the energy of activation for flow.

In terms of relative viscosity $\mu_r = \mu / \mu_p$ where $\mu_p$ is the viscosity of the plasma:

$$\mu_r = (B/B_p)\, e^{+(E-E_p)/RT}$$

differentiating with respect to 1/T:

$$\frac{\partial \ln \mu_r}{\partial (1/T)} = (E - E_p)/R$$

From a plot of $\ln \mu_r$ and 1/T, $(E - E_p)$ may be obtained. It has been found to be 1.23 kcals. for a hematocrit level of blood of 44%.

Merrill et al (38) have shown that at low shear rates the absolute viscosity of blood becomes very large in magnitude and independent of temperature; their explanation for this is the movement of aggregate rouleaux past each other, i.e., the plastic deformation of the three-dimensional networks which increasingly control dynamic rheology. They have also noted a substantial independence of the relative viscosity, of blood to water, on temperature at shear rates greater than 1 $sec^{-1}$.

### 2.3.3 The variation of yield stress with hematocrit level

The variation of yield stress with hematocrit up to a level of 80% is given by:

$$\tau_y^{1/3} = A(H - H_c)$$

where $\tau_y$ = yield stress

$H$ = hematocrit

$H_c$ = critical hematocrit below which there is no yield stress

$A$ = constant - approx. 0.008

This equation is similar to the one proposed by Norton (39) for clay suspensions, where the volume per cent of dispersed mineral phase corresponds to the hematocrit level.

Above hematocrit levels of 50% the following equation first proposed by Green (40) proves to be a better correlation:

$$\tau_y = ae^{bH}$$

where a and b are empirical constants.

There is very little dependence of yield stress on temperature, indicating that the energies of interaction holding the red cells together are much greater than the thermal energy.

## 2.4 The Nature of the Flow of Blood in Capillaries

### 2.4.1 Capillaries of the same size as red cells

#### 2.4.1.1 Bolus flow

Studies (23) have clarified the role of important variables influencing the resistance to flow in relatively large tubes. In the systematic circulation both the rate of shear and the tube radius are large compared to the values in the capillary circulation. It is quite probable that an appreciable fraction of the capillaries permit only one red cell to enter at a time (41). Also the average velocity of the flow of blood in capillaries is only about one thousanth of that in the aorta.

In capillaries where only one red cell enters at a time, the plasma is effectively trapped between successive red cells and moves along in segments. This is commonly referred to as bolus flow. When bolus flow occurs in capillaries, the red cells are deformed and there is probably some frictional force between the endothelial wall and the membrane of the cell. Also the plasma between the red cells undergoes some motion which may be expected to increase the rate of gaseous equilibrium within the plasma, as well as to increase the viscous resistance.

Visual observations (42) of the motion of a dye in the "core" of a bolus in a glass tube, show that it is carried through the bolus at a velocity roughly twice the

average (or "transport") velocity of the bolus. The dye then reaches the upper interface of the bolus where it is carried radially towards the wall of the glass tube. Upon reaching the wall, the dye adheres to the glass and remains in that position until the bottom interface of the bolus reaches it. Then the radial components carry the dye back into the core, then the circuit is repeated again. A circuit was completed every time the bolus had travelled about twice its own length.

2.4.1.2 Diffusion

The flow pattern described above is in contrast to that in Poiseuille flow, in so far as strong radial components are associated with bolus flow. These radial velocity components which exist at the terminal surfaces of the bolus increase the rate of transfer of a material (i.e., oxygen) from the periphery of the bolus into the interior.

During the first micron or so bolus flow considerably facilitates equilibrium, after which the plasma rapidly becomes saturated. In the capillary circulation, the red cells act as sinks for oxygen, so that a greater total amount of oxygen is required for saturation than experimentation of Prothero has suggested (42). This is because his model ignored the diffusion into the red cells. Also the oxygen gradient is maintained longer. In this circumstance saturation occurs much less rapidly and thus it is possible that bolus flow in the plasma may increase the rate of equilibriation by as much

as 100% over the rate which would be obtained if the motion in the plasma was that of Poiseuille flow.

It is known (43), that the pulmonary capillary blood has essentially reached gaseous equilibrium with the oxygen tension in the alveolar space in the course of traversing only a fraction of the length.

Roughton et al (44) have considered the series of resistances to diffusion in the whole process, i.e., the diffusion through the vessel wall from alveolus to lumen, the diffusion through the plasma into the body of the red cell, and the kinetics of chemical association with the haemoglobin in the red cell. They conclude that the last factor could be the most important. In their analysis they assume complete mixing in the plasma.

The problem of diffusion of gases between blood and tissue is much more complicated in the peripheral capillaries. Instead of an alveolar space where a uniform oxygen tension down the length of a capillary may be assumed, there will be gradients of $PO_2$ in the tissues surrounding the capillary, not only in a direction at right angles to the axis of flow, but also along the length. The gradients will probably be considerable, since modern measurements of the $PO_2$ cells indicate levels far below the venous $PO_2$. It appears that equilibrium is never achieved even in the full length of the capillaries.

Forster has proceeded to analyse the diffusion into the red cell with the continuous sink of the hemoglobin throughout the cell, to derive the successive "shells" of oxygen tension within the discoid erythrocytes. However, microscopic observations of red cells in bolus flow suggests that the red cell is continually changing shape due to the non-uniformity of the capillary. Therefore, mixing of the contents of the cell will occur. Even when the capillary is larger than the cell, a transfer of the energy of motion to the contents of the cell resulting in flow and mixing in the red cell may occur. Mason (45) has shown that such a circulation occurs within oil droplets suspended in water when the suspension is flowing.

2.4.1.3 Pressure required to force red cells through narrow capillaries

Work done on a millipore filter apparatus through which the rate of filtration of erythrocytes was measured (46), has shown that mammalian red cells may be sufficiently deformed to enable them to pass through pores 5 to 3 micra in diameter, for relatively long periods, under pressure of 4 cms. of water or less. These pressures are less than the generally accepted values for the driving pressure available in the capillary circulation. However, the authors do not believe that their experiments furnished reliable evidence on the viscous resistance to flow through capillaries in vivo.

Their calculated velocities through these pores containing cells are only about 1/500 of the *in vivo* values; the reason being that the red cells adhere rather firmly to the filter material, which is not the case for the endothelial lining of capillaries.

2.4.1.4 Deformation

With the use of improved optical techniques and high-speed cinemicrography, the flow behaviour of individual cells has been observed (47, 48, 49). At zero flow they appear to be edge on, with their faces orientated perpendicular to the vessel. As the flow rate increases, they begin to deform into U-shapes, thimble-shapes or teardrop-shapes, the degree of deformation increasing with increasing flow rates. This phenomena is also observed with liquid bubbles in tube flow (50), but not with rigid discs having diameters slightly less than that of a rigid tube; they, instead, rotate in complex orbits.

2.4.2 Capillaries of a larger size than the red cells

2.4.2.1 Rotation

The velocity gradient or shear rate which increases with the radius, gives rise to fluid stresses which exert a torque on the surface of the suspended cells causing them to rotate. Studies of human red cells in heparinized plasma were made by following the particles (concentration 2%)

down propylene or glass tubes (51, 52). Analysis of cinefilms verifies a theory put forward by Jeffreys in 1922, that the angular velocities of rod- and disc-like particles are a maximum when the particle major axis lies across the direction of flow, and minimum, but not zero, when aligned with the flow. This applies to single erythrocytes as well as to straight-chain rouleaux from 2 to 20 cells. As a result of the erythrocytes' periodic angular motion, the particle spends more of its time aligned with the flow than across it.

In Poiseuille flow, rouleaux containing n cells in a linear array, of regular shape and not deformed by the velocity gradient, rotate as rigid discs (for $n = 2, 3$) or rod (if $n = 5$) (52). Similar results have been obtained in Couette flow with physical models of rouleaux consisting of linear stacks of rigid discs (53).

2.4.2.2 Deformation

The deformation of red cells in tubes with diameters equal to or less than the cell diameter has been frequently reported (47, 48). But the deformation, in a tube with a larger diameter than that of the cell, has only been demonstrated adequately after the advent of high-speed cinematographic techniques. According to Bloch (49) "the erythrocytes spin about their long and short axes, deform readily and travel across the 'lamina' in an irregular helical spiral" in arterioles 2 to 5 times the cell diameter.

Rand and Burton (54) determined the stiffness of the red-cell membrane by measuring the pressure required to suck the cells into a micropipette. The membrane tension was found to be $2 \times 10^{-2}$ dyne/cm. and a red cell could be forced out of the micropipette having a tip of 2 micra internal diameter, with a pressure drop of less than 1 mm. of water. Apparently the membrane can withstand large bending strains, but only limited tangential strains as the erythrocyte folds over during outflow. So if a long tongue of a cell is sucked into a micropipette, the membrane within the tube spontaneously collapses on itself (55). This is similar to the breakup of a flowing, long, cylindrical bubble in a tube after being brought to rest.

Observations made on rouleaux of red cells having more than 10 cells, indicate that they have spring orbits (51, 52), i.e., the rouleaux while rotating are subjected to compressive forces in alternate quadrants as a result of the normal forces in flow. If the rouleaux axis ratio (thickness/diameter), or the velocity gradient is sufficiently high, these compressive forces can lead to buckling. The rouleaux will then tend to straighten out in the next quadrant where the forces are tensile - this orbit is called a "springy" orbit. At a given shear rate, increasing the number of cells increases the flexibility of the rouleaux, so that the ends become capable of independent movement (cells 20). Such

orbits are called snake orbits.

2.4.2.3 Axial migration

The classical visual evidence is that in a healthy mammal, the flow is streamline in small arteries and veins but that the erythrocytes move in an axial stream surrounded by a peripheral concentric layer of plasma (17, 18). It has been claimed (56) that "the cells of this stream were arranged in concentric laminae, the centre one passing along most rapidly and each additional layer passing more slowly than the one inside it. The wall of each lamina of this system consisted of unagglutinated blood cells; each layer was exactly one red cell thick. The blood flowed so rapidly in most arterioles and venules which were from 60 to 120 micra in diameter, that individual red cells could not be seen." Copely and Staple (57) examined arterial and venal flow in hamster pouches and clearly observed the cell-free layer which could be altered in width from 7.6 micra to zero micra, by reducing the flow rate to zero in a venule of 72.2 micra diameter. For an arteriole 19.2 micra in diameter, the cell-free layer varied in width from 0 to 3.5 micra, depending on the flow rate.

However, Merrill and Wells (10) claim that in the arterioles and venules of a hamster pouch, the flow is granular and they observed no axial drift of the cells. Müller (21) maintains that blood flow is laminar, and the red

cells move at random, and Bloch (58) has shown that what to the eye appears a homogeneous laminar flow, becomes at a film speed of 3000 frames/sec., a turbulent flow with continuous reorientation of cellular components. This work was done on the mysentery and liver of frogs.

This contradictory evidence regarding axial migration ties in directly with the Farhaeus-Lindqvist effect whose proponents support the existence by the marginal zone theory and the sigma phenomenon - both assume axial migration. Hence, any conclusions reached must inevitably be speculative.

2.4.2.4 Concentrated suspensions

It is extremely difficult to follow individual particles in the tube flow of concentrated dispersions of 5 - 10% by volume, and over 10% it is virtually impossible because of multiple reflection and refraction of the transmitted light. There are techniques to overcome this problem though it is not possible to use them with red blood cells. In this case transparent suspensions have been prepared using human ghost cells, which, after hemolysis and washing, were reconstituted in biconcave form in plasma (51) at concentrations of 10 - 70%. About 1% by volume of the original unhemolysed red cells was then added and these could be easily seen during flow.

The behaviour of human erythrocytes in ghost cell suspension has been studied by Goldsmith at various velocities.

At concentrations above 20%, the cell velocities in tubes of radius less than 50 micra began to deviate from a parabolic profile. Above 30% there was appreciable blunting of the profile, but less so than that of a similar concentration of rigid discs. Also this blunting was greater at low flow rates than at high ones.

The cells also exhibited erratic radial displacements, the frequency of which decreased with decreasing radial distances. They also deformed into various shapes such as triangular and U-shaped structures. When the red cells were hardened with gluteraldehyde similar erratic paths were observed, but no deformation.

Unlike the regular periodic rotational orbits of the red cells in very dilute suspensions, the rotational orbits in suspensions above 30% fluctuated tremendously, occasionally "flipping" over, completing a half-orbit. In this case, there was a greater alignment of the red cells with flow than in the case of dilute solutions, and the degree of alignment at any given concentration increased with increasing flow rate.

The major difference between the behaviour of the ghost cells in heparinized plasma and normal red cell suspensions, is that in the former, rouleaux are not formed. Although the velocity distributions varied with the flow rate, there was not the same drastic change in flow regime that is observed with whole blood. At mean flow rates greater than 10 tube diameters/sec., the blood is evenly distributed across the

lumen of the tube; at the wall there is a cell-depleted layer of varying thickness from 0 to 8 micra (57, 59) with single red cells being jostled about by collisions during flow. At creeping flow rates, there is a central core network of rouleaux moving as a plug. At the periphery, where the velocity gradient is predominant, the red cells and rouleaux rotate and deform. In tubes where the radius is 20 micra, blunting of the velocity profile at concentrations of 40% occurs at low flow rates, the velocity profile becoming increasingly parabolic with increasing flow rates (59). This change in velocity profile is not observed in concentrated suspensions of erythocytes in Ringer's Solution (60) where rouleaux do not form, and where, in a Couette viscometer, erythocytes exhibit Newtonian behaviour at all velocity gradients.

## 2.5 The Difficulties of "In Vivo" Measurements

There are several practical difficulties involved in making rheological measurements on blood flow *in vivo*, and this has led several investigators to concentrate their research on *in vitro* experiments. These difficulties are due to the need for simultaneous measurements of the instantaneous flow rate, pressure drop, and the cell orientation, shape, spacing and number. Because of the obvious difficulty of making these measurements on a living mammal, investigators have usually concentrated on studying one variable at a time, without the simultaneous measurement or control of the others.

The other obstacle is due to the clotting of fresh blood. Therefore, investigators have seldom been able to use fresh blood without the addition of anti-coagulants, or they tend to use serum instead of plasma, or they use a suspending agent other than plasma (e.g. A.C.D.). Even under these circumstances, it is fairly difficult to record blood flow without clotting in glass capillaries smaller than about 30 microns in diameter (22). This could be due to the absence of a fibrin coating on the glass surface which apparently permits blood to flow more easily over it (12, 57); however, ultimate blockage would come about by the formation of a coagulated mass of cells in the capillary. Since it is a recognized fact that for successful hydraulic transport of

solid particles, the tube diameter must be at least three times the largest dimension of the transported particle, one might expect blockages in capillaries smaller than 24 micra, if one considers the maximum dimension of the red cell to be 8 micra. This is of course under the proviso that the flexibility of the cell does not alter the effective maximum dimension. This is of the order of the smallest diameter of capillaries which have been successfully used in practice (13).

## 2.6 Other Empirical Equations

The only empirical equation that is considered important in its application to blood is the Casson equation (63) first derived for printing inks. The equation may be represented by:

$$\tau^{\frac{1}{2}} = a^{\frac{1}{2}}\dot{\gamma}^{\frac{1}{2}} + b^{\frac{1}{2}}$$

where $\tau$ = shear stress

$\dot{\gamma}$ = shear rate

a and b are constants

Merrill et al. (64) have shown that the parameter b is identical to the yield stress $\tau_y$ and Merrill and Pelletier (65) have shown that a is identical to the point value of the absolute viscosity $\eta$ = constant, in the limit of zero yield stress, ($\tau_y = b = 0$).

Charm and Kurland (66) have used a series of viscometers with shear rate ranges from 2 to 100,000 $sec^{-1}$

and maintain that the Casson equation may be applied to blood over the whole range. However, the constants a and b take different values for different viscometers, as used for different shear rate ranges.

Merrill and Pelletier (65) refute this claim by using one rotational viscometer over a wider range of shear rate, viz. 0.1 - 300 $sec^{-1}$, and testing eleven blood samples adjusted to 40% hematocrit in the viscometer, at 37°C. They plotted shear-stress as a function of shear rate on square-root co-ordinates (See Fig. ). They "offer the conjecture that the data over the range of 0.1 to 20 $sec^{-1}$ shear rate can be approximated by the Casson equation, the slope being the square root of the constant a, and that above 100 $sec^{-1}$, the data follow the equation

$$\eta = \tau / \dot{\gamma}$$

with constant viscosity so that the slope is the square root of the Newtonian viscosity."

Consequently, Merrill and Pelletier cover the entire shear rate range with a 2-parameter, 2-equation model, i.e.,

$$\tau^{\frac{1}{2}} = \eta^{\frac{1}{2}} \dot{\gamma}^{\frac{1}{2}} + \tau_y^{\frac{1}{2}} \qquad \text{(Casson equation)}$$

$$\tau^{\frac{1}{2}} = \eta^{\frac{1}{2}} \dot{\gamma}^{\frac{1}{2}} \qquad \text{(Newtonian equation)}$$

A major drawback of this model is the range limitation. The Casson equation is applicable over a shear rate range of zero

to approximately 20 $sec^{-1}$, and the Newtonian equation from 100 $sec^{-1}$ to higher. Transition from the Casson equation to the Newtonian one occurs over the shear rate range of about 16 $sec^{-1}$ to 100 $sec^{-1}$, with no relation to approximate or predict this transition. Clearly there is a need for an improved model.

## 3. THEORY

### 3.1 Capillary Flow

The equation of motion, in symbolic form may be represented as:

$$(D\bar{V}/Dt) = -\nabla p - (\nabla \cdot \bar{\bar{\tau}}) + \sum_s \rho_s F_s \qquad (1)$$

where $(D\bar{V}/Dt)$ = the mass per unit volume times accelaration

$\nabla p$ = the pressure force per unit volume

$\sum_s \rho_s F_s$ = the sum of all the field forces per unit volume

In cylindrical co-ordinates (r, θ, z), equation (1) may be represented, in terms of $\tau$, by the following equations, assuming gravity to be the only field force present:

r-component:

$$\rho\left(\frac{\partial V_r}{\partial t} + V_r\frac{\partial V_r}{\partial r} + \frac{V_\theta}{r}\frac{\partial V_r}{\partial \theta} - \frac{V_\theta^2}{r} + V_z\frac{\partial V_r}{\partial z}\right)$$
$$= -\frac{\partial p}{\partial r} - \left(\frac{1}{r}\frac{\partial}{r}(r\tau_{rr}) + \frac{1}{r}\frac{\partial \tau_{r\theta}}{\partial \theta} - \frac{\tau_{\theta\theta}}{r} + \frac{\partial \tau_{rz}}{\partial z}\right) + \rho g_r \qquad (2)$$

θ-component:

$$\rho\left(\frac{\partial V_\theta}{\partial t} + V_r\frac{\partial V_\theta}{\partial r} + \frac{V_\theta}{r}\frac{\partial V_\theta}{\partial \theta} + \frac{V_r V_\theta}{r} + V_z\frac{\partial V_\theta}{\partial z}\right)$$

$$= -\frac{1}{r}\frac{\partial p}{\partial \theta} - \left(\frac{1}{r^2}\frac{\partial}{\partial r}(r^2\tau_{r\theta}) + \frac{1}{r}\frac{\partial \tau_{\theta\theta}}{\partial \theta} + \frac{\partial \tau_{\theta z}}{\partial z}\right) + \rho g_\theta \qquad (3)$$

z-component:

$$\rho\left(\frac{\partial V_z}{\partial t} + V_r\frac{\partial V_z}{\partial r} + \frac{V_\theta}{r}\frac{\partial V_z}{\partial \theta} + V_z\frac{\partial V_z}{\partial z}\right)$$

$$= -\frac{\partial p}{\partial z} - \left(\frac{1}{r}\frac{\partial}{\partial r}(r\tau_{rz}) + \frac{1}{r}\frac{\partial \tau_{\theta z}}{\partial \theta} + \frac{\partial \tau_{zz}}{\partial z}\right) + \rho g_z \qquad (4)$$

Now steady pipe (capillary) flow has the velocity components $(0,0,V_z(r))$ and the stress tensor takes the form:

$$\sigma_{ij} = -p\delta_{ij} + \tau_{ij} = \begin{pmatrix} \tau_{rr} - p & 0 & \tau_{rz} \\ 0 & \tau_{\theta\theta} - p & 0 \\ \tau_{rz} & 0 & \tau_{zz} - p \end{pmatrix}$$

where $\tau_{\theta\theta}$ is zero if there is to be no helical flow. The shear rate $dV_z/dr$ is always negative, since r is measured from the centre line and $\tau_{rz}$ is always positive, i.e., the momentum is transferred from the centre line towards the wall. Therefore, to define an apparent viscosity which will not be constant, we have:

$$\tau_{rz} = -\mu_a\,(dV_z/dr) \qquad (5)$$

where $\mu_a$ is the apparent viscosity.

Assuming:

(i) steady continuum flow

(ii) no forces acting in the radial or flow directions

(iii) the flow is symmetrical with respect to z, (i.e., $\tau_{r\theta} = \tau_{\theta z} = 0$)

the equations (2), (3) and (4) reduce to:

$$0 = -\frac{\partial p}{\partial r} - \frac{1}{r}\frac{\partial}{\partial r}(r\tau_{rr}) - \frac{\tau_{\theta\theta}}{r} \tag{6}$$

$$0 = -\frac{\partial p}{\partial z} - \frac{1}{r}\frac{\partial}{\partial r}(r\tau_{rz}) \tag{7}$$

From equation (7):

$$\partial(r\tau_{rz}) = -\frac{\partial p}{\partial z}\, r\,\partial r$$

i.e. $$\tau_{rz} = -\frac{r}{2}\frac{dp}{dz} \tag{8}$$

At the wall, $r = r_o$ and $\tau_{rz} = \tau_w$

$\therefore$ $$\tau_w = -\frac{r_o}{2}\frac{dp}{dz} \tag{9}$$

Dividing (8) by (9) we get:

$$\tau_{rz} = \frac{r}{r_o}\tau_w \tag{10}$$

The boundary condition is $V_z = 0$ at $r = r_o$, for no slip at the wall.

The volume flow rate is given by:

$$Q = \int_o^{r_o} 2\pi r V_z dr \qquad (11)$$

We have from equation (10) that:

$$r = r_o \tau_{rz} / \tau_w$$

$\therefore$ equation (11) becomes:

$$Q = 2\pi \left(\frac{r_o}{\tau_w}\right)^2 \int_o^{\tau_w} \tau_{rz} V_z d\tau_{rz} \qquad (12)$$

The velocity may be given by:

$$V_z = \int_r^{r_o} \left(-\frac{dV_z}{dr}\right) dr$$

i.e. $$V_z = \frac{r_o}{\tau_w} \int_{\tau_{rz}}^{\tau_w} \left(-\frac{dV_z}{dr}\right) d\tau_{rz} \qquad (13)$$

Combining equations (12) and (13):

$$Q = 2\pi \left(\frac{r_o}{\tau_w}\right)^3 \int_o^{\tau_w} \tau_{rz} \int_{\tau_{rz}}^{\tau_w} \left(-\frac{dV_z}{dr}\right) d\tau_{rz} d\tau_{rz}$$

i.e. $$\frac{4Q}{\pi r_o^3} = \frac{8}{\tau_w^3} \int_0^{\tau_w} \tau_{rz} \int_{\tau_{rz}}^{\tau_w} \left(-\frac{dV_z}{dr}\right) d\tau_{rz} d\tau_{rz} \qquad (14)$$

Integrating by parts:

$$\frac{4Q}{\pi r_o^3} = \frac{4}{\tau_w^3} \int_0^{\tau_w} \tau^2_{rz} \left(-\frac{dV_z}{dr}\right) d\tau_{rz} \qquad (15)$$

Equation (15) is the general equation which relates the flow to the velocity gradient in the system.

For a non-Newtonian fluid, it is possible to define an apparent viscosity as:

$$\frac{1}{\mu_{ap}} = \frac{4Q/\pi r_o^3}{\tau_w} = \frac{4}{\tau_w^4} \int_0^{\tau_w} \tau^2_{rz} \left(-\frac{dV_z}{dr}\right) d\tau_{rz} \qquad (16)$$

where $\mu_{ap}$ may be distinguished from $\mu_a$ as defined by equation (5), i.e.,

$$\tau_w = -\mu_a \left(\frac{dV_z}{dr}\right)_w = \mu_{ap} \frac{4Q}{\pi r_o^3}$$

The term $4Q/\pi r_o^3$ is, at times called the pseudo-shear rate.

Weissenberg, Rabinowitsch and Mooney obtained a simple relation between the flow rate and the wall shear rate (or between $\mu_a$ and $\mu_{ap}$):

Differentiation of equation (15) gives:

$$\frac{d[\tau_w^3 (4Q/\pi r_o^3)]}{d\tau_w} = 4\tau_w^2 \left(-\frac{dV_z}{dr}\right)_w \qquad (18)$$

i.e. $$\frac{4Q}{\pi r_o^3} \cdot \frac{1}{4\tau_w^2} \cdot 3\tau_w^2 + \frac{\tau_w^3}{4\tau_w^2} \frac{d}{d\tau_w}\left(\frac{4Q}{\pi r_o^3}\right) = \left(-\frac{dV_z}{dr}\right)_w \qquad (19)$$

$$\therefore \quad \left(-\frac{dV_z}{dr}\right)_w = \frac{3}{4}\left(\frac{4Q}{\pi r_o^3}\right) + \frac{\tau_w}{4} \cdot \frac{d(4Q/\pi r_o^3)}{d\tau_w} \qquad (20)$$

Equation (20) can now be used to obtain the basic shear diagram, i.e., for any given value of $\tau_w$ the value of $4Q/\pi r_o^3$ may be obtained from the data, and the slope of the curve may also be obtained at the point, hence $(-dV_z/dr)_w$ may be calculated. Both $\tau_w$ and $(-dV_z/dr)_w$ are obtained at the same point and hence are the terms of the basic shear diagram. There is no need to assume any kind of rheological law for this calculation.

## 3.2 Slip at the Wall

The above equations may be modified for slip-at-the-wall conditions by allowing for a slip velocity $V_s$; i.e., the new boundary condition at the wall becomes $V_z = V_s$ as opposed to $V_z = 0$

∴equation (13) becomes:

$$V_z = V_s + \int_r^{r_o} \left(-\frac{dV_z}{dr}\right) dr$$

$$V_z = V_s = \frac{r_o}{\tau_w} \int_{\tau_{rz}}^{\tau_w} \left(-\frac{dV_z}{dr}\right) d\tau_{rz} \qquad (21)$$

Combining equation (21) with equation (12) we have a relation similar to equation (14), i.e.,

$$\frac{4Q}{\pi r_o^3} = \frac{4V_s}{r_o} + \frac{8}{\tau_w^3} \int_o^{\tau_w} \tau_{rz} \int_{\tau_{rz}}^{\tau_w} \left(-\frac{dV_z}{dr}\right) d\tau_{rz} d\tau_{rz} \qquad (22)$$

Integrating by parts, as before, we have an equation similar to equation (15):

$$\frac{4Q}{\pi r_o^3} = \frac{4V_s}{r_o} + \frac{4}{\tau_w^3} \int_o^{\tau_w} \tau^2_{rz} \left(-\frac{dV_z}{dr}\right) d\tau_{rz} \qquad (23)$$

Oldroyd (61) defines:

$$\xi = \frac{V_s}{\tau_w} \quad \text{and} \quad \phi = \frac{4}{\tau_w^4} \int_o^{\tau_w} \tau^2_{rz} \left(-\frac{dV_z}{dr}\right) d\tau_{rz}$$

Substituting the above relations into equation (23) we have:

$$\frac{4Q}{\pi r_o^3} = (4\xi/r_o + \phi)\,\tau_w \qquad (24)$$

A plot of $4Q/\pi r_o^3$ versus $1/r_o$ will determine both $\xi$ and $\phi$.

As can be seen from equation (24), at any constant $\tau_w$, for a system with slip, increasing the diameter, will decrease $4Q/\pi r_o^3$, but there is no effect of length if steady state is obtained. Hence a plot of $4Q/\pi r_o^3$ versus $\tau_w$ will determine the existence or the absence of slip. If slip is present then the slip velocity may be easily determined from Oldroyd's parameters.

However, it should be recognized that both slip at the wall and thrixotropic behaviour may cause complications in the capillary shear diagram. To distinguish between the two it is better to have a rotational viscometer available, so that the change in viscosity with time may be known, at a given rate of shear. If no time dependence exists, the non-coincidence of the curves of the $4Q/\pi r_o^3$ versus $\tau_w$ plot may be attributed to slip at the wall.

## 4. THE DEVELOPMENT OF THE MODEL

The data of Haynes and Burton (23, 62) and Merrill et al. (60) were utilized in the development of the model. Haynes and Burton, and Merrill et al. had obtained a set of values of pressure drop and volume flow through capillaries, for a series of radii and hematocrits. The data used were at the following radii:

A. Haynes and Burton at 25.5°C.

(i) Radius: 57.04 $\mu$

Hematocrits: 21%, 38.7%, 61.8%

(ii) Radius: 184.7 $\mu$

Hematocrits: 8.8%, 28.5%, 43.3%, 76%

(iii) Radius: 472.4 $\mu$

Hematocrits: 13.6%, 35.5%, 40%, 56%, 61%

(iv) Radius: 747.4 $\mu$

Hematocrits: 27.4%, 50.4%, 66.9%, 82.5%

B. Merrill et al. at 19.9°C.

Hematocrit: 39.3%

Radii: 144 $\mu$, 183 $\mu$, 192 $\mu$, 261.5 $\mu$, 425

The equation (20) derived earlier was used to evaluate the shear rate, i.e.,

$$\left(-\frac{dV_z}{dr}\right)_w = \frac{3}{4}\left(\frac{4Q}{\pi r_o^3}\right) + \frac{\tau_w}{4}\cdot\frac{d(4Q/\pi r_o^3)}{d\tau_w} \qquad (20)$$

Knowing the pressure drop and volume flow at each hematocrit for each of the radii, the computer program No. 1 (See Appendix II), was used to evaluate the pseudo-shear rate, $4Q/\pi r_o^3$ and the shear stress $\tau_w$ from the relation:

$$\tau_w = -\frac{r_o}{2}\frac{dp}{dz} \qquad (9)$$

In order to evaluate the term $\frac{d(4Q/\pi r_o^3)}{d\tau_w}$ which appears on the R.H.S. of equation (20) plots of the pseudo-shear rate and shear stress were made. (Figs. 2, 3, 4, 5, for the data of Haynes and Burton, and Figs. 15, 16, 17, 18, 19, for the data of Merrill et al.)

Now knowing all the terms on the R.H.S. of equation (20), the shear rate was calculated using computer program No. 2 (See Appendix II). Both $\tau_w$ and $(-dV_z/dr)_w$ are calculated at the same point and are thus the terms of the basic shear diagram. The basic shear diagram for each of the above mentioned radii and hematocrits are shown (Figs. 6, 7, 8, 9, for the data of Haynes and Burton, and Figs. 20, 21, 22, 23, 24, for the data of Merrill et al.).

From the rheological properties of blood it was obvious that the model should incorporate a yield stress, $\tau_y$, and an asymptotic viscosity, $\mu_\infty$, due to the Newtonian behaviour of blood after a certain shear rate.

*All figures are shown in Section 7.

Close examination of all the basic shear diagrams indicated the existence of the yield stress (intercept on $\tau_w$ axis) and a straight line section which would correspond to the asymptotic viscosity. The point of yield stress and the beginning of the straight line section was connected by a smooth curve for each case. Consequently, there was a family of curves, each member having the same basic shape consisting of a linear segment, which when extended backwards intersected with the positive $\tau_w$-axis; this point of intersection was called the apparent yield stress, $\tau_{yap}$, the yield stress that blood would exhibit if it behaved as an ideal Bingham plastic. There was also a non-linear segment which passed through the point of yield stress. (See Fig. 1).

Any straight line section on the basic shear diagram may be represented by the relation:

$$\dot{\gamma}_w = \phi \tau_w - C \qquad (25)$$

where $\dot{\gamma}_w = (-dV_z/dr)_w$ = shear rate

$\phi$ = slope of the linear segment = fluidity of blood

$C$ = intercept on the negative $\tau_w$ axis

Now C may be expressed by the relation:

$$C = \phi \tau_{yap} \qquad (26)$$

FIGURE 1: SHEAR RATE VS. SHEAR STRESS

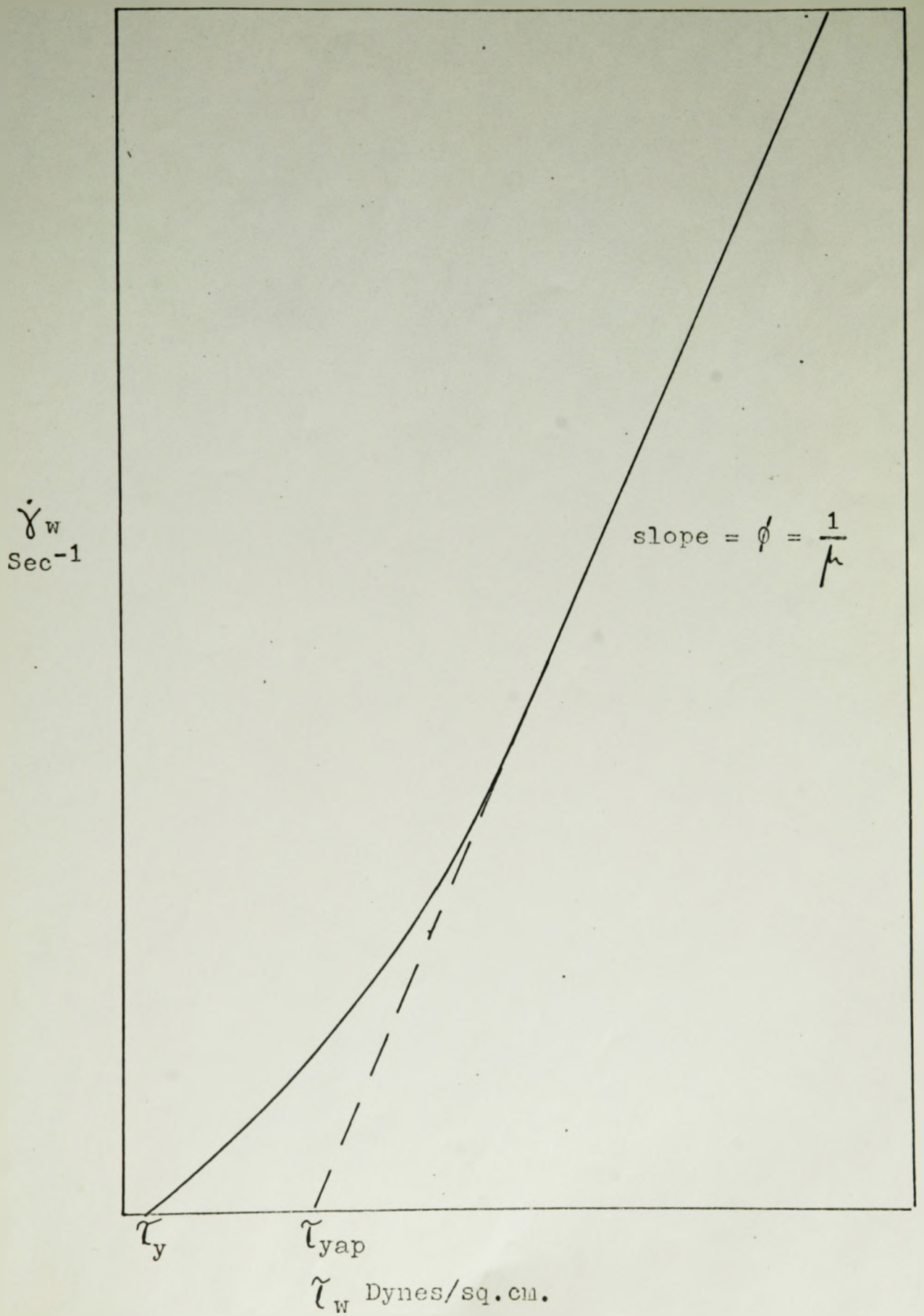

where $\tau_{yap}$ = intercept on positive $\tau_w$-axis

= apparent yield stress

i.e. $$\gamma_w = \phi \tau_w - \phi \tau_{yap} \qquad (27)$$

Since the non-linear segment intersects with the positive $\tau_w$-axis, to give the yield stress, equation (27) may be modified to

$$\gamma_w = \phi(\tau_w - \tau_y) - \phi(\tau_{yap} - \tau_y) \qquad (28)$$

In order to represent the non-linear section, it was clear that the second term on the R.H.S. of equation (28), i.e., $\phi(\tau_{yap} - \tau_y)$ would have to be multiplied by a function which is zero at the point of yield stress, $\tau_y$, and approaches unity in such a way that the non-linear segment is "smoothly" joined to the linear section as the shear rate is increased. A simple function which satisfies these requirements is:

$$\left[1 - \exp\left\{-A(\tau_w - \tau_y)\right\}\right] \qquad (28a)$$

where A is a constant that characterizes the rate of approach to unity.

The author does not maintain that this is the only function that would satisfy the requirements; there are obviously several others. The choice of this one over others was made on its simplicity.

Consequently, the full shear diagram may be represented by:

$$\dot{\gamma}_w = \phi(\tau_w - \tau_y) - \phi(\tau_{yap} - \tau_y)\left[1 - \exp\left\{-A(\tau_w - \tau_y)\right\}\right] \quad (29)$$

i.e. $$\dot{\gamma}_w = \phi\left[(\tau_w - \tau_y) - (\tau_{yap} - \tau_y)\left[1 - \exp\left\{-A(\tau_w - \tau_y)\right\}\right]\right] \quad (30)$$

Now $\phi$, the fluidity, is the reciprocal of the asymptotic viscosity, i.e.,

$$\phi = 1/\mu$$

and since this model holds for any shear stress and shear rate measured at the same point, the equation, (30), may be written as:

$$\dot{\gamma} = \frac{1}{\mu}\left[(\tau - \tau_y) - (\tau_{yap} - \tau_y)\left[1 - \exp\left\{-A(\tau - \tau_y)\right\}\right]\right] \quad (31)$$

From the basic shear diagram all the parameters are directly obtained except one, A. However, A may be determined by choosing a point on the non-linear segment of the basic shear diagram (since A characterizes the rate of approach to unity)* thus determining the shear stress and shear rate at that point, and hence using equation (32), i.e.,

*This is a trial-and-error procedure

$$A = \frac{-\left[\ln\left\{1 + \frac{\mu\dot{\gamma}}{(\tau_{yap} - \tau_y)} - \frac{(\tau - \tau_y)}{(\tau_{yap} - \tau_y)}\right\}\right]}{\tau - \tau_y} \qquad (32)$$

Computer program No 3 (See Appendix II), is designed to evaluate A, and predict the value of the shear rate, at any given shear stress, and compare it with the actual value. These are shown as Figs. 10, 11, 12, 13, for the data of Haynes and Burton, and Figs. 25, 26, 27, 28, 29, for the data of Merrill et al.

## 5. THE DEVELOPMENT OF "THE NO SLIP AT THE WALL" CONDITIONS

To show the presence or absence of slip at the wall, it was necessary to have data at a constant hematocrit and temperature, at several different radii. The data of Merrill et al. were only used in this case, as those of Haynes and Burton did not meet this requirement.

Computer program No. 1, (See Appendix II), was used to determine the pseudo-shear rate and the shear stress at the five different radii. The results were plotted on the same graph paper, for all the radii, to determine if there was a decrease in the pseudo-shear rate, with increasing radii, at a constant shear stress. This is shown in Fig. 31.

## 6. RESULTS AND DISCUSSION

The basic shear diagrams as derived from the data of Haynes and Burton (Figs. 6-9) and of Merrill et al. (Figs. 20-24), are of the same basic shape as those obtained by other investigators (11, 64). They show the existence of a small yield stress and the transition from non-Newtonian to Newtonian behaviour, this transition being effected at a shear rate of approximately 100 $sec^{-1}$.

The yield stress that is obtained in each case is higher than the true yield stress of blood. This is most probably due to the insufficiency of available data at extremely low pressure-drops, which necessitates the extrapolation of the non-linear segment from the lowest available point. The curvature in that region is vital for the accurate determination of the yield stress graphically, and hence, an extrapolation technique is not likely to yield the true value. This has been borne out by Merrill and his co-workers (64) where the five extrapolated yield stresses were found to range from 0.09 dynes/sq.cm. to 0.15 dynes/sq.cm., whereas the true yield stresses for this particular work were 0.053 dynes/sq.cm. for each.

It was considered worthwhile to determine the variation of the asymptotic viscosity with hematocrit level

## TABLES OF RHEOLOGICAL PARAMETERS

A. From the Data of Haynes and Burton

Temperature 25.5°C.

### TABLE I

RADIUS = 57.04 $\mu$

| RHEOLOGICAL PARAMETERS | HEMATOCRIT IN % | | |
|---|---|---|---|
| | 21.0 | 38.7 | 61.8 |
| $\phi = 1/\mu$ | 54.0 | 36.3 | 20.0 |
| $\tau_y$ | 0.2 | 0.79 | 1.15 |
| $\tau_{yap}$ | 0.95 | 3.1 | 2.45 |
| A | 0.258 | 0.211 | 0.21 |

## TABLE II

RADIUS = 184.7 $\mu$

| RHEOLOGICAL PARAMETERS | HEMATOCRIT IN % | | | |
|---|---|---|---|---|
| | 8.8 | 28.5 | 43.3 | 76.0 |
| $\phi = 1/\mu$ | 73.0 | 42.0 | 29.4 | 12.1 |
| $\tau_y$ | 0.1 | 0.4 | 0.6 | 0.9 |
| $\tau_{yap}$ | 0.5 | 0.7 | 1.75 | 4.35 |
| A | 0.365 | 0.23 | 0.226 | 0.226 |

## TABLE III

RADIUS = 472.4 $\mu$

| RHEOLOGICAL PARAMETERS | HEMATOCRIT IN % | | | | |
|---|---|---|---|---|---|
| | 13.6 | 35.5 | 40.0 | 56.0 | 61.0 |
| $\phi = 1/\mu$ | 47.6 | 25.0 | 21.3 | 13.5 | 10.7 |
| $\tau_y$ | 0.5 | 0.7 | 0.9 | 1.0 | 1.2 |
| $\tau_{yap}$ | 1.2 | 2.7 | 3.3 | 5.5 | 7.7 |
| A | 0.365 | 0.26 | 0.25 | 0.24 | 0.24 |

TABLE IV

RADIUS = 747.4 $\mu$

| RHEOLOGICAL PARAMETERS | HEMATOCRIT IN % | | | |
|---|---|---|---|---|
| | 27.4 | 50.4 | 66.9 | 82.5 |
| $\phi = 1/\mu$ | 36.8 | 18.5 | 11.35 | 7.5 |
| $\tau_y$ | 0.25 | 0.9 | 1.5 | 1.7 |
| $\tau_{yap}$ | 0.65 | 1.55 | 3.2 | 3.9 |
| A | 0.31 | 0.25 | 0.25 | 0.25 |

B. From the Data of Merrill et al.

Hematocrit 39.3%

Temperature 19.9°C.

TABLE V

| | RADIUS IN MICRA | | | | |
|---|---|---|---|---|---|
| RHEOLOGICAL PARAMETERS | 144 | 183 | 192 | 261.5 | 425 |
| $\phi = 1/\mu$ | 2.66 | 2.45 | 2.5 | 2.4 | 2.55 |
| $\tau_y$ | 0.13 | 0.22 | 0.16 | 0.15 | 0.14 |
| $\tau_{yap}$ | 18.7 | 17.1 | 14.5 | 16.0 | 13.5 |
| A | 0.0404 | 0.0417 | 0.0428 | 0.0448 | 0.05 |

and radius, for the basic shear diagrams (which are identical to those predicted by the model - see Tables I - V). Fig. 14 represents the situation for the data of Haynes and Burton. The family of curves appears to have an asymptotical approach to the fluidity ($\phi = 1/\mu$) axis. This seems reasonable as can be seen from Figs. 6-9, or Figs. 10-13, that as the hematocrit level is decreased, the curves become more vertical, i.e., the slope, which is equal to the fluidity, approaches infinity. The approach to the hematocrit axis seems to indicate a finite value of the asymptotic viscosity at 100% hematocrit level. The approaches in both cases are shown by the dotted lines, whereas the thick line indicates the variation as calculated from the basic shear diagrams.

An interesting phenomenon that can be deduced from Fig. 14, is the existence of a Farhaeus-Lindqvist effect, i.e., decreasing asymptotic viscosity with decreasing radii. This has been supported by Haynes (27) but refuted by Cerney et al. (11). Both groups used identical samples of blood which were different from those considered in this work. However, Fig. 14 indicates a Farhaeus-Lindqvist effect between the radii of 57.04 $\mu$ and 184.7 $\mu$, and a reverse Farhaeus-Lindqvist effect from radii 747.4 $\mu$ and 472.4 $\mu$. The existence of this reverse effect has also been suggested by Haynes (11), but only for low shear rates. Since the asymptotic viscosity is present only at high shear rates, this reverse effect unfortunately cannot be explained by the author. Since neither the existence

nor the absence of Farhaeus-Lindqvist effect has been established, more experimental work obviously needs to be done.

The absence of this effect has also been mentioned by Merrill et al. (29), and their observations are in agreement with Fig. 30, where the fluidity is plotted against the radius for a constant hematocrit level of 39.3%. There is no variation of viscosity with radius.

These contradictory observations may perhaps be explained on the basis of the different techniques utilized in obtaining the pressure-drop volume flow data points and/or by the fact that whereas Haynes and Burton used A.C.D. as the suspending medium, Merrill used plasma. A.C.D. is supposed to have the properties of plasma except that A.C.D. is a Newtonian fluid whereas plasma is now known to be slightly non-Newtonian.

The model developed is as shown below:

$$\dot{\gamma} = \frac{1}{\mu}\left[(\tau - \tau_y) - (\tau_{yap} - \tau_y)\left[1 - \exp\left\{-A(\tau - \tau_y)\right\}\right]\right] \quad (31)$$

where $\dot{\gamma}$ = shear rate

$\tau$ = shear stress

$\mu$ = asymptotic viscosity

$\tau_y$ = yield stress

$\tau_{yap}$ = apparent yield stress

$A$ = constant

Figs. 10-13 and 25-29, compare the basic shear diagrams as predicted by the model with those obtained from the original data. The straight lines represent the model and the dark circles represent the points obtained from the data. As can be seen, the fit is an excellent one, the maximum error at any point being less than 5%. It was initially considered to test for "Goodness of Fit", but this idea was later rejected on the grounds that the null hypothesis would definitely be accepted at the 5% level.

The ranges over which the model was been developed are given below:

Shear stress: from the yield stress to 80 dynes/sq.cm.

Shear rate: 0 - 900 $sec^{-1}$

However, it should be noted that the form of the model is such that it corresponds directly with the form of the basic shear diagram, i.e., the non-Newtonian section is accommodated for by the complete model, in which the term $\left[1 - \exp\left\{- A(\tau - \tau_y)\right\}\right]$ is less than unity, and the Newtonian section is accommodated for by the same term equalling unity; hence, the complete model in this latter case is essentially the equation of a straight line, which has no upper bound. Therefore, theoretically, this model whould be valid from a shear rate of 0 $sec^{-1}$ to any shear rate greater than 100 $sec^{-1}$, where Newtonian behaviour is predominant. This validity of the model over any shear rate range is its major advantage over the 2-equation model proposed by Merrill and his co-workers (65).

Fig. 31 shows that there is no change in the pseudo-shear rate with radius. The points fall fairly close to one another, and the thick black line has been drawn to show the trend. Consequently, one may surmise that up to a hematocrit level of 39.3% there is no slip at the wall, viz., the assumptions of Merrill et al. (60) are valid. However, it cannot justifiably be maintained that that conclusion would be true at higher hematocrits. In fact, it is quite possible, that on increasing the red blood cell concentration, the chances of slip existing at the wall may increase due to the closer "packing" of the cells.

## 7. GRAPHICAL REPRESENTATION OF THE RESULTS

The figures shown in this section are the graphical representation of the results.

The results obtained from the data of Haynes and Burton (23, 62) are shown in Figs. 2-14. (Due to typographical errors in reference 23, for Radius = 472.4 , reference 62 has been mentioned where these errors are corrected.) Figs. 15-31 refer to the data of Merrill et al. (60), Figs. 32-34 refer to the data of Merrill and Pelletier (65) and Figs. 35-36 refer to the data of Merrill et al. (38).

FIGURE 2: PSEUDO-SHEAR RATE VS. SHEAR STRESS

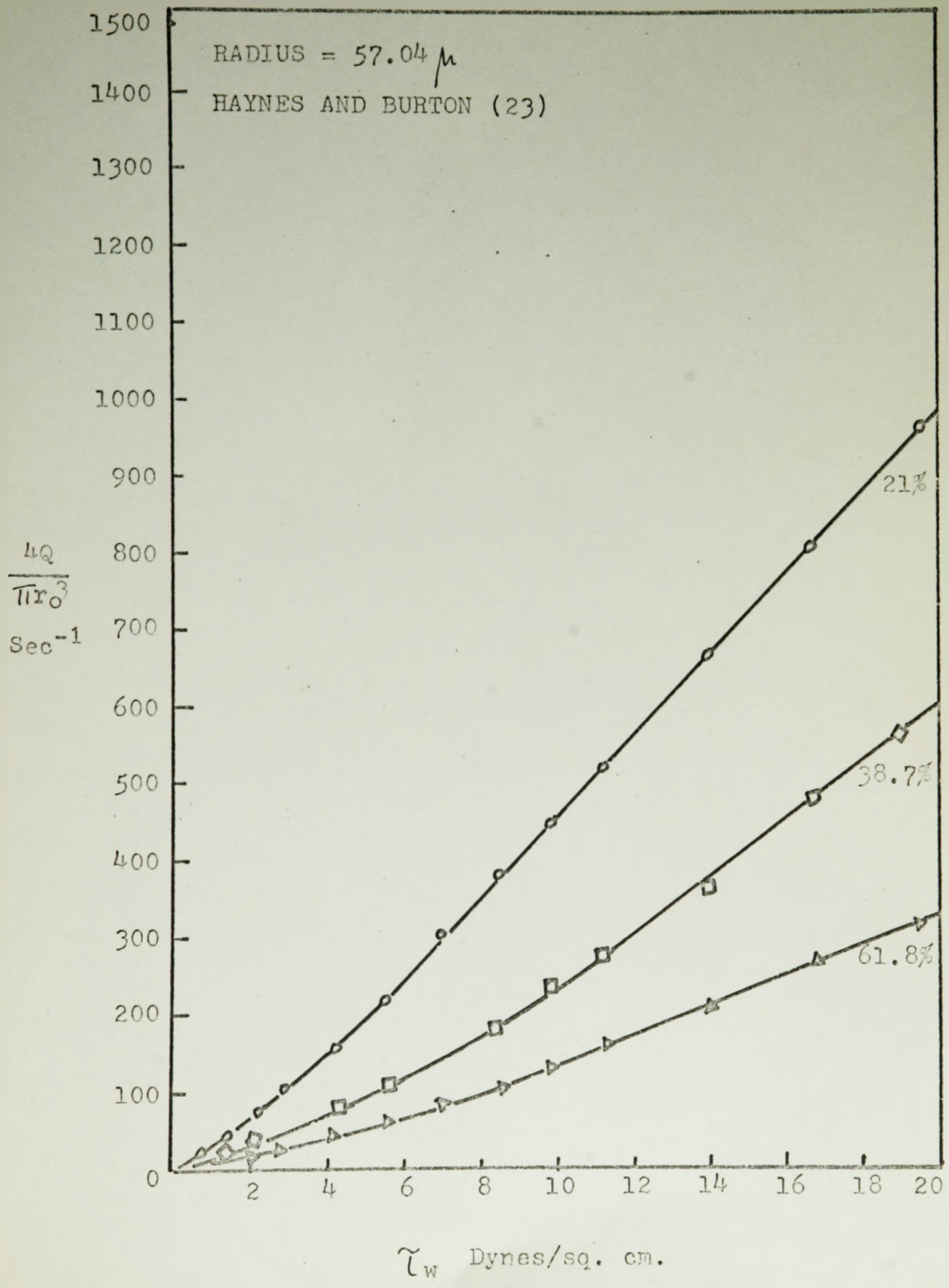

FIGURE 3: PSEUDO-SHEAR RATE VS. SHEAR STRESS

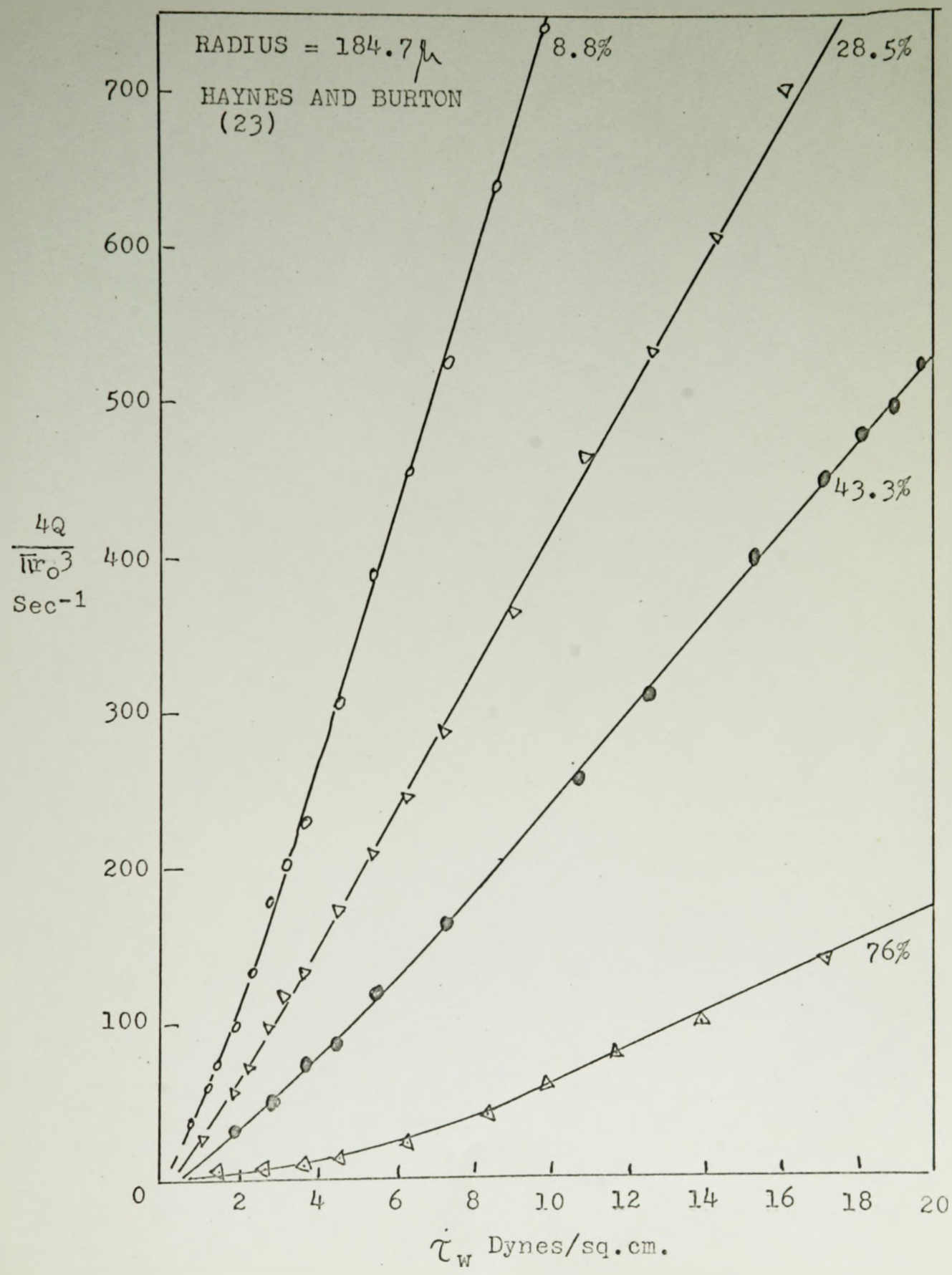

FIGURE 4: PSEUDO-SHEAR RATE VS. SHEAR STRESS

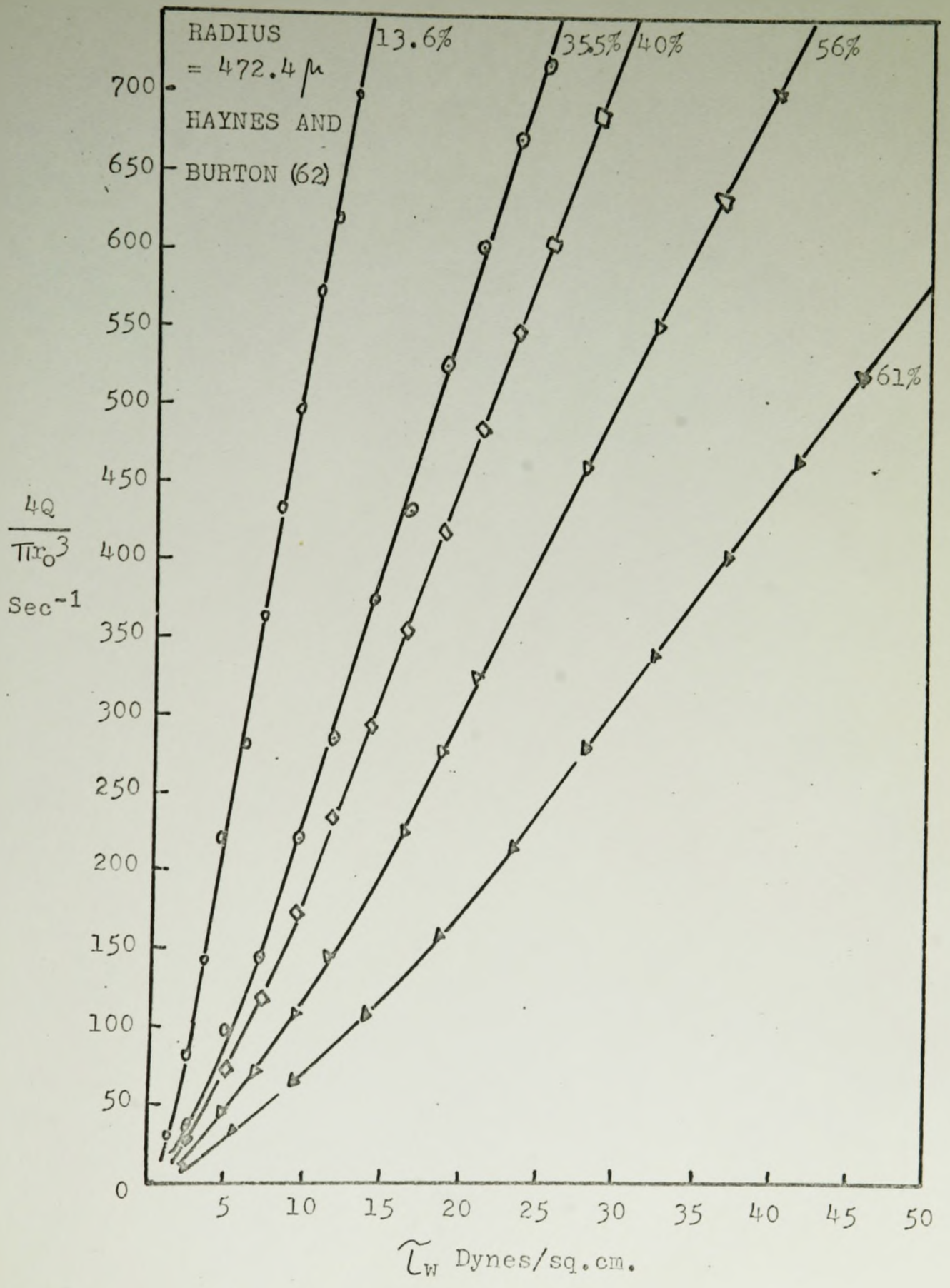

FIGURE 5: PSEUDO-SHEAR RATE VS. SHEAR STRESS

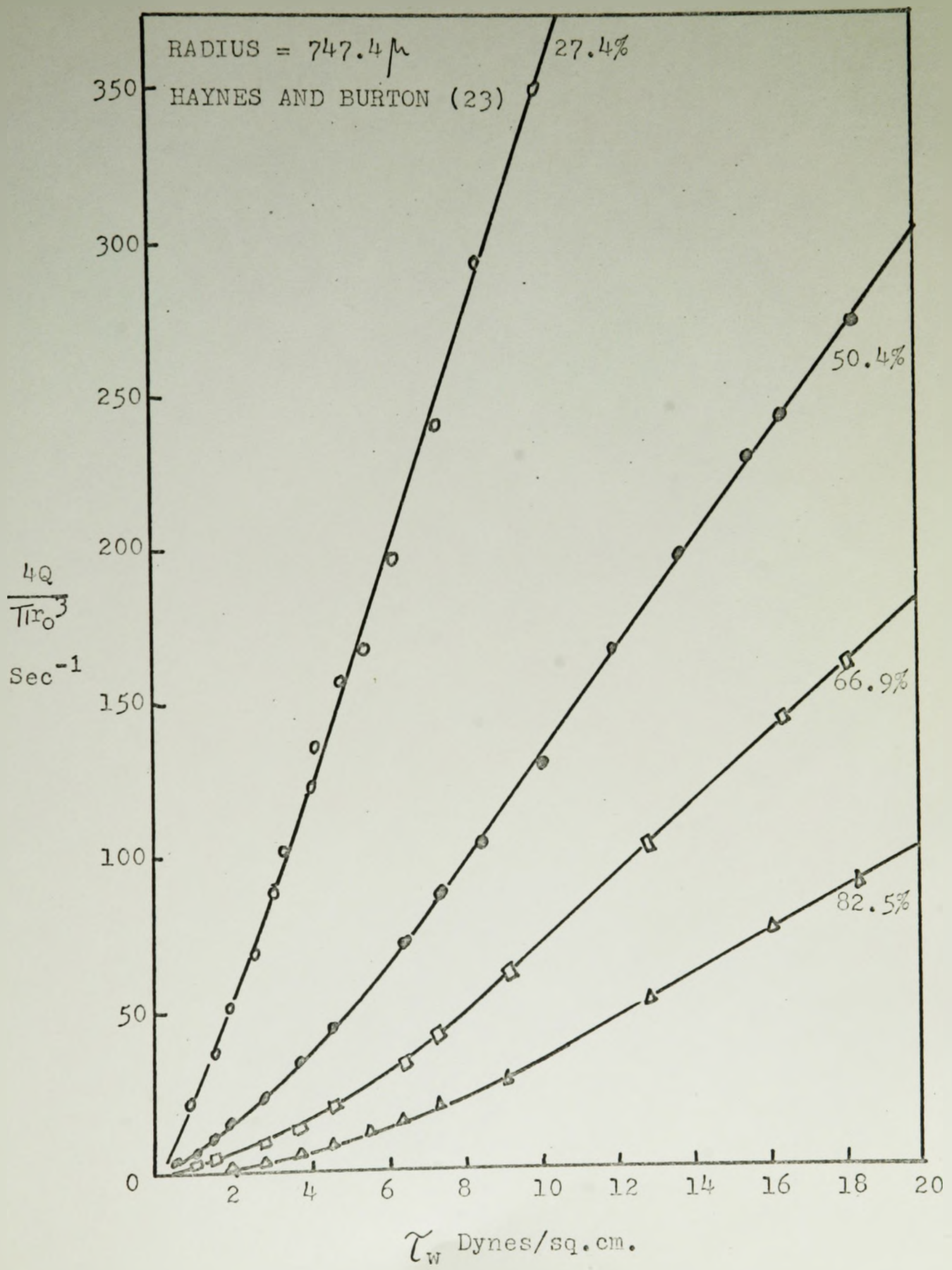

FIGURE 6: SHEAR RATE VS. SHEAR STRESS

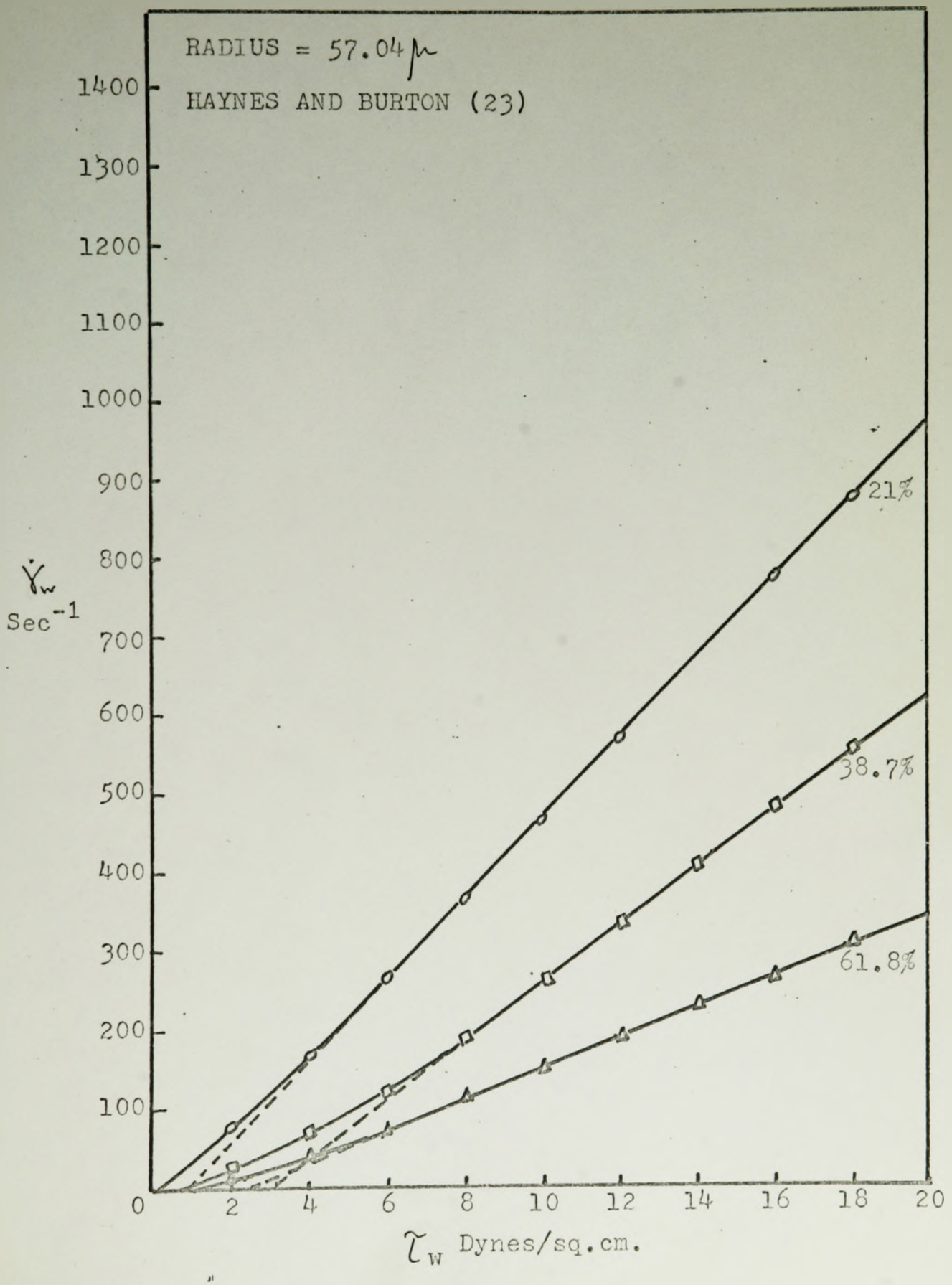

FIGURE 7: SHEAR RATE VS. SHEAR STRESS

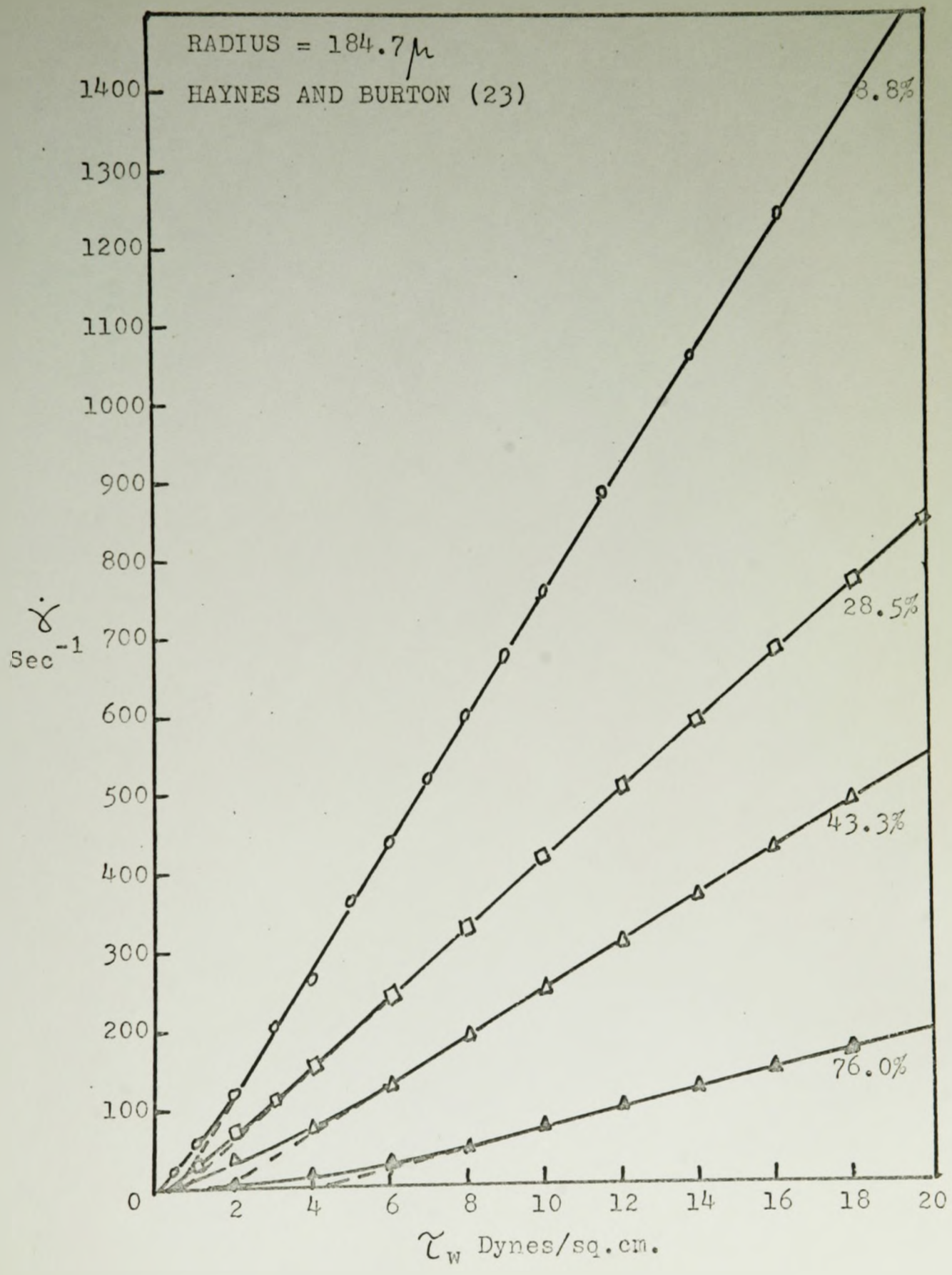

FIGURE 8: SHEAR RATE VS. SHEAR STRESS

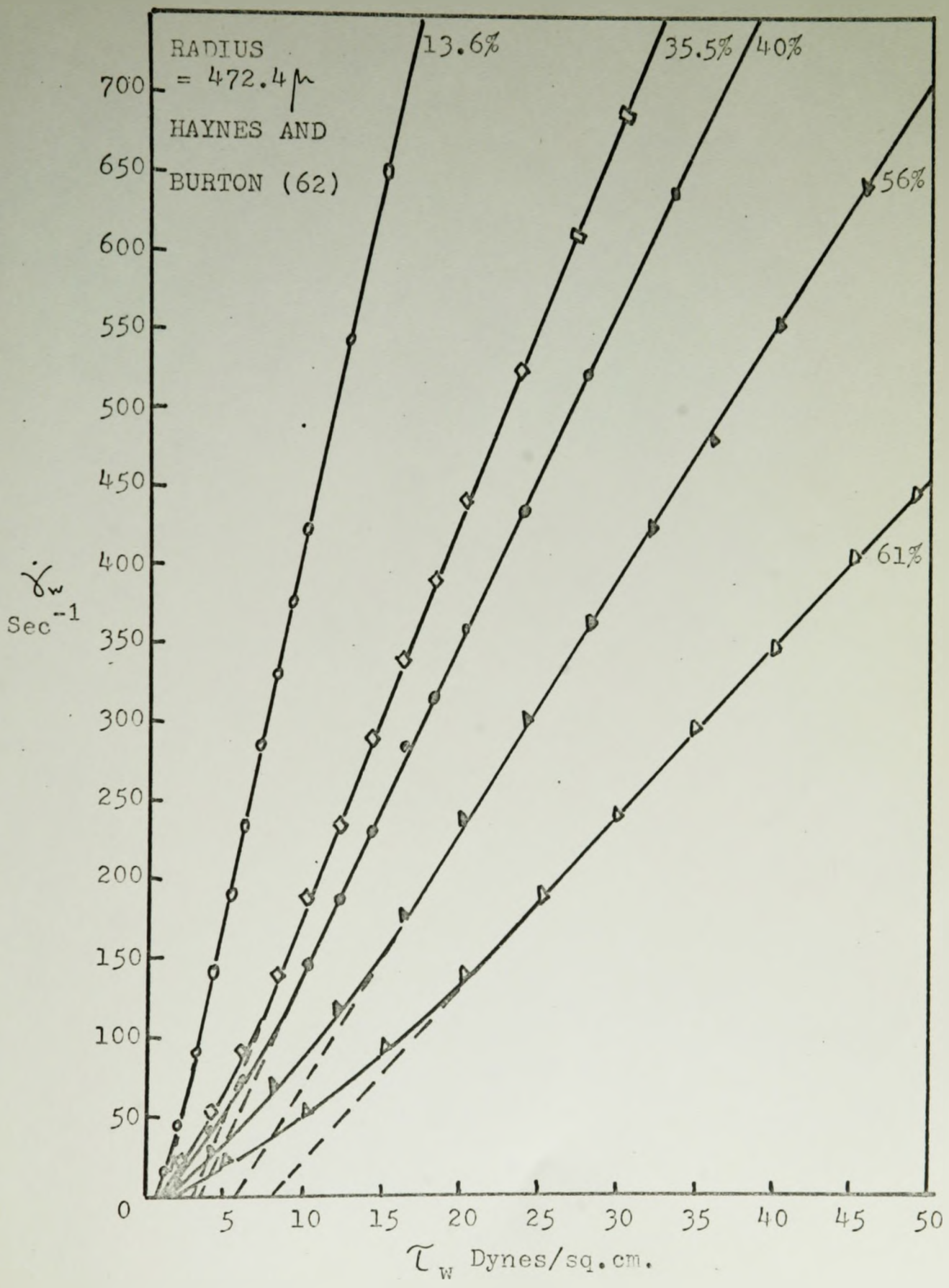

FIGURE 9: SHEAR RATE VS. SHEAR STRESS

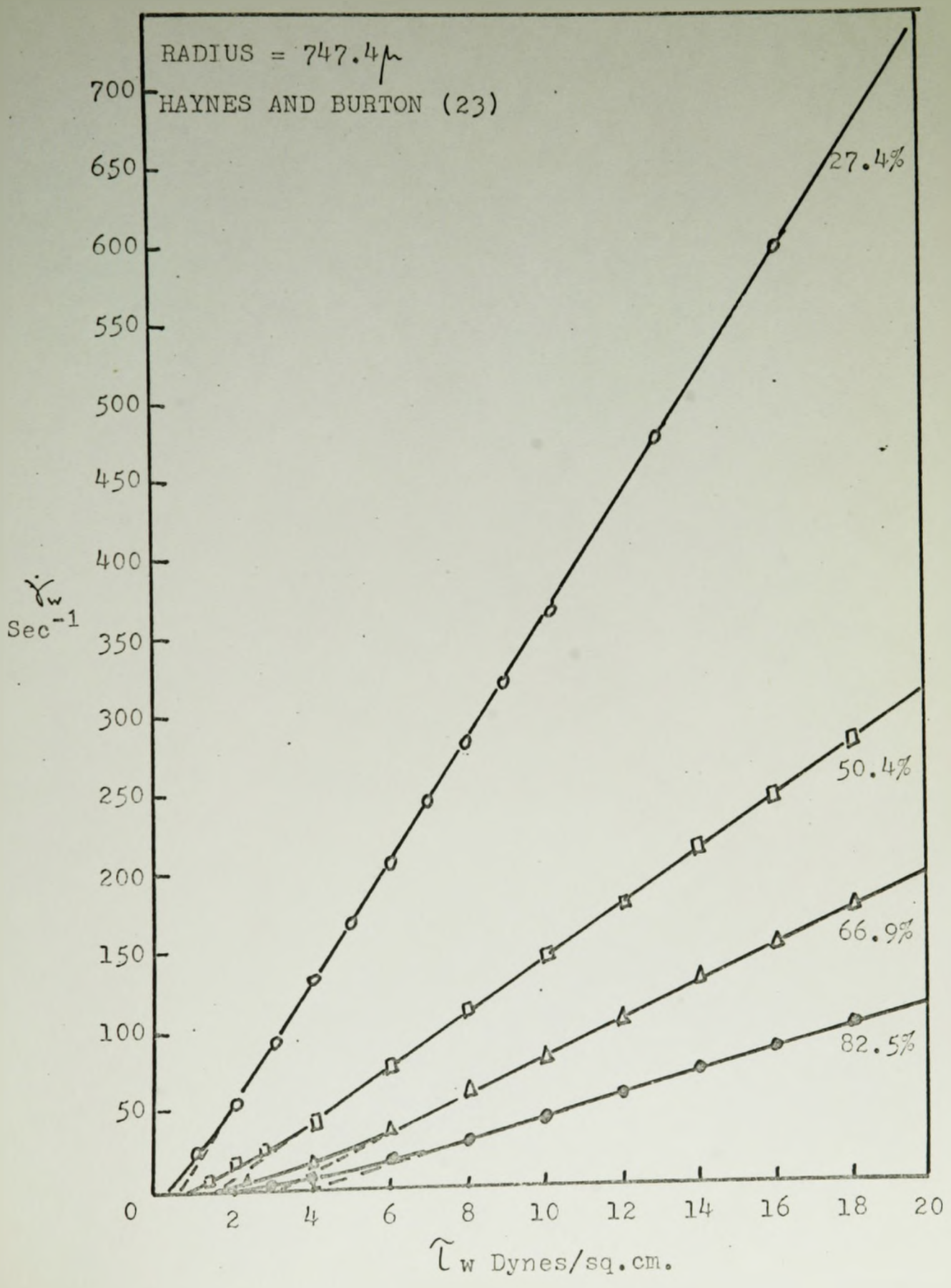

FIGURE 10: SHEAR RATE VS. SHEAR STRESS

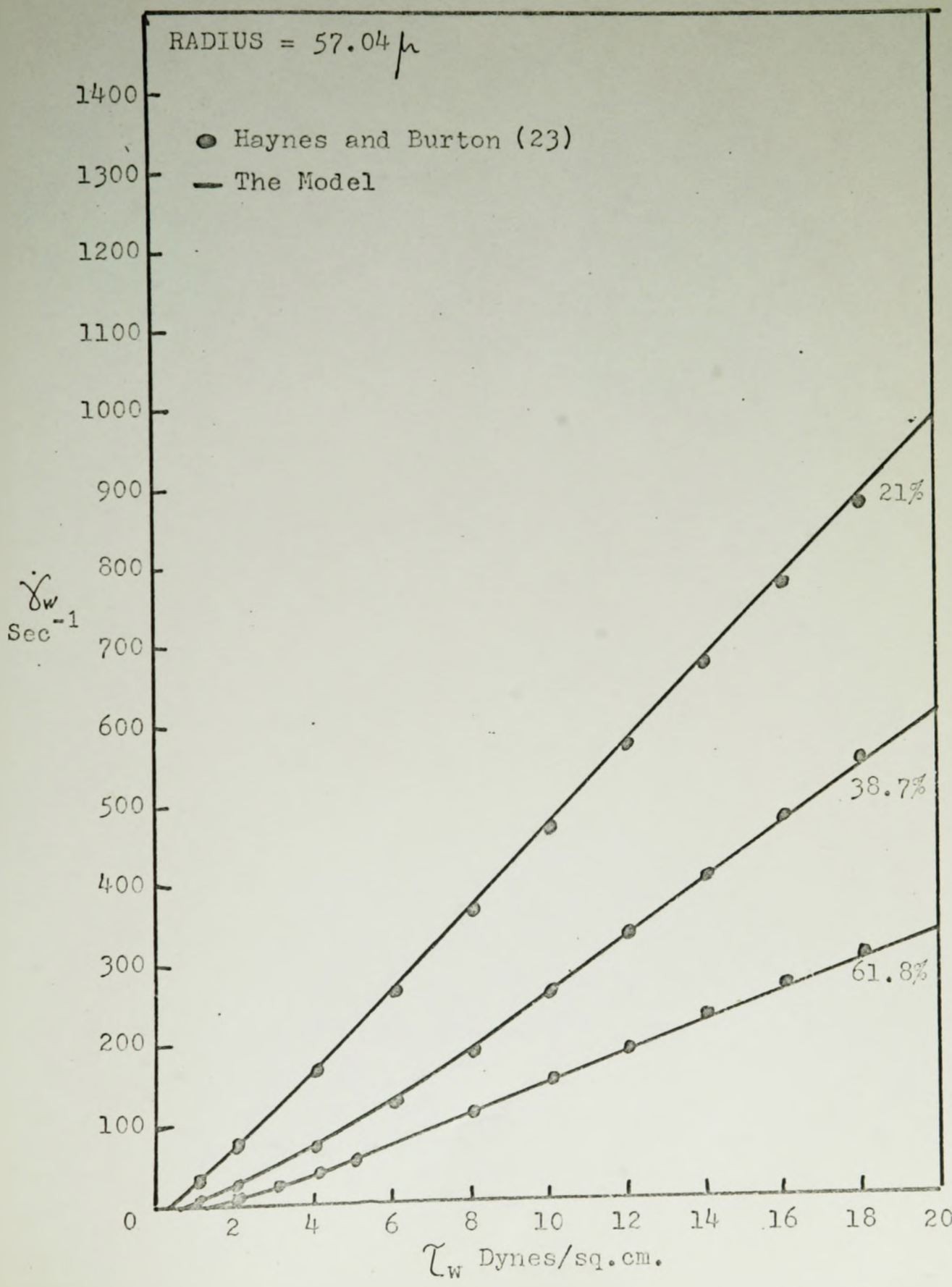

FIGURE 11: SHEAR RATE VS. SHEAR STRESS

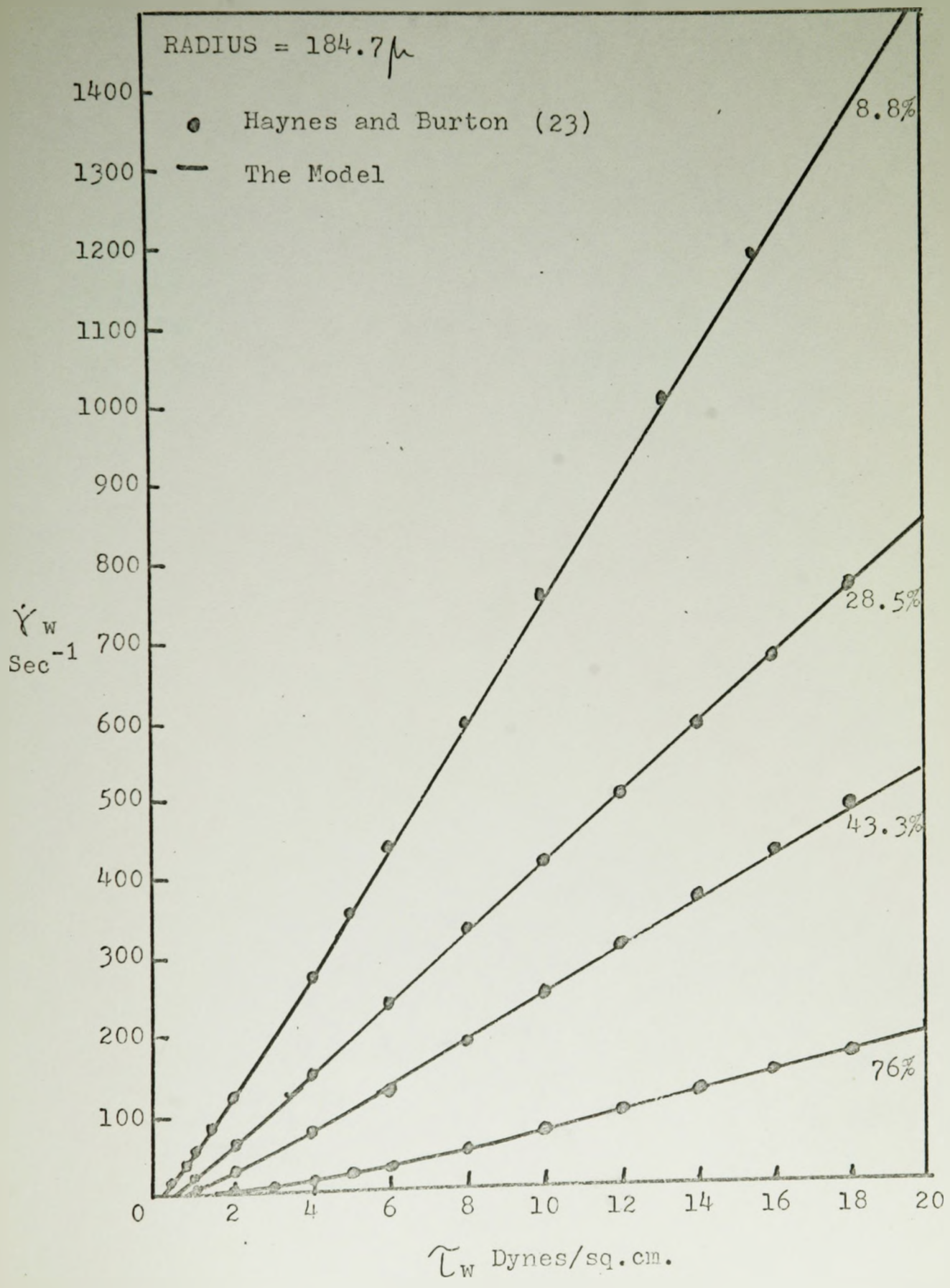

FIGURE 12: SHEAR RATE VS. SHEAR STRESS

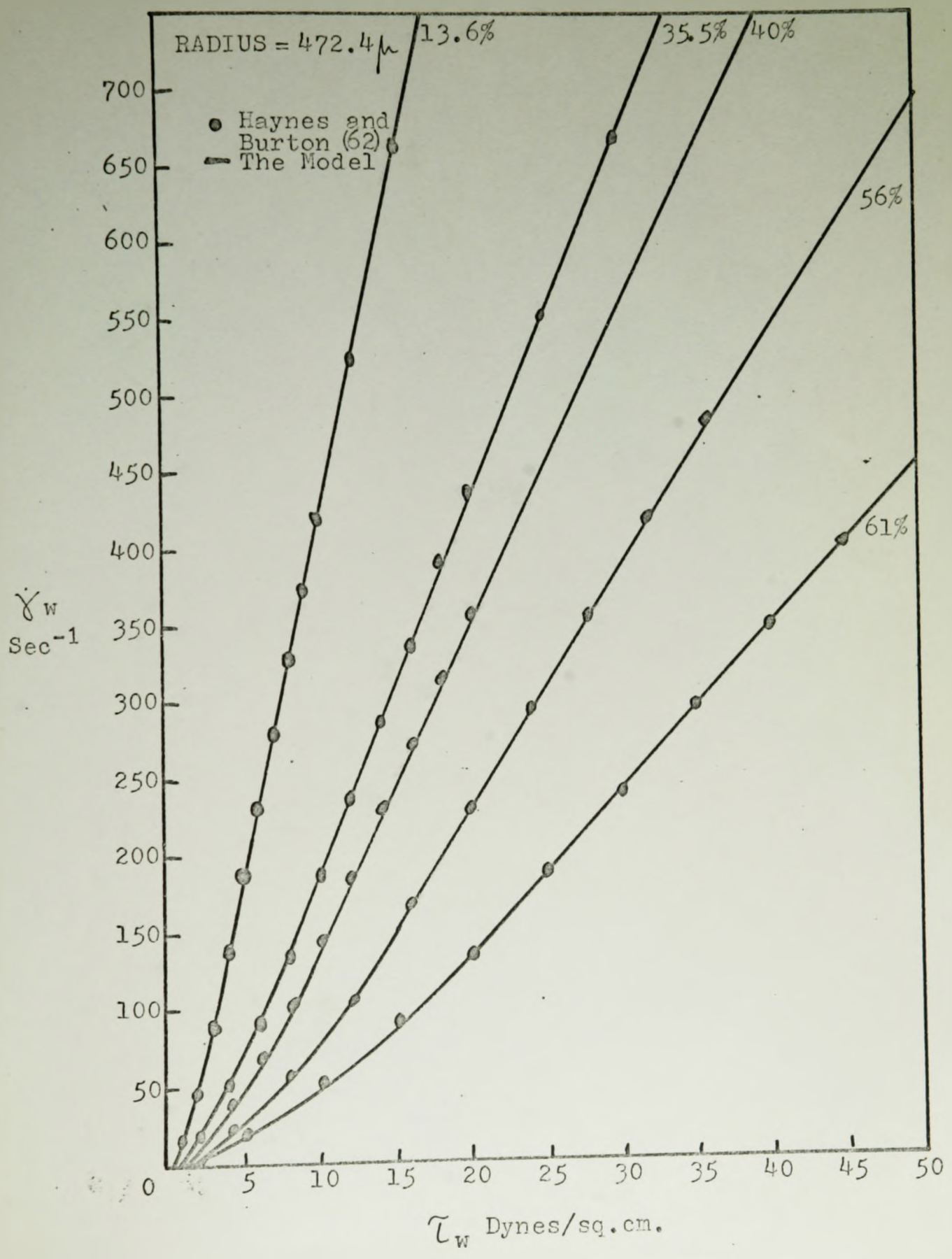

FIGURE 13: SHEAR RATE VS. SHEAR STRESS

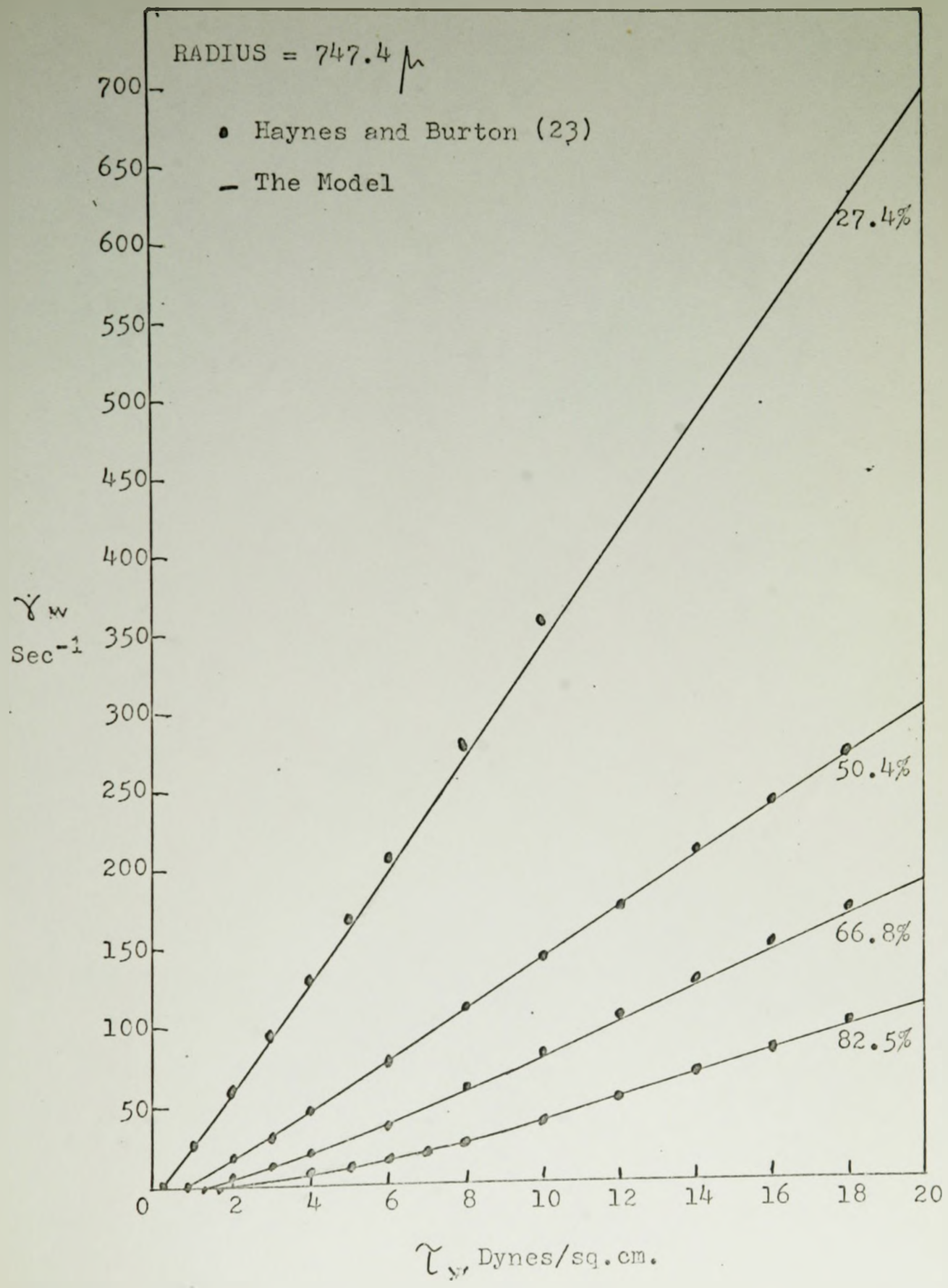

FIGURE 14: FLUIDITY ( = 1/μ ) VS. HEMATOCRIT

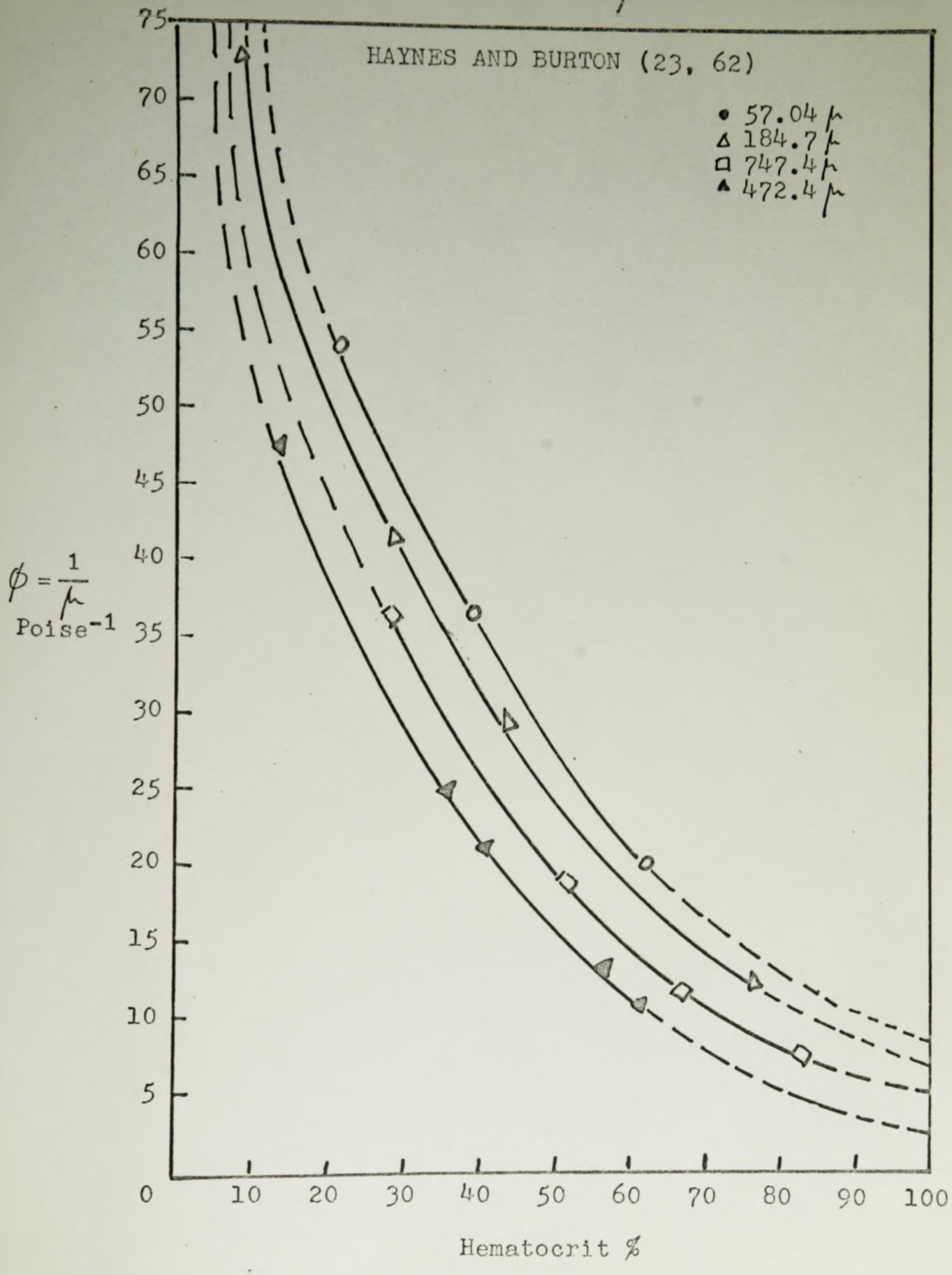

FIGURE 15: PSEUDO-SHEAR RATE VS. SHEAR STRESS

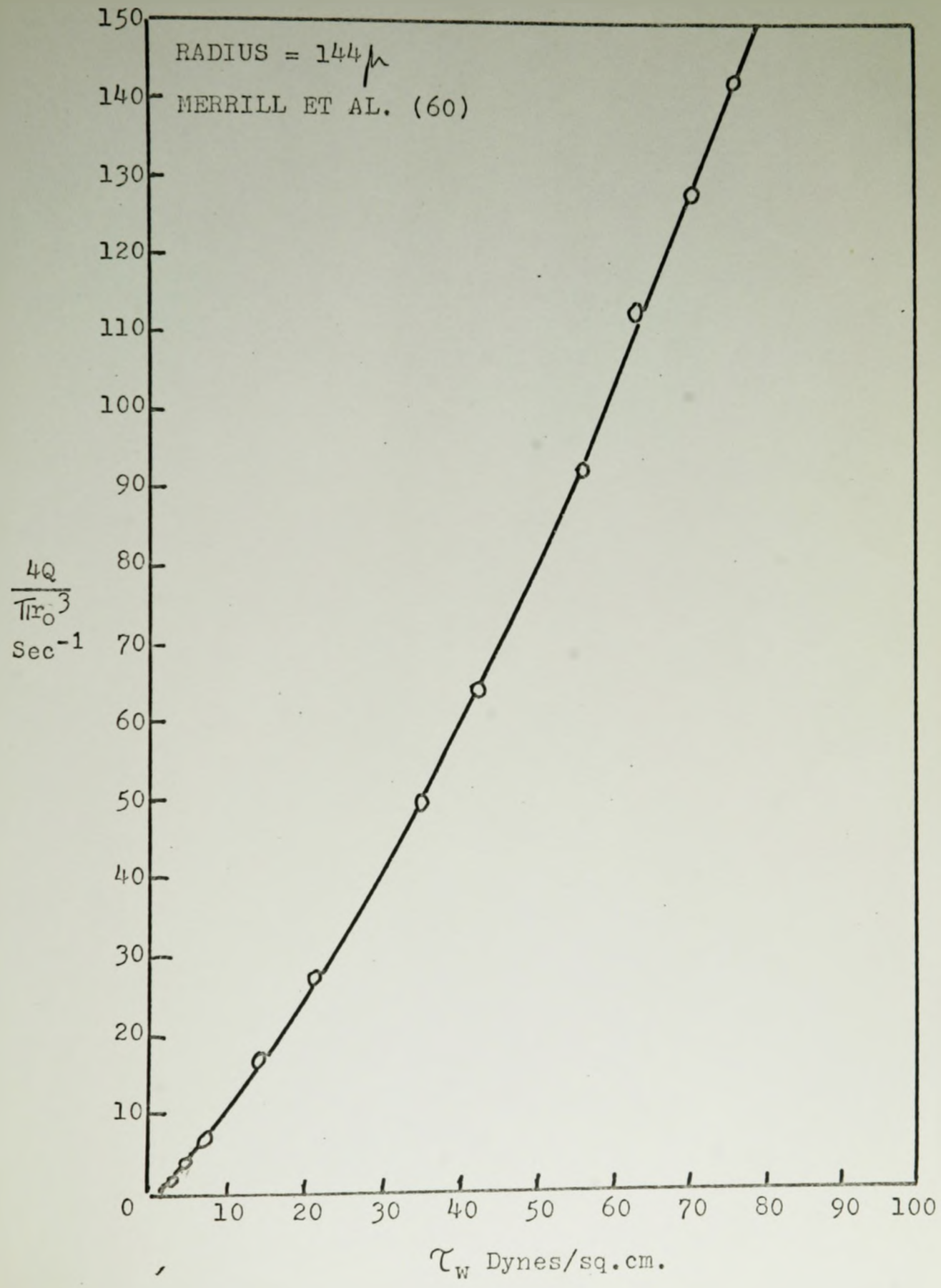

FIGURE 16: PSEUDO-SHEAR RATE VS. SHEAR STRESS

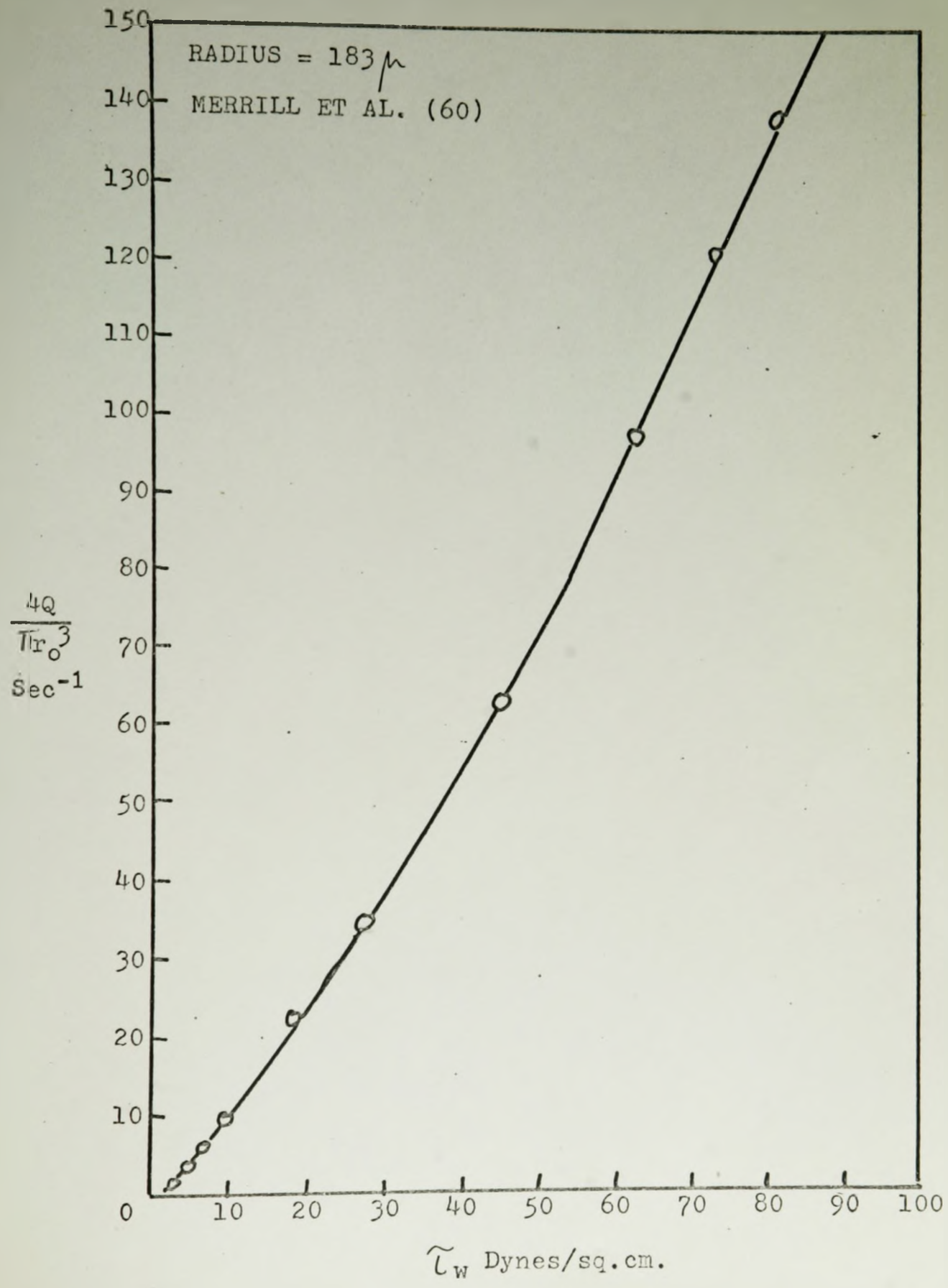

FIGURE 17: PSEUDO-SHEAR RATE VS. SHEAR STRESS

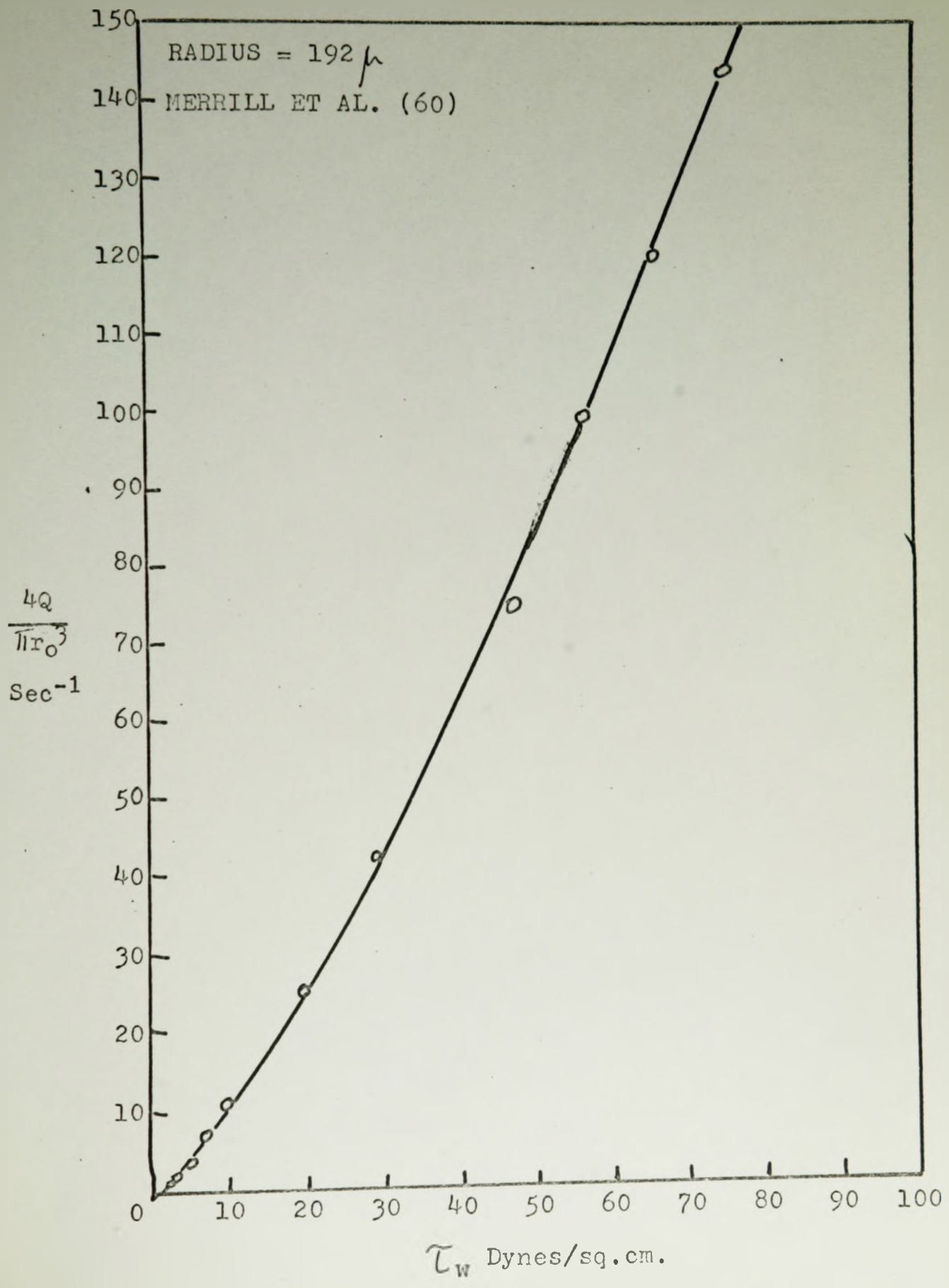

FIGURE 18: PSEUDO-SHEAR RATE VS. SHEAR STRESS

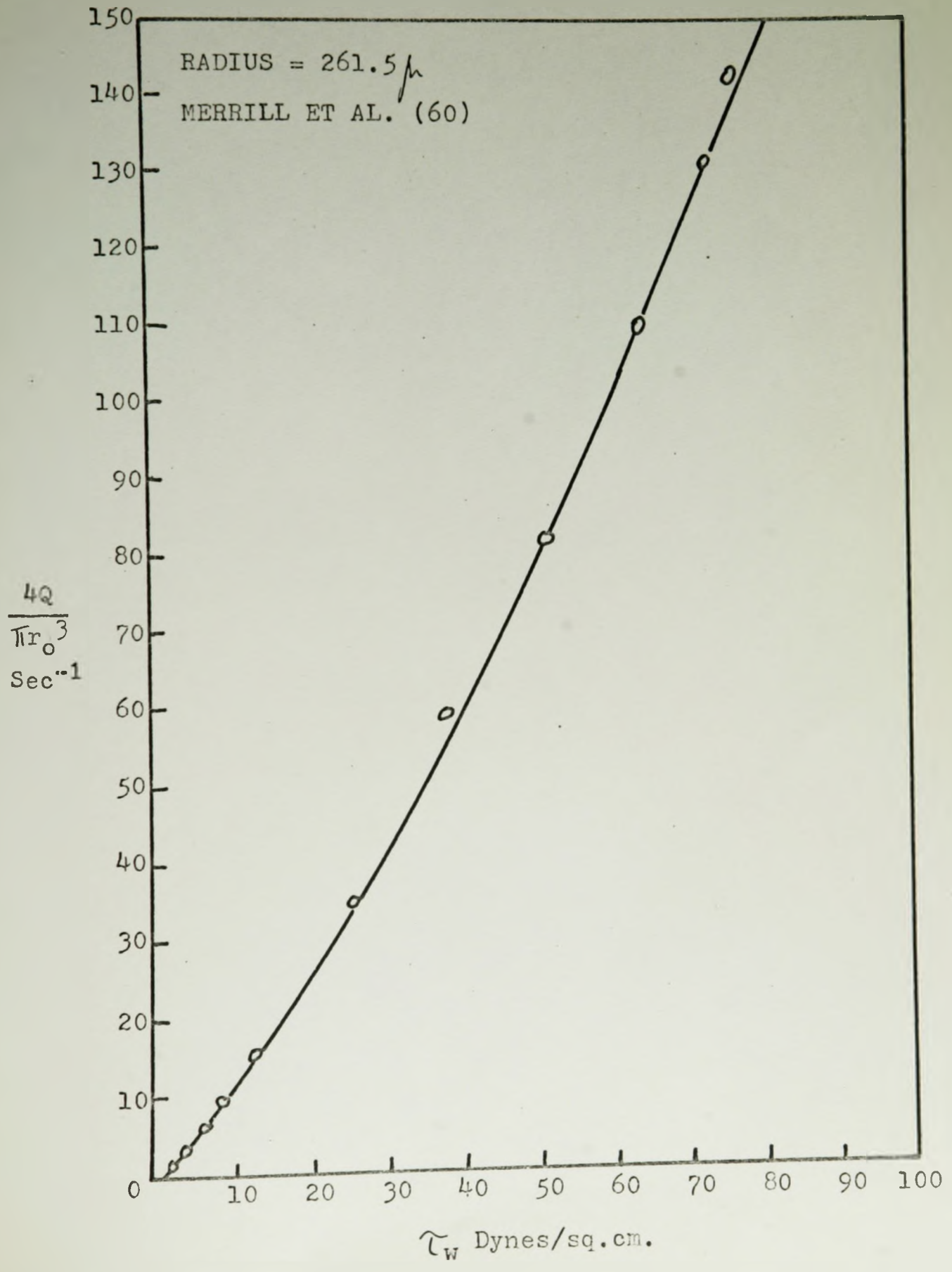

FIGURE 19: PSEUDO-SHEAR RATE VS. SHEAR STRESS

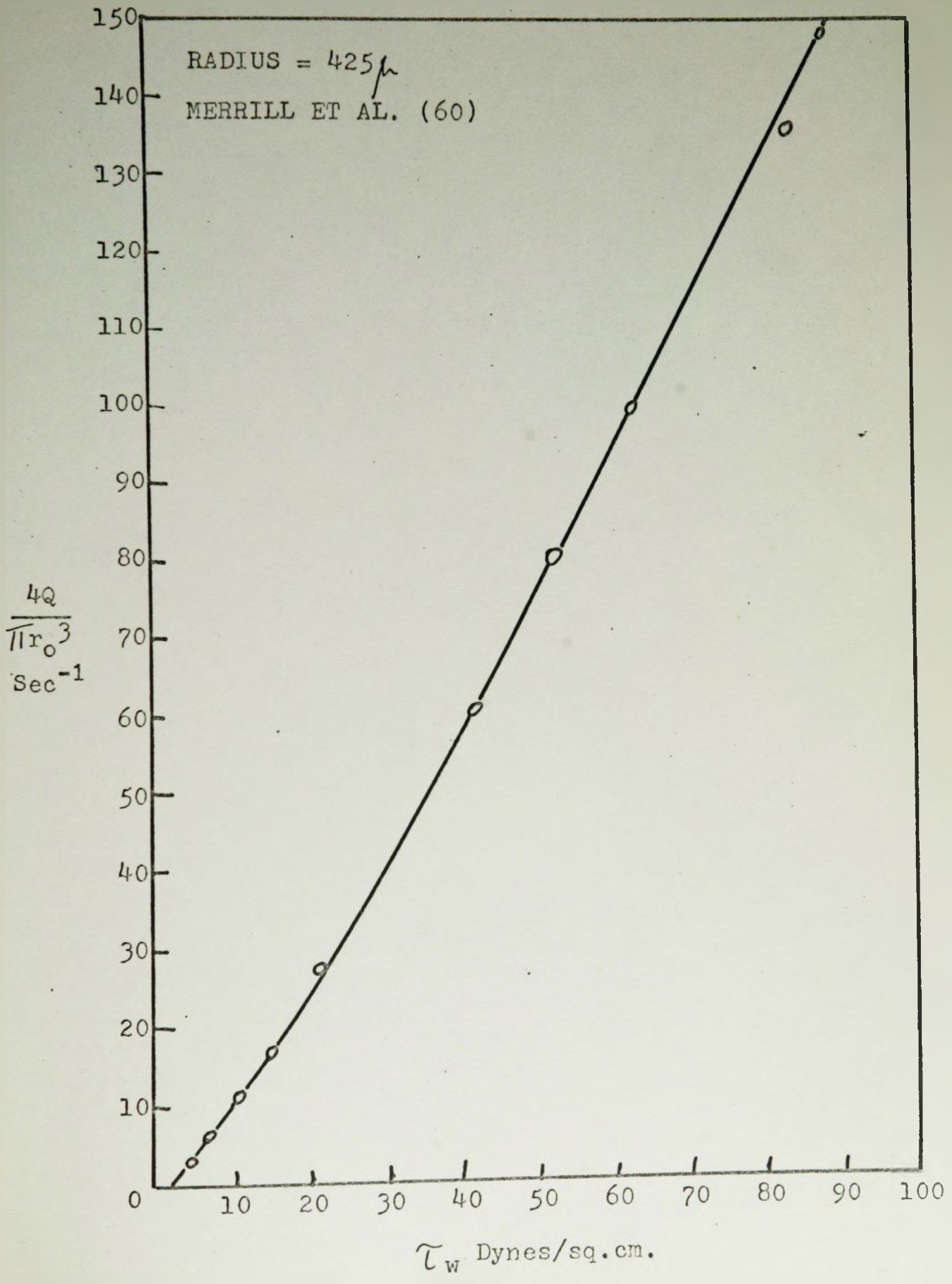

FIGURE 20: SHEAR RATE VS. SHEAR STRESS

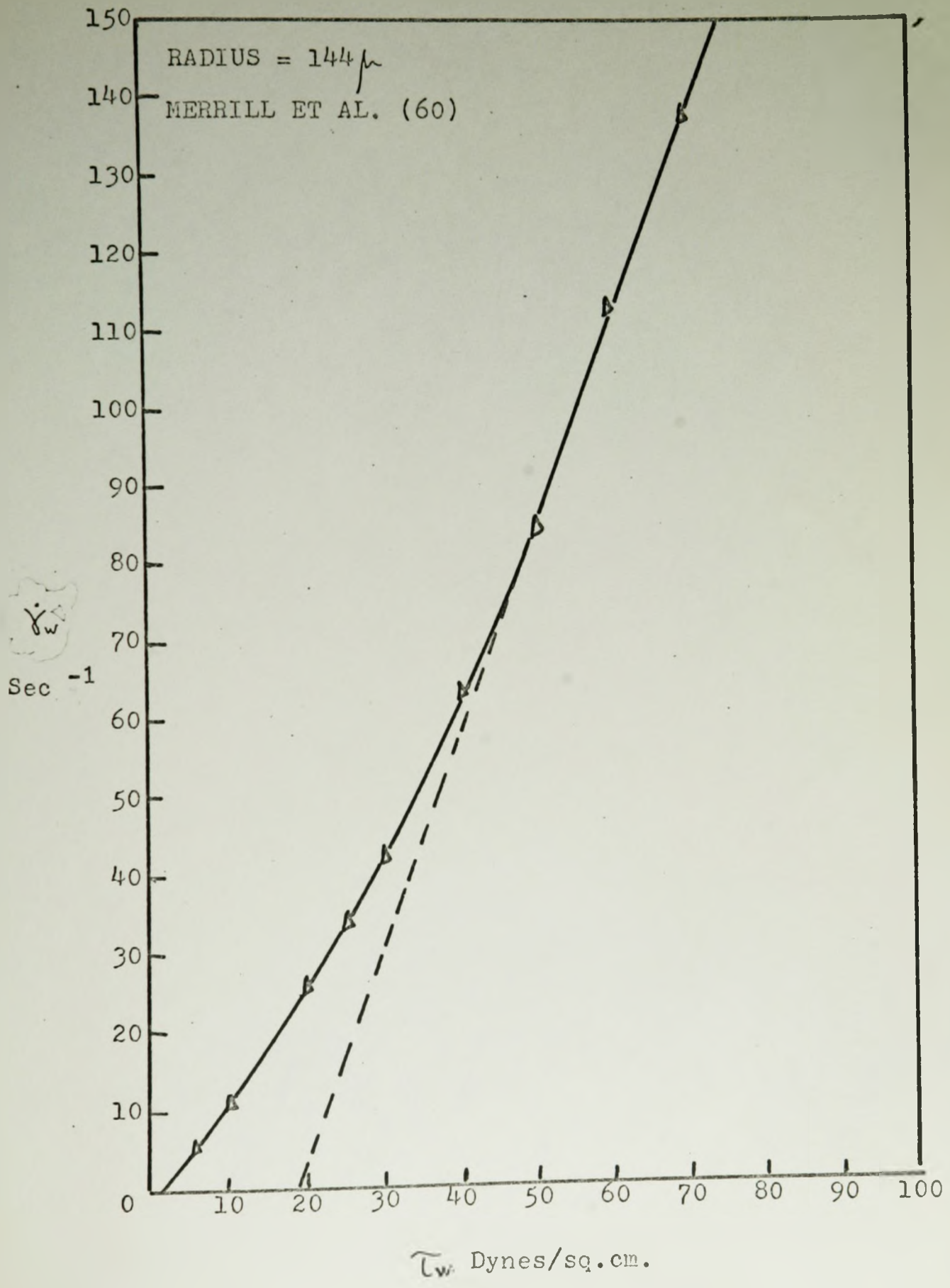

FIGURE 21: SHEAR RATE VS. SHEAR STRESS

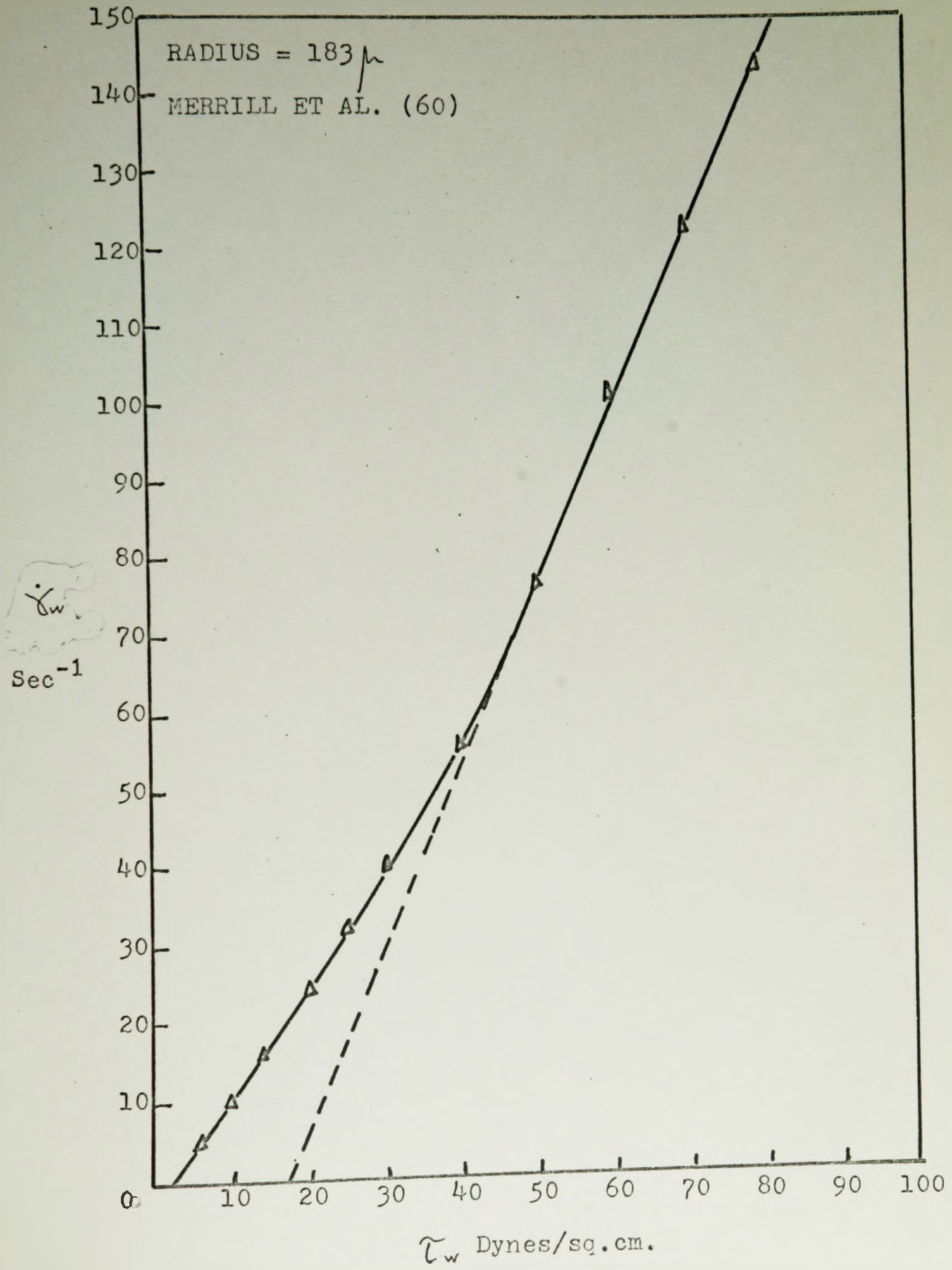

FIGURE 22: SHEAR RATE VS. SHEAR STRESS

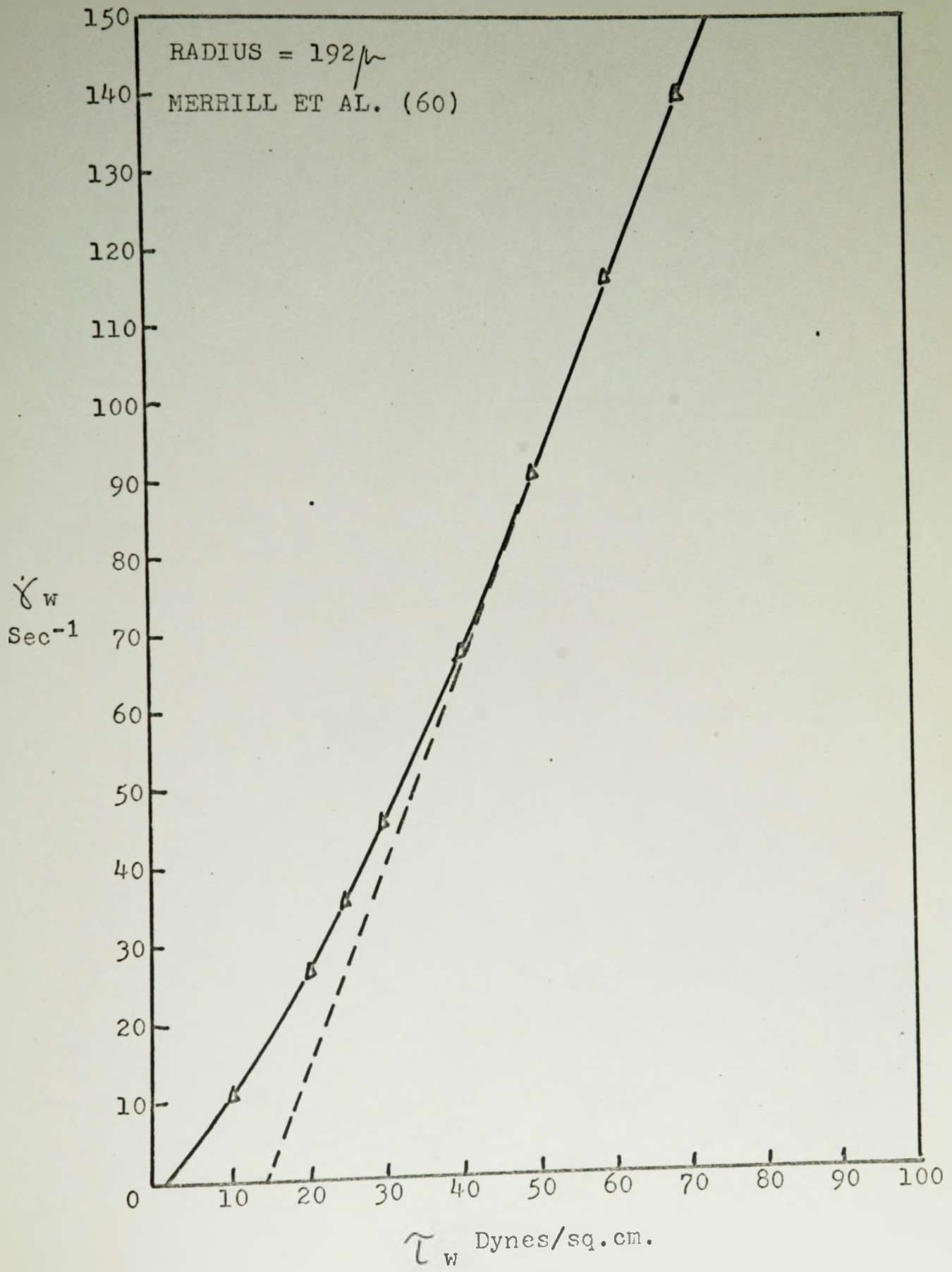

FIGURE 23: SHEAR RATE VS. SHEAR STRESS

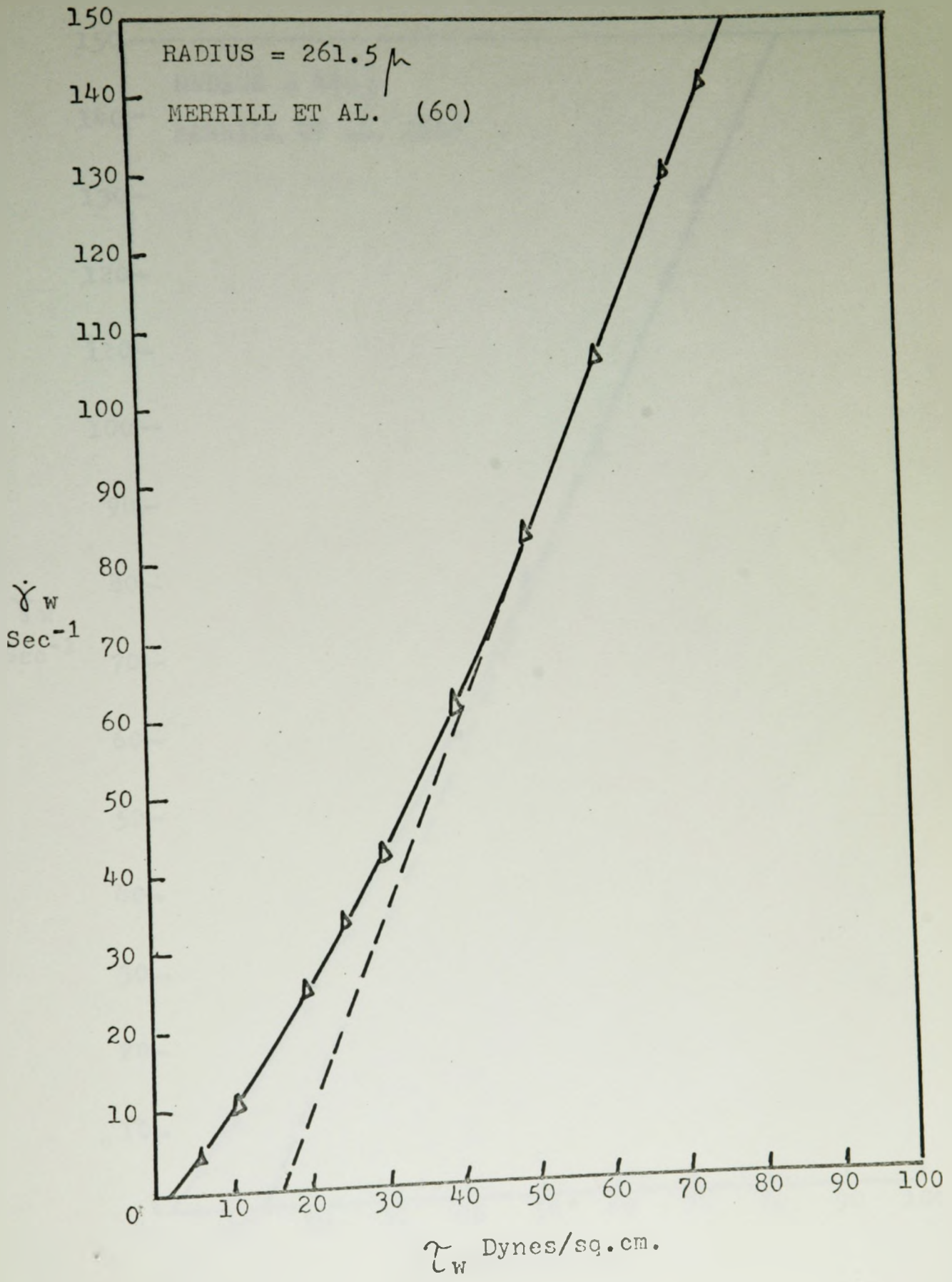

FIGURE 24: SHEAR RATE VS. SHEAR STRESS

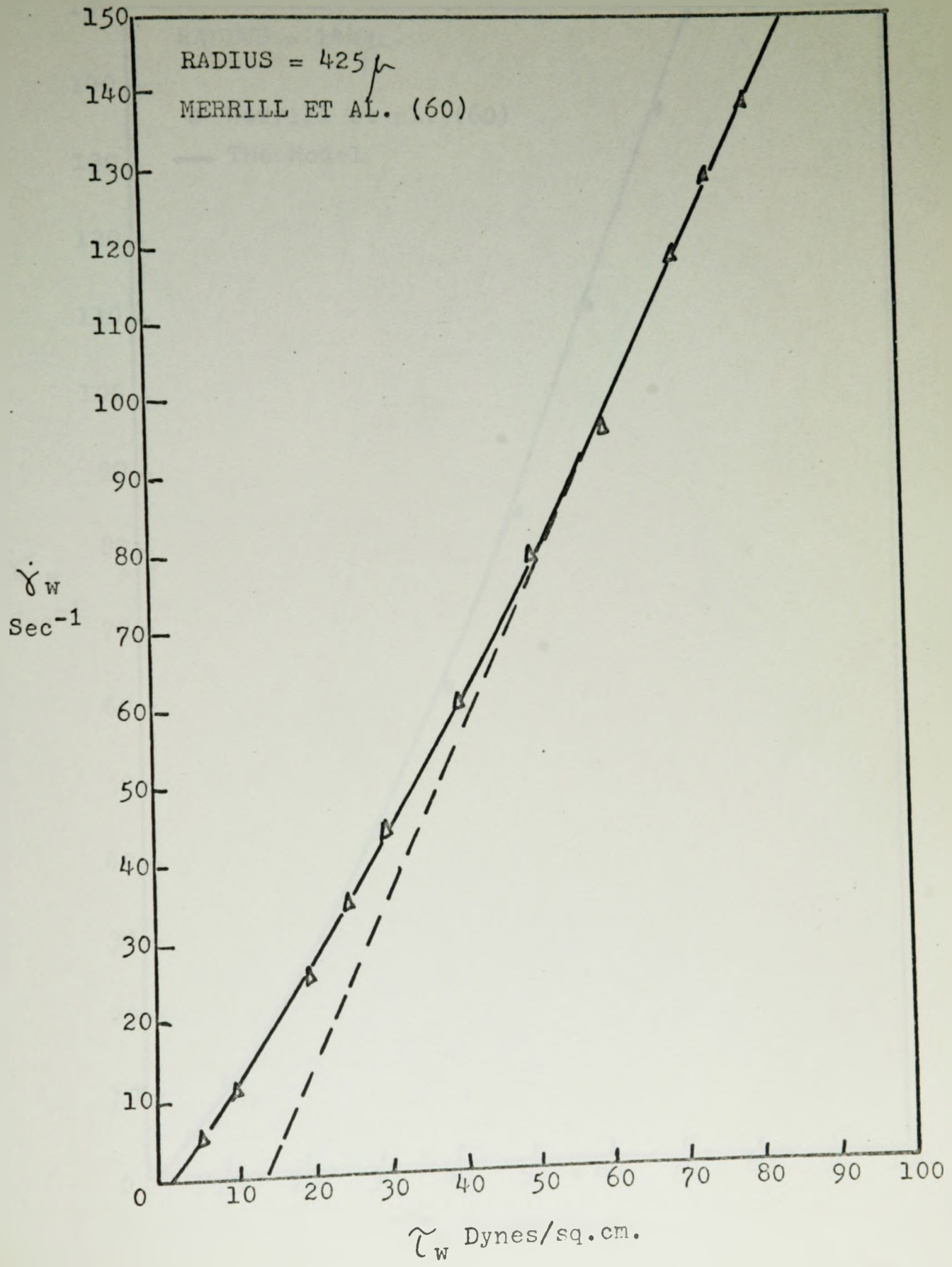

FIGURE 25: SHEAR RATE VS. SHEAR STRESS

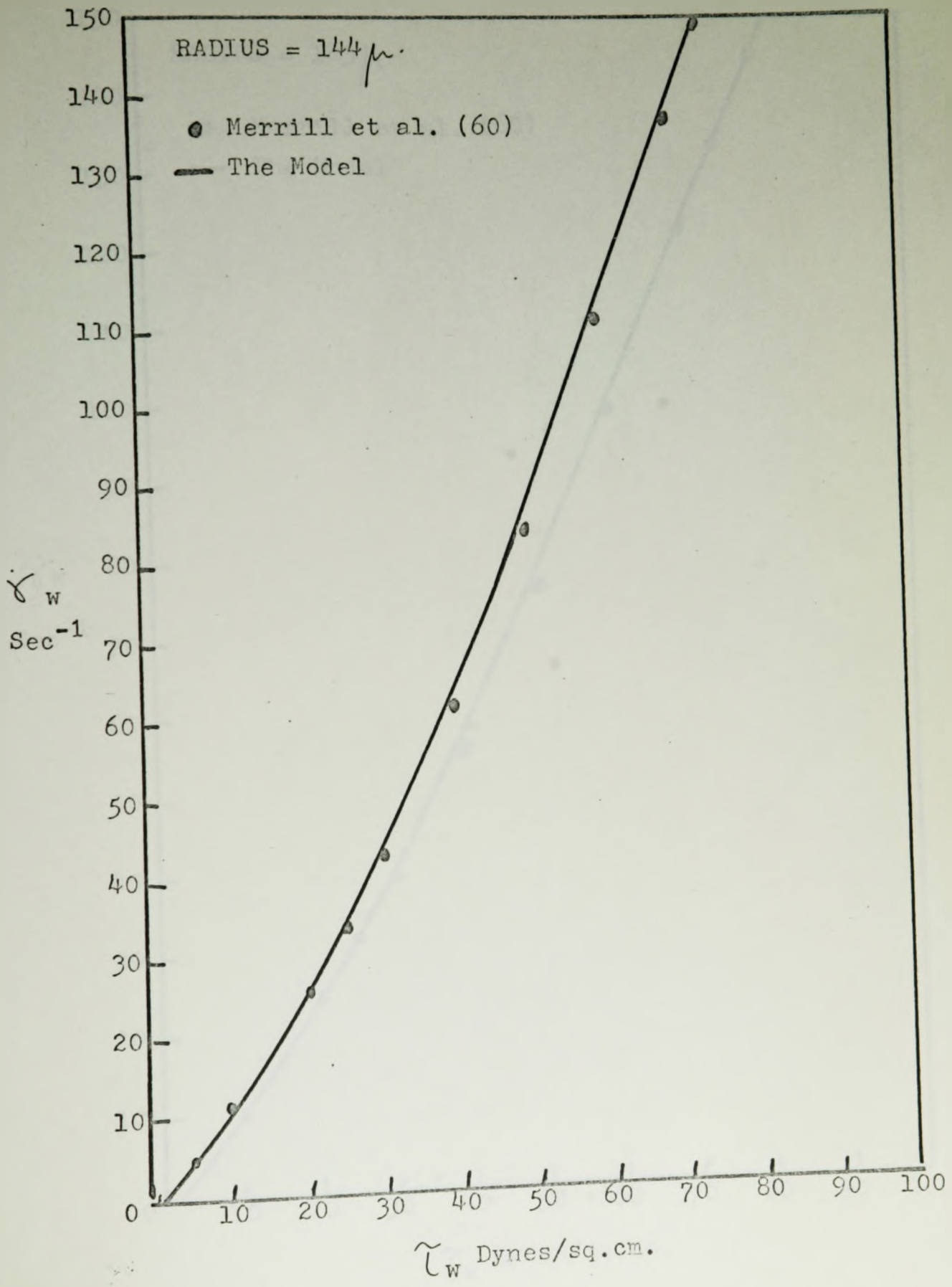

FIGURE 26: SHEAR RATE VS. SHEAR STRESS

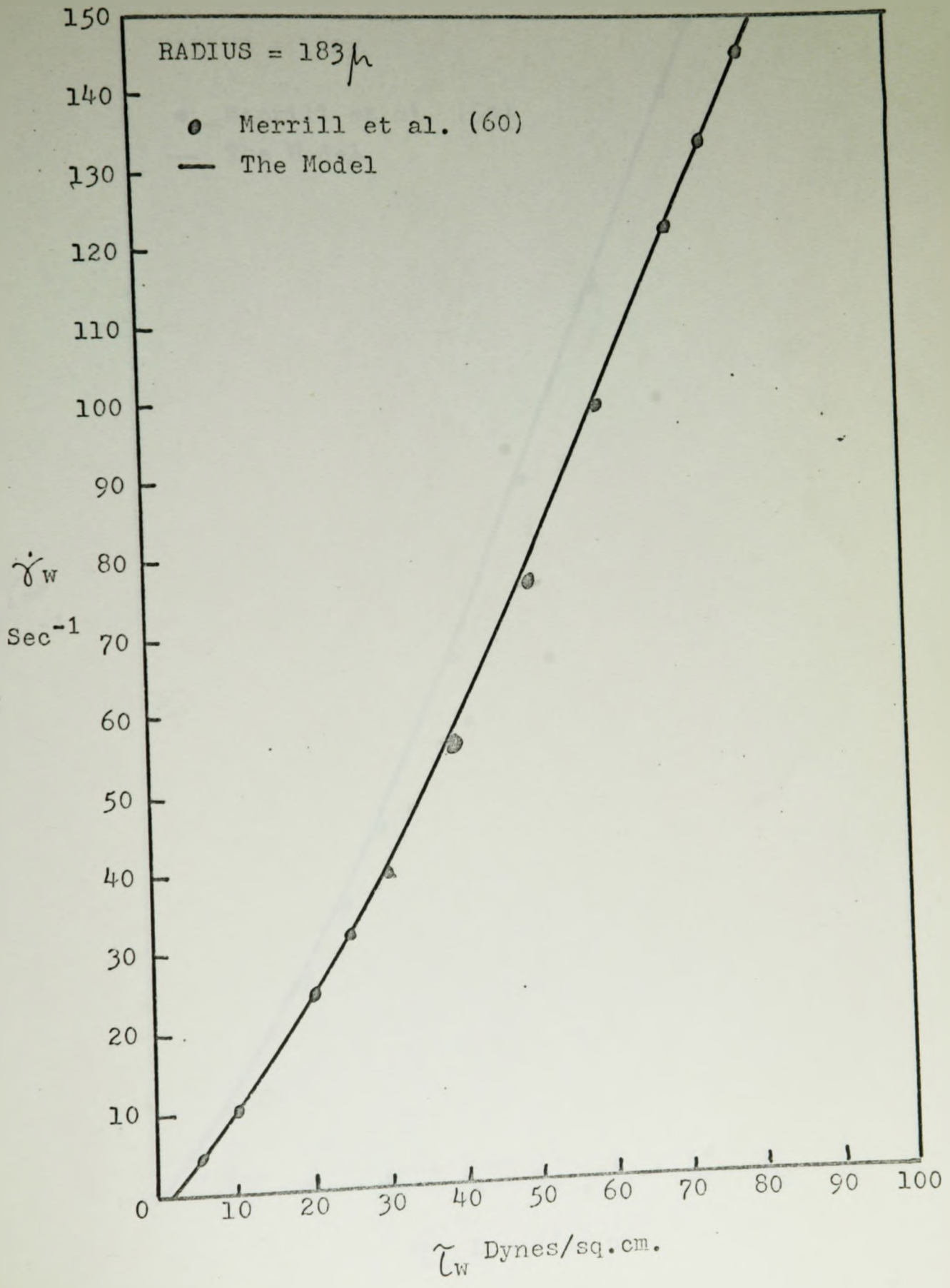

FIGURE 27: SHEAR RATE VS. SHEAR STRESS

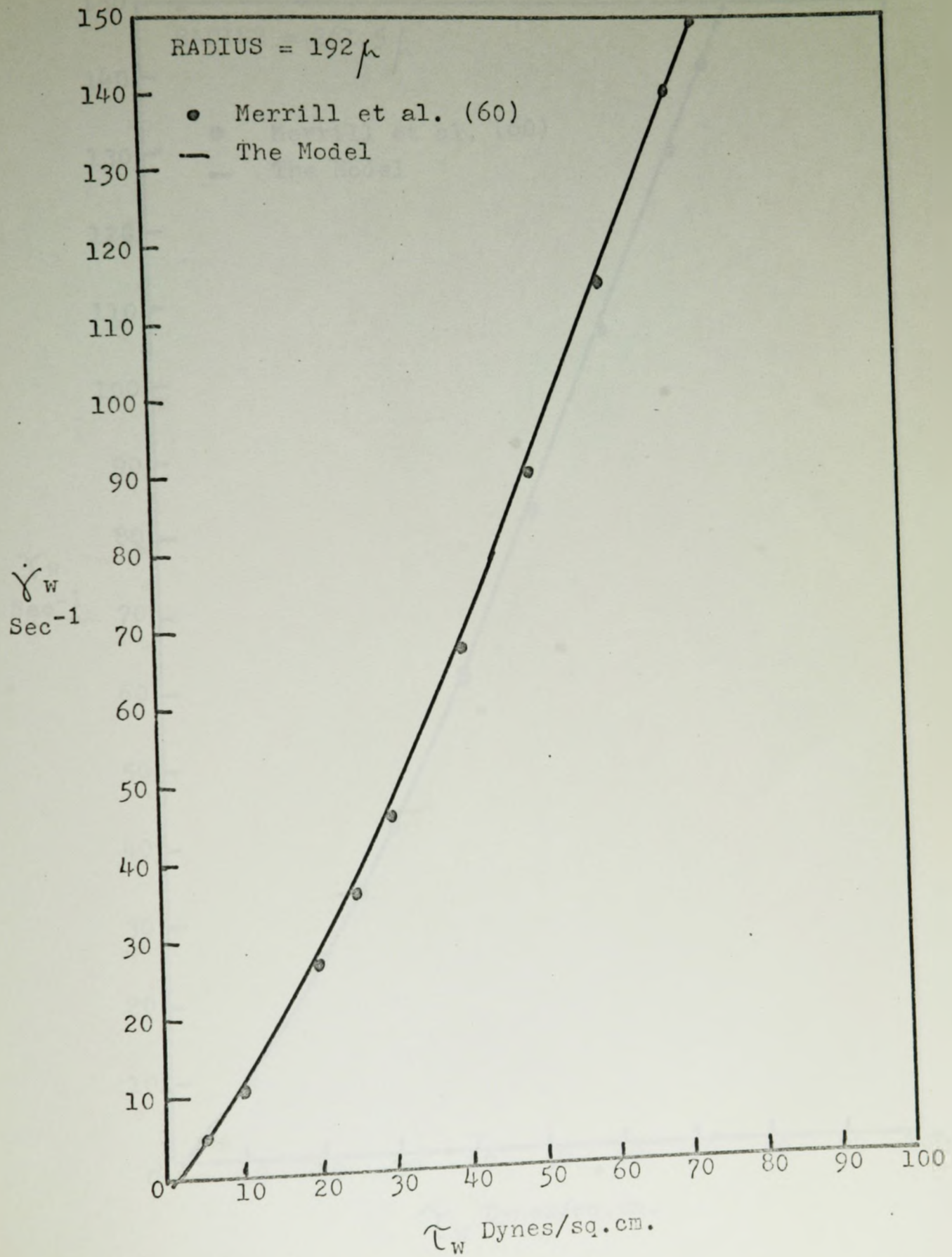

FIGURE 28: SHEAR RATE VS. SHEAR STRESS

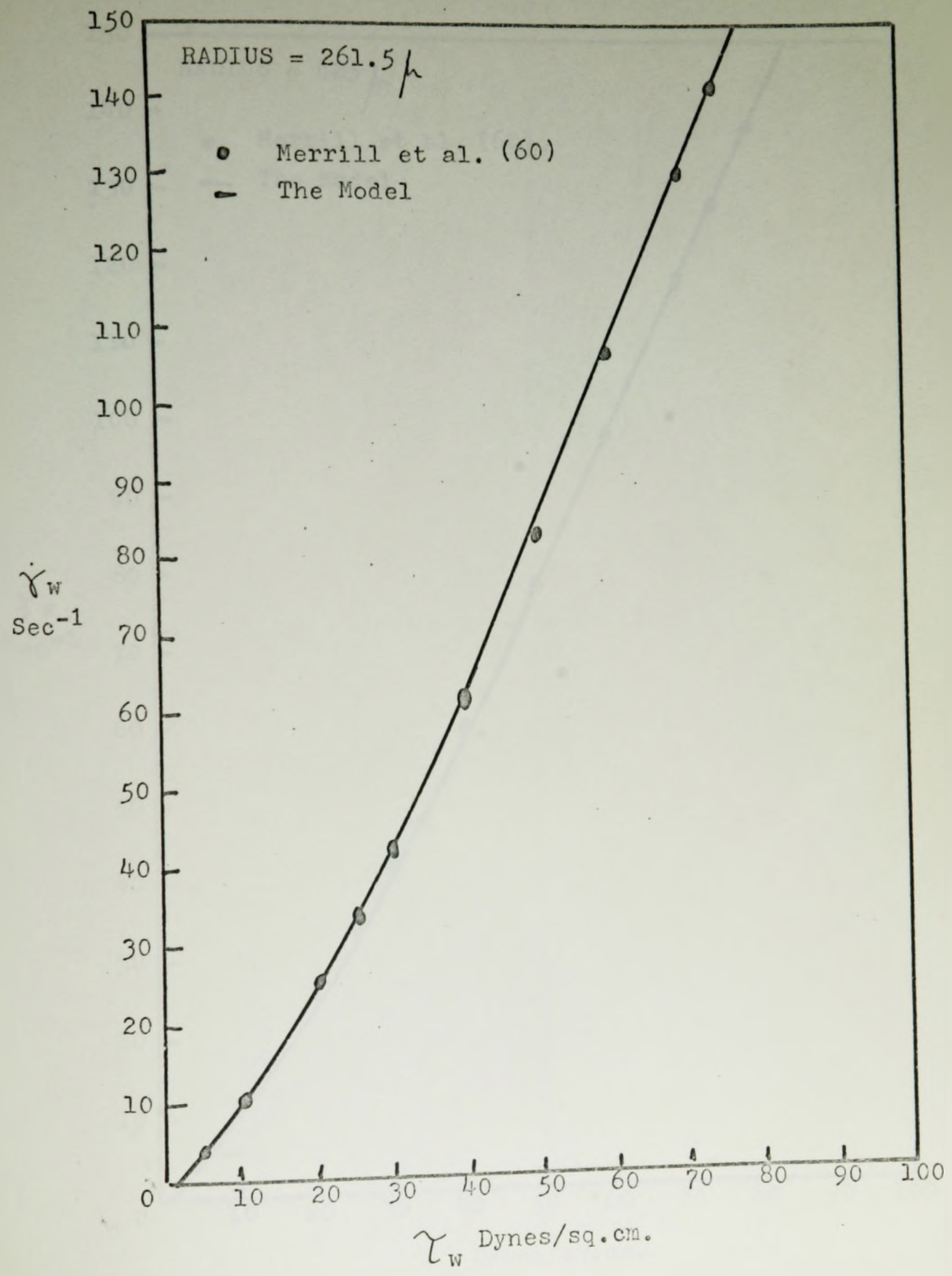

FIGURE 29: SHEAR RATE VS. SHEAR STRESS

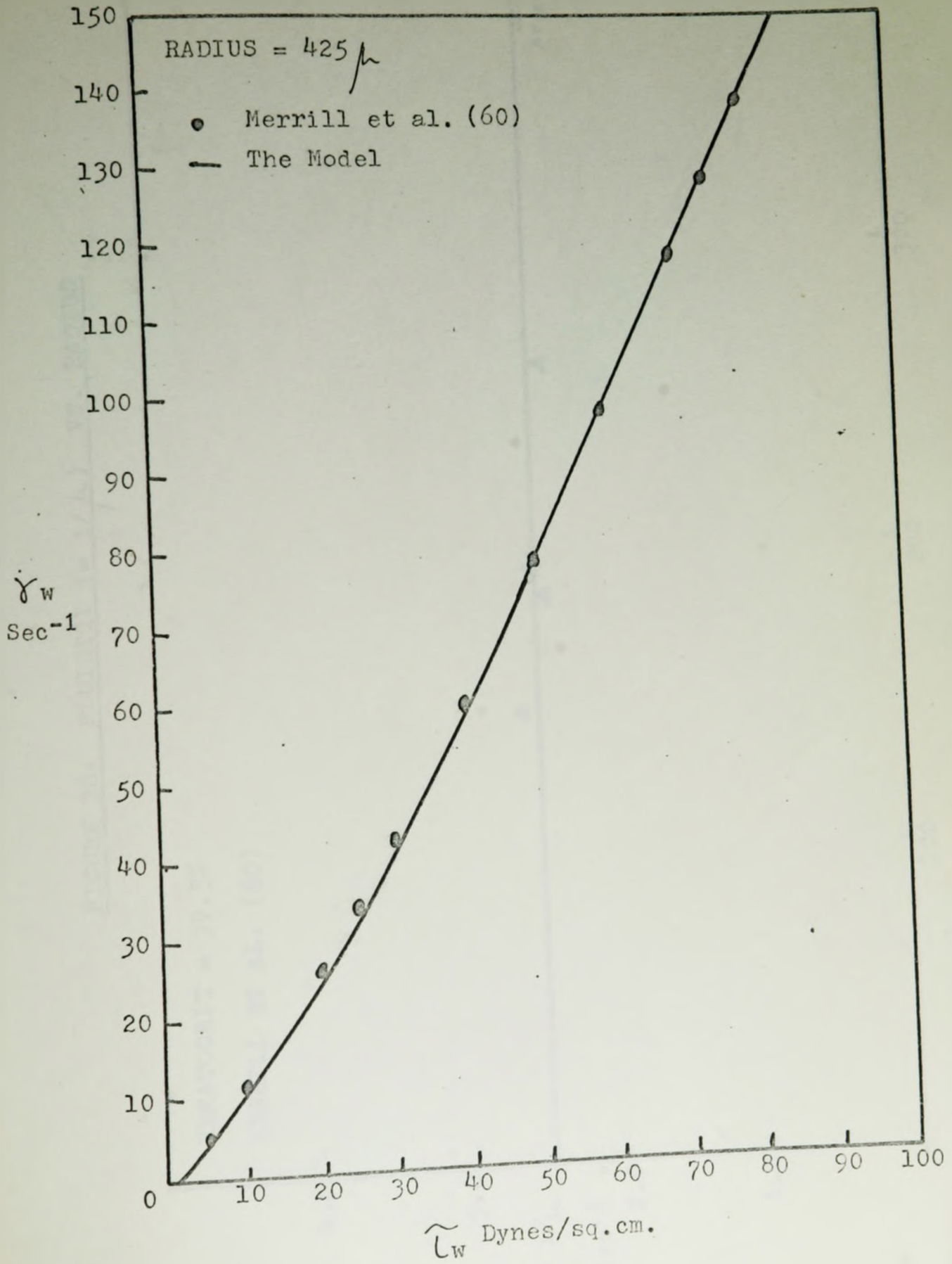

FIGURE 30: FLUIDITY (= $1/\mu$) VS. RADIUS

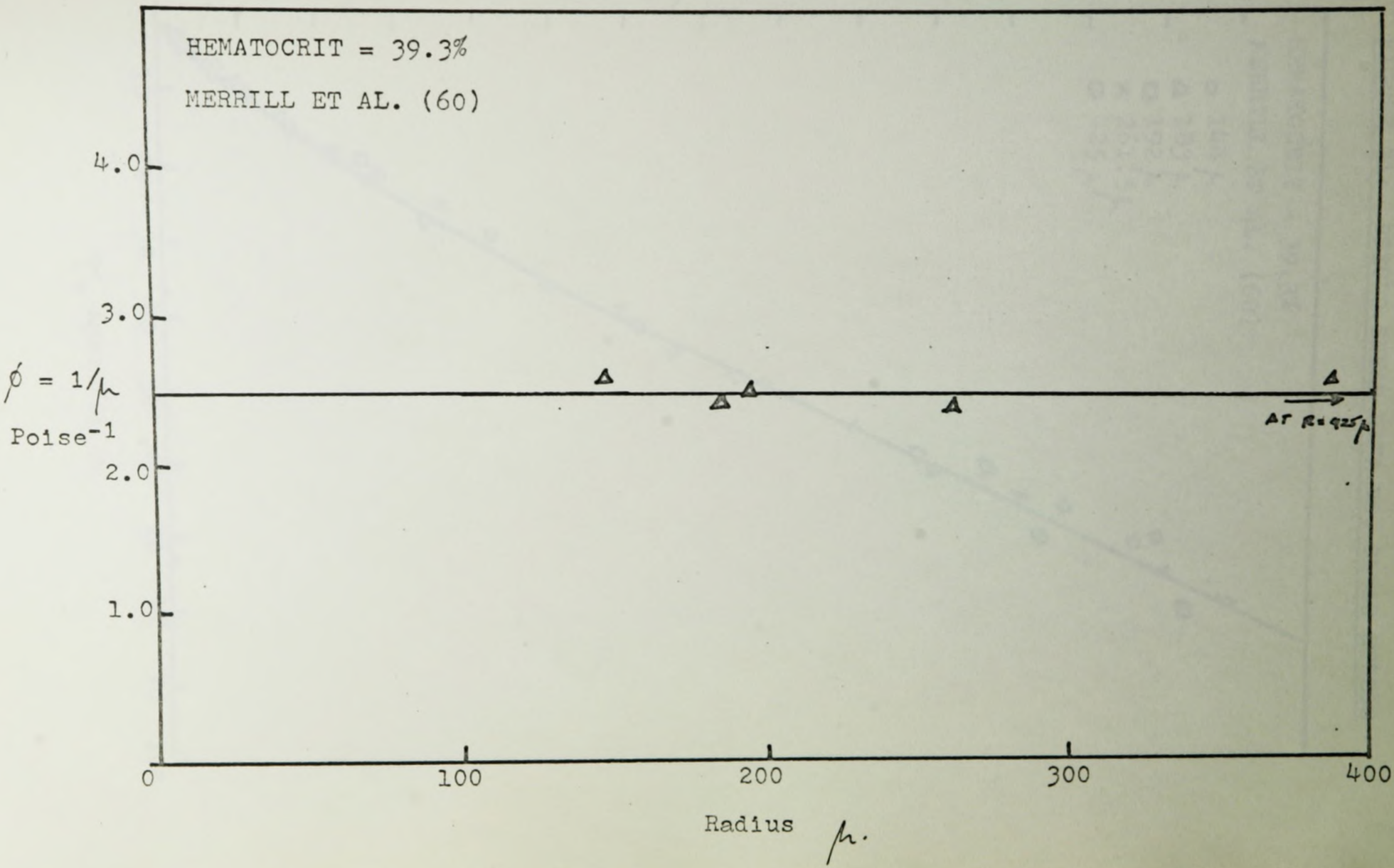

FIGURE 31: PSEUDO-SHEAR RATE VS. SHEAR STRESS

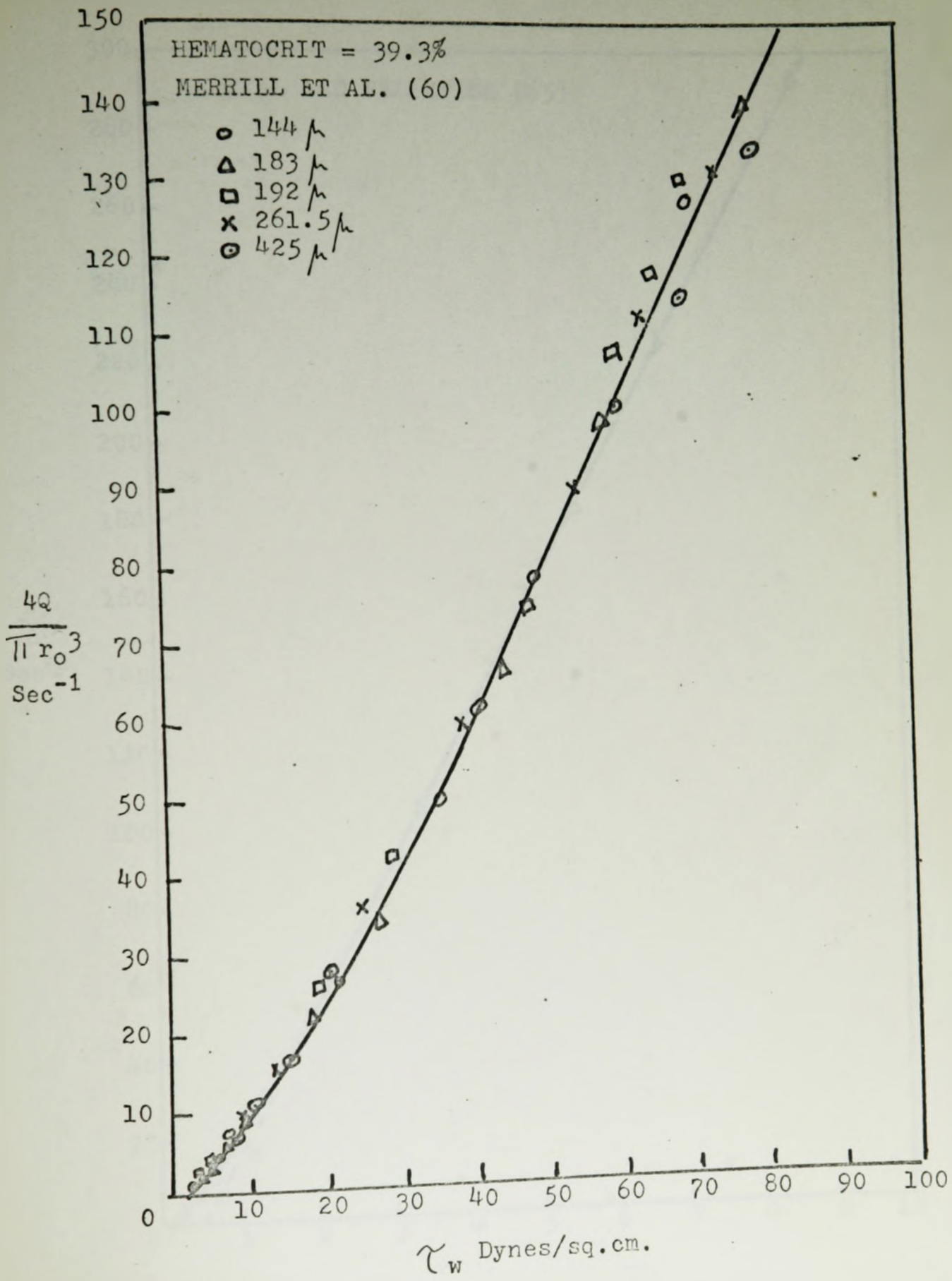

FIGURE 32: SHEAR RATE VS. SHEAR STRESS

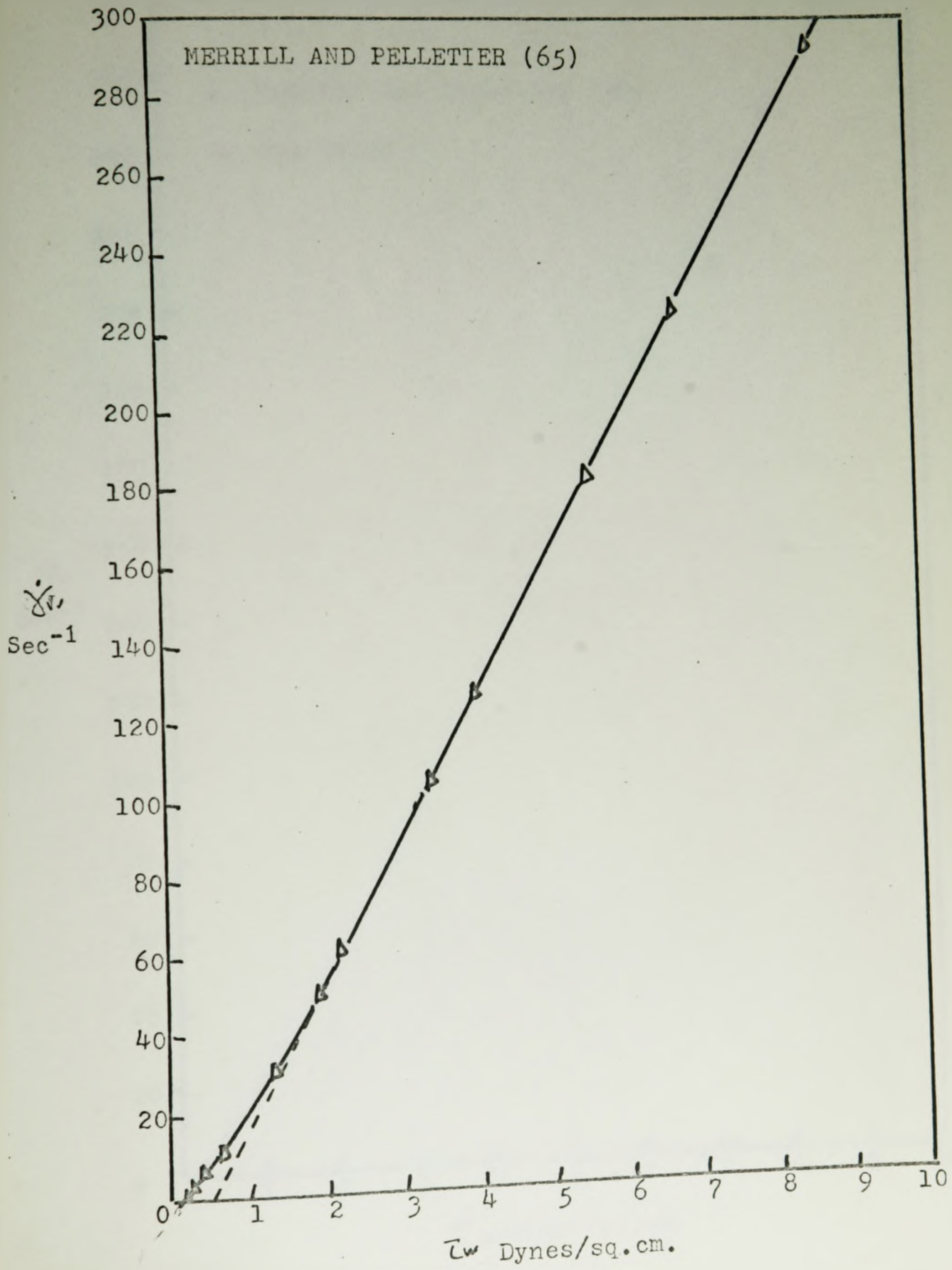

FIGURE 33: SHEAR RATE VS. SHEAR STRESS

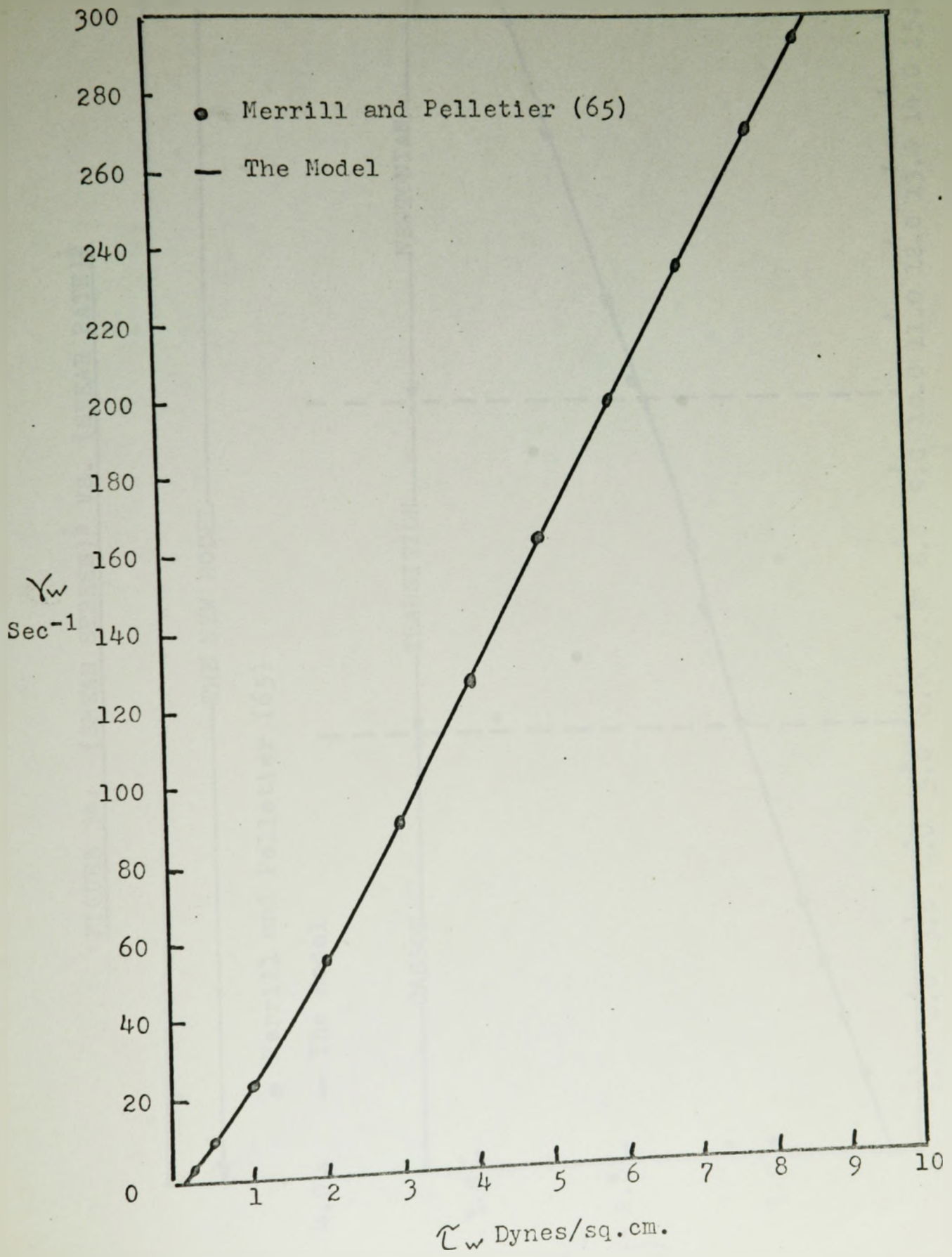

FIGURE 34: (SHEAR STRESS)$^{\frac{1}{2}}$ VS. (SHEAR RATE)$^{\frac{1}{2}}$

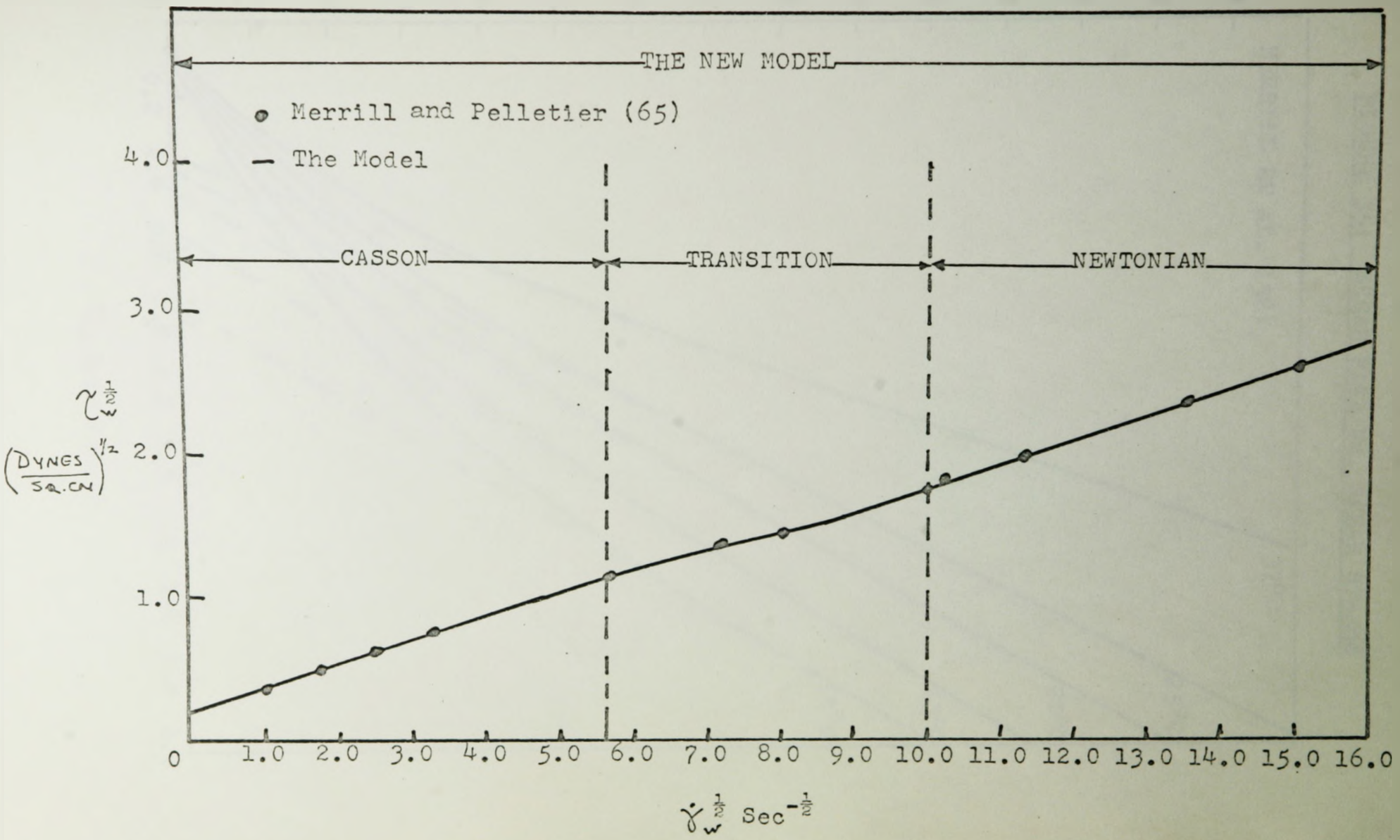

FIGURE 35: SHEAR RATE VS. SHEAR STRESS

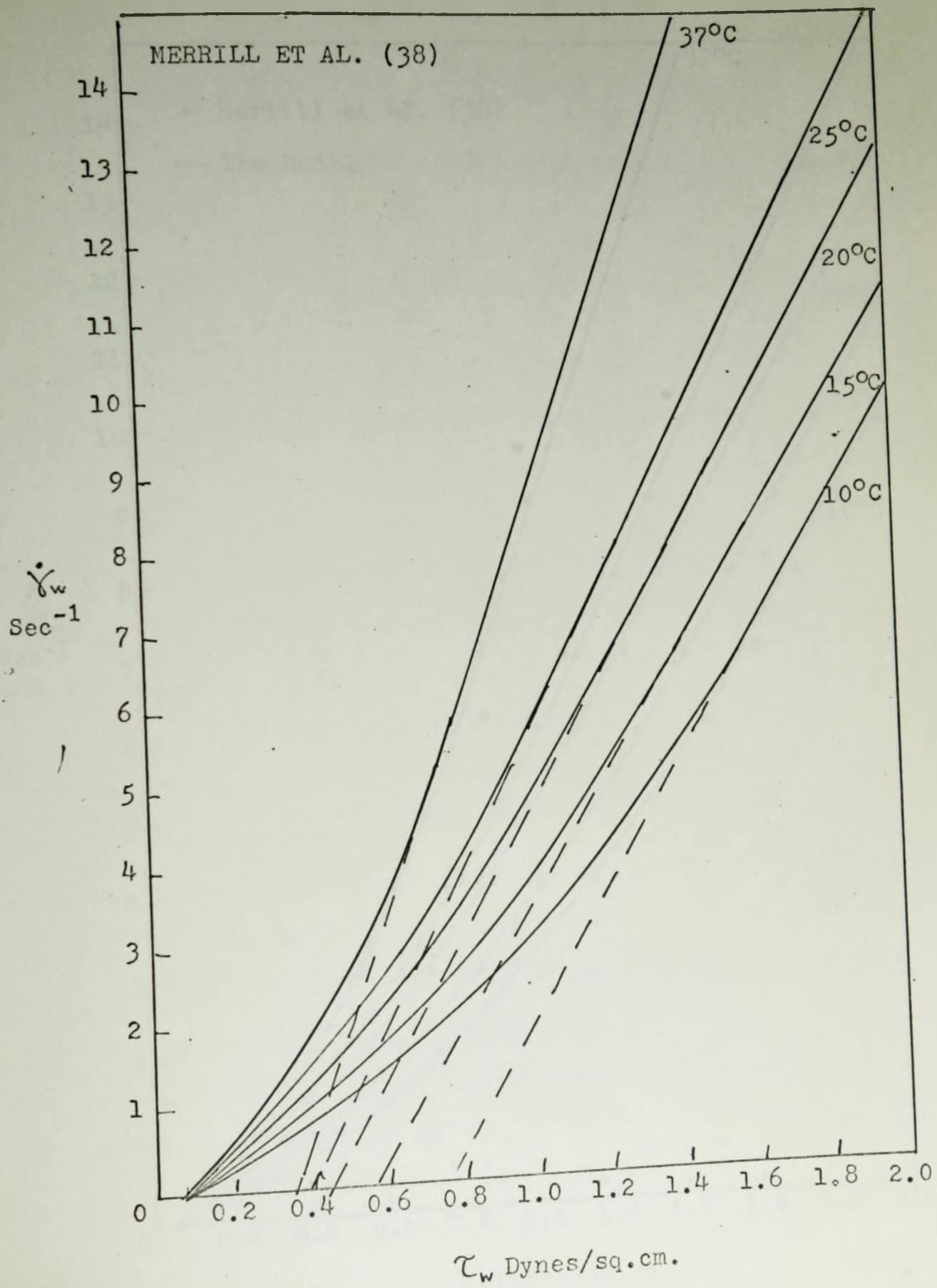

FIGURE 36: SHEAR RATE VS. SHEAR STRESS

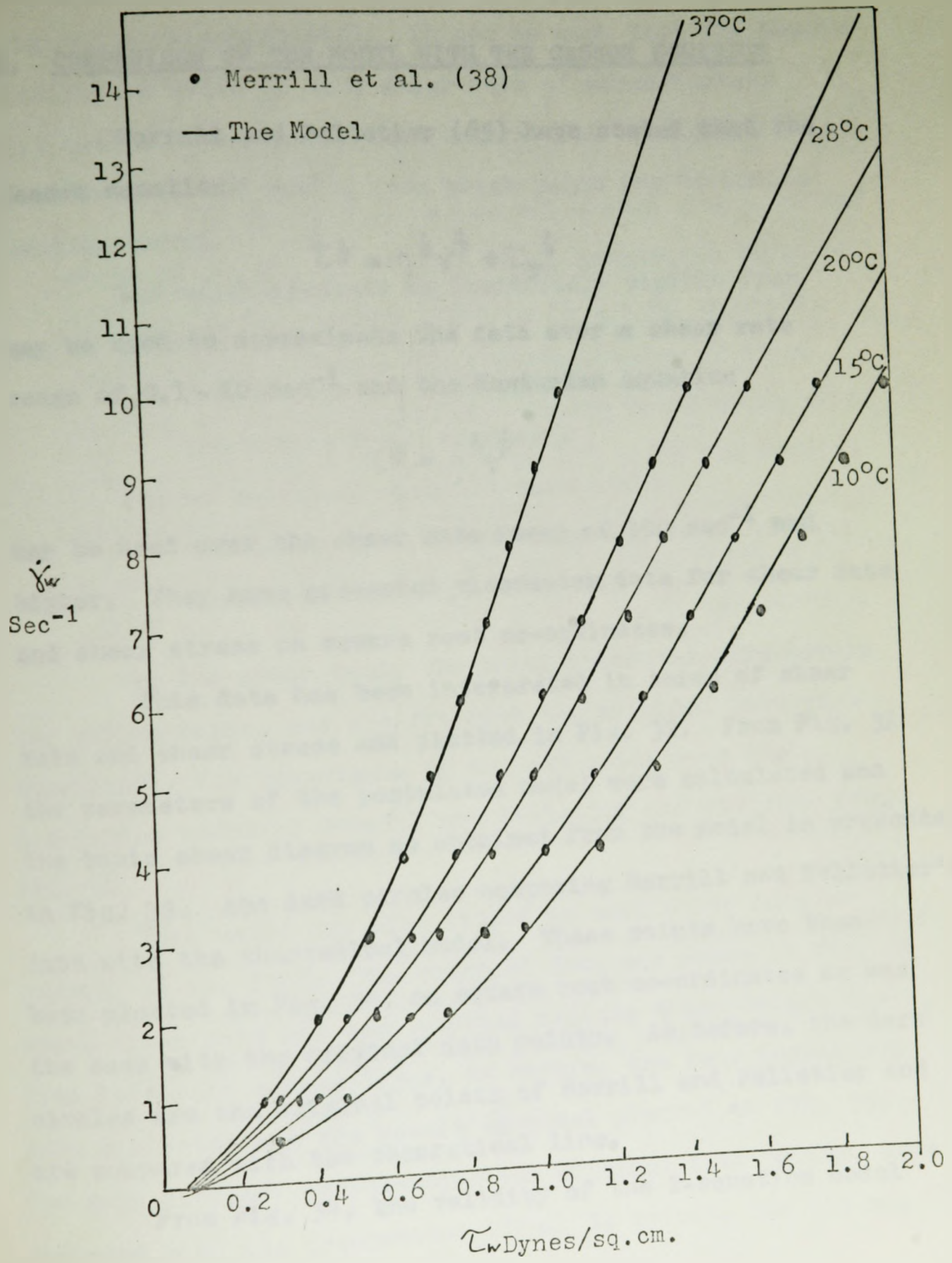

## 8. COMPARISON OF THE MODEL WITH THE CASSON EQUATION

Merrill and Pelletier (65) have stated that the Casson equation

$$\tau^{\frac{1}{2}} = \eta^{\frac{1}{2}}\dot{\gamma}^{\frac{1}{2}} + \tau_y^{\frac{1}{2}}$$

may be used to approximate the data over a shear rate range of 0.1 - 20 $sec^{-1}$ and the Newtonian equation

$$\tau^{\frac{1}{2}} = \eta^{\frac{1}{2}}\dot{\gamma}^{\frac{1}{2}}$$

may be used over the shear rate range of 100 $sec^{-1}$ and higher. They have presented viscometer data for shear rate and shear stress on square root co-ordinates.

This data has been interpreted in terms of shear rate and shear stress and plotted in Fig. 32. From Fig. 32 the parameters of the postulated model were calculated and the basic shear diagram as obtained from the model is presented in Fig. 33; the dark circles comparing Merrill and Pelletier's data with the theoretical model. These points have then been plotted in Fig. 34, on square root co-ordinates as was the case with the original data points. As before, the dark circles are the original points of Merrill and Pelletier and are compared with the theoretical line.

From Fig. 34, the validity of the 2-equation model

of Merrill and Pelletier has shown, as was done in the original publication (65). It can be seen that the Casson equation is valid up to a shear rate of approximately 31.5 $sec^{-1}$, a transition zone exists from that point to a shear rate of 100 $sec^{-1}$, from which point the Newtonian equation holds.

The major drawback is immediately visible from Fig. 34 in that

(a) 2 equations are necessary to cover the entire range as shown,

(b) no empirical equation covers the transition zone between the non-Newtonian and Newtonian behaviour of blood.

On the other hand, the model presented here covers the entire range, and the fit with the original data is excellent. The advantages of the new model over the 2-equation model of Merrill and Pelletier are obvious, from Fig. 34.

This model was also fitted to some other data of Merrill et al. (38). The original data are shown in Fig. 35 where shear rate has been plotted against shear stress for five different temperatures. As before, the four parameters were evaluated and the resulting model plotted in Fig. 36. The dark circles, representing the original data points, were compared with the theoretical line. As before, the fit was confirmed to be very good.

## 9. CONCLUSION

(i) $$\dot{\gamma} = \frac{1}{\mu}\left[(\tau - \tau_y) - (\tau_{yap} - \tau_y)\left[1 - \exp\left\{-A(\tau - \tau_y)\right\}\right]\right]$$

The model shown above was tested over a radius range of 57.04$\mu$ to 747.4$\mu$ and a hematocrit range of 8.8% to 82.5%. It was found to be a very accurate representation of the basic shear diagram of blood flowing through capillaries. It was found to be valid over a shear rate range of 0 to 900 $sec^{-1}$ and because of the Newtonian (straight line) behaviour of blood at shear rates greater than 100 $sec^{-1}$, this model would be valid up to any shear rates of 100 $sec^{-1}$ and greater.

The model was also shown to have a decided advantage over the 2-equation one proposed by Merrill and Pelletier.

(ii) Work on the data of Merrill et al. showed that their assumption of no slip at the wall was valid up to a hematocrit level of 39.3%. Data at a higher hematocrit level was not available, hence no statement can be made about the validity of this assumption at hematocrits higher than 39.3%.

## 10. NOMENCLATURE

| | | |
|---|---|---|
| $A$ | = a constant which characterizes the rate of approach to unity | |
| $C$ | = a constant - intercept on the negative $\tau_w$ axis | |
| $Q$ | = volume flow rate | cc./sec. |
| $dp/dz$ | = pressure drop across the length of the capillary | cms. $H_2O$/cm. tube |
| $r_o$ | = radius of the capillary | micra |
| $V_s$ | = slip velocity at the wall | cms./sec. |
| $V_z$ | = velocity of flow in the z direction | cms./sec. |
| $(-dV_z/dr)$ | = shear rate | $sec^{-1}$ |
| $\dot{\gamma}$ | = shear rate | $sec^{-1}$ |
| $\gamma_w$ | = shear rate at the wall | $sec^{-1}$ |
| $\delta_{ij}$ | = Kronecker Delta | |
| $\mu$ | = asymptotic viscosity of non-Newtonian fluid | poise |
| $\mu_a$ | = apparent viscosity of Newtonian fluid | poise |
| $\mu_{ap}$ | = apparent viscosity of non-Newtonian fluid | poise |
| $\xi$ | = Oldroyd's parameter | |
| $\sigma_{ij}$ | = stress tensor | dynes/sq.cm. |
| $\tau_y$ | = yield stress | dynes/sq.cm. |

| | | |
|---|---|---|
| $\tau_{yap}$ | = apparent yield stress, i.e., the yield stress blood would exhibit if it behaved as an ideal Bingham plastic. | dynes/sq.cm. |
| $\tau_{ij}$ | = stress tensor | dynes/sq.cm. |
| $\tau_w$ | = shear stress at the wall | dynes/sq.cm. |
| $\phi$ | = Oldroyd's parameter | |
| $\phi$ | = fluidity | $poise^{-1}$ |

## REFERENCES


1. B.W. ZWEIFACH. Functional Behaviour of Microcirculation. Charles C. Thomas, Springfield, Illinois, 1961.
2. E.H. BLOCH. The American Journal of Anatomy. 110. 125-153 (1962).
3. N.L. HOERR. Medical Physics. 1. 127-134, Otto Glasser ed., Year Book Medical Publishers, Chicago, 1944.
4. R.H. HAYNES. Trans. Soc. Rheol. 5. 85-101 (1961).
5. T.A.J. PRANKERD. The Red Cell. Blackwell, Oxford, 1961.
6. E.W. MERRILL, G.C. COKELET, A. BRITTEN and R.E. WELLS JR. Circulation Research. 13. 48-55 (1963).
7. G.C. COKELET. D.Sc. Thesis. M.I.T., January, 1963.
8. A.M. BENIS. D.Sc. Thesis. M.I.T., May, 1964.
9. R.E. WELLS, R. DENTON, E.W. MERRILL. J. Lab. Clin. Med. 57. 646, 1961.
10. R.E. WELLS, E.W. MERRILL. Appl. Mech. Rev. 149. 1961.
11. L.C. CHINEY, F.B. COOK, C.C. WALKER. Amer. J. Physiol. 202. 1188, 1962.
12. A.L. COPLEY. Flow Properties of Blood and Other Biological Systems. Copley and Stainsby (editors), Pergamon Press, London, 1960.
13. S. CHARM and G.S. KURLAND. Amer. J. Physiol. 203. 417, 1962.
14. J.T. BRUNDAGE. Amer. J. Phsyiol. 110. 657, 1934-5.

15. E.C. BINGHAM and R.R. POEPKE. J. Gen. Physiol. 28. 79, 1944.

16. F. KREUZER. Helv. Physiol. Acta. 8. 486, 1950.

17. L.E. BAYLISS. Deformation and Flow in Biological Systems. A. Frey-Wyssling (editor), North-Holland, Amsterdam, 1952.

18. G. SCOTT BLAIR. Rheologica Acta. 1. 123, 1958.

19. R.H. HAYNES. Blood Vessels and Lymphatics. (D.I. Abramson, ed.), Academic Press, New York, 1962, p. 26

20. G.R. COKELET, E.W. MERRILL, E.R. GILLILAND, H.E. SHIN, A. BRITTEN, R.E. WELLS, Society of Rheology Conference. Baltimore, U.S.A., 1962.

21. A. MULLER. Helv. Physiol. Acta. 6. 181, 1948.

22. L.E. BAYLISS. Flow Properties of Blood and Other Biological Systems. Copley and Stainsby (editors), Pergamon Press, London, 1960.

22a. N.A. COULTER JR. and J.R. PAPPENHEIMER. Amer. J. Physiol. 159. 401, 1949.

23. R.H. HAYNES and A.C. BURTON. Amer. J. Physiol. 197. 943, 1959.

24. R. FARHAEUS and T. LINDQVIST. Amer. J. Physiol. 96. 562, (1931).

25. M.G. TAYLOR. Australian J. Exper. Biol. & M. Sc. 33. 1, 1955.

26. R.H. HAYNES and A.C. BURTON. In: Proceedings of the First National Biophysics Conference. New Haven, Yale Univ. Press, 1959, p.452.

27. R.H. HAYNES. Amer. J. Physiol. 198(6). 1193-1200, 1960.

28. K. KUMIN. Inaugural Dissertation. Bern, 1948.

29. E.W. MERRILL, E.R. GILLILAND, G. COKELET, H. SHIN, A. BRITTEN, and R.E. WELLS JR. J. Appl. Physiol. 18. 255, (1963).

30. A.D. MAUDE and R.L. WHITMORE. J. Appl. Physiol. 12. 105, 1958.

31. R. FARHAEUS. Acta Med. Scand. 161. 151, 1958.

32. J.J. HERMANS. Flow Properties of Disperse Systems. North-Holland, Amsterdam, 1953.

33. R.ST.J. MANLEY and S.G. MASON. J. Colloid Sci. 7. 354, 1952.

34. H.L. GOLDSMITH and S.G. MASON. J. Fluid Mech. 12. 88, 1962.

35. F. EIRICH and J. SVERAK. J. Proc. Faraday Soc. B42. 57, 1946.

36. R.L. WHITMORE. J. Inst. Fuel. 30. 238, 1957.

37. E.G. RICHARDSON. Dynamics of Real Fluids. London, Arnold, 1950, p.119.

38. E.W. MERRILL, E.R. GILLILAND, G. COKELEY, H. SHIN, A. BRITTEN, and R.E. WELLS JR. Bioph. J. 3, 199, 1963.

39. F.H. NORTON, A.L. JOHNSON, and W.G. LAWRENCE, Fundamental Study of Clay: VI Flow Properties of Kaolinite-Water Suspension, J. Amer. Ceram. Soc. 27. 149, 1944.

40. H. GREEN and R. WELTMANN. J. Appl. Physics. 14, 569, 1943.

41. J.W. IRWIN, W.S. BARRAGE, C.E. AIMAR, R.W. CHESTNUT JR. Anat. Rec. 119, 391, 1954.

42. J. PROTHERO and A.C. BURTON. Biophys. J. 1, 565, 1961.

43. J.H. COMROE, R.E. FORRESTER, A.B. DUBOIS, W.A. BRISCOE and E. CARLSEN. The Lung. Chicago, The Year Book Publishers, 1955, Ch. 5, p.86.

44. F.J.W. ROUGHTON and R.E. FORRESTER. J. Appl. Physiol. 11, 290, 1957.

45. S.G. MASON and F.D. RUMSCHEIDT. Pulp & Paper Research Inst. of Can. Technical Report, 177, 1960.

46. J. PROTHERO and A.C. BURTON. Biophys. J. 2, 213, 1962.

47. P.I. BRANEMARK and J. LINDSTROM. Biorheology. 1, 139, 1963.

48. M.M. GUEST, T.P. BOND, R.G. COOPER and J.R. DERRICK. Science. 142. 1319, 1963.

49. E.H. BLOCH. Am. J. Anat. 110, 125, 1962.

50. H.L. GOLDSMITH and S.G. MASON. J. Colloid Sci. 18, 237, 1963.

51. H.L. GOLDSMITH. Federation Proc. 26, 1813, 1967.

52. H.L. GOLDSMITH. Science. 153, 1406, 1966.

53. I.Y. ZIA, R.G. COX, S.G. MASON. Science. 153, 1405, 1966

54. R.P. RAND and A.C. BURTON. Biophys. J. 4, 115, 1964.

55. R.P. RAND. Biophys. J. 4, 304, 1964.

56. H.H. KNISELY, E.H. BLOCH, T.S. ELIOT, and L. WARNER. Trans. Am. Ther. Soc. 48, 95, 1950.

57. A.L. COPELY and P.H. STAPLE. Biorheology. 1, 3, 1962.

58. E.H. BLOCH. Anat. Rec. 115. 283, 1953.

59. G. BUGLIARELLO, C. KAPUR, G. HSIAO. Proc. Intern. Congr. Rheol. 4th PROVIDENCE, R.I., Interscience Publishers, Inc. New York, 351, 1965.

60. E.W. MERRILL, A.M. BENIS, E.R. GILLILAND, T.K. SHERWOOD and E.W. SALZMAN. J. Appl. Physiol. 20, 954, 1965.

61. J.G. OLDROYD. Rheology. (Eirich, editor), Vol. I, Ch. 16, Academic Press, New York, (1956).

62. R.H. HAYNES. Trans. Soc. Rheol. 5, 85, 1961.

63. N. CASSON. In Rheology of Disperse Systems. (C.C. Mill, editor), Pergamon, London, 1959

64. G.R. COKELET, E.W. MERRILL, E.R. GILLILAND, H. SHIN, A. BRITTEN and R.E. WELLS JR. Trans. Soc. Rheol. 7, 303, 1963.

65. E.W. MERRILL and G. PELLETIER. J. Appl. Phys. 23, 178, 1967.

66. S. CHARM and G. KURLAND. Nature. 206. 617, 1965.

## APPENDIX I

### A.1 A POSSIBLE PRACTICAL APPLICATION

Knowing the four parameters of the model, viz: $\phi$, $\tau_y$, $\tau_{yap}$, and A, it is possible to obtain volume flow through a capillary of given radius for any given pressure drop across the capillary.

The procedure would be to obtain the basic shear diagram using equation (31), i.e.,

$$\gamma = \frac{1}{\mu}\left[(\tau - \tau_y) - (\tau_{yap} - \tau_y)\left[1 - \exp\left\{-A(\tau - \tau_y)\right\}\right]\right] \quad (31)$$

The basic shear diagram may also be represented by equation (20), i.e.,

$$\left(-\frac{dV_z}{dr}\right)_w = \frac{3}{4}\left(\frac{4Q}{\pi r_o^3}\right) + \frac{\tau_w}{4}\frac{d(4Q/\pi r_o^3)}{d\tau_w} \quad (20)$$

Any infinitely small section of the curve may be represented by a straight line of the form:

$$y = mx + c$$

Now, for any pressure drop, $\tau_w$ may be calculated from the relation:

$$\tau_w = -\frac{r_o}{2}\frac{dp}{dz} \quad (9)$$

and the slope of the curve corresponding to that point value of $\tau_w$ may be obtained readily.

That slope m may be given by:

$$m = \frac{1}{4} \frac{d(4Q/\pi r_o^3)}{d\tau_w} \tag{33}$$

i.e. $$Q = \int_o^Q dQ = \pi r_o^3 \int_o^\tau m \, d\tau_w \tag{34}$$

Equation (34) may be integrated numerically to obtain the volume flow rate Q.

## APPENDIX II

### A.2 COMPUTER PROGRAMS

#### A.2.1 Program No. 1

This Program is designed to evaluate

(i) the shear stress at the wall using the relation:

$$\tau_w = - \frac{r_o}{2} \frac{dp}{dz} \qquad (9)$$

where $r_o$ = the radius of the tube

$dp/dz$ = the pressure drop,

(ii) the pseudo-shear rate $\frac{4Q}{\pi r_o^3}$

where Q = the volume flow rate

$r_o$ = the radius of the tube.

These two relations may be evaluated for

(i) a maximum of 10 different radii,

(ii) a maximum of 10 different hematocrits at <u>each</u> of the above radii,

(iii) a maximum of 20 shear stresses and pseudo-shear rates for each of the above hematocrits at each particular radius.

The program reads in a number of parameters and prints out the same parameters in the order that has been read in. This provides a useful check against incorrect data

being fed into the computer.

After the necessary computations, the pseudo-shear rates and shear stresses are printed out for each hematocrit at each particulat radius. The output is self explanatory.

Notation Used in the Program

R = radius in cms.

H = hematocrit in per cent.

L = no. of different radii.

M = no. of different hematocrits.

N = no. of different pressure drop and volume flow points.

AUTHOR = name of author whose data is being used.

P = pressure drop in cms. of water/cm. of tube.

Q = volume flow rate in cc./sec.

TWALL = shear stress at the wall in dynes/sq.cm.

EETA = pseudo-shear rate in $sec^{-1}$

```
C     PROGRAM NUMBER 1
C     4Q/PR3 VS. TW RELATIONSHIP
C     DATA FROM PRESSURE VS VOLUME FLOW CURVES
C     R=RADIUS IN CMS.
C     H=HEMATOCRIT IN PER CENT
C     L = NO. OF DIFFERENT RADII
C     M = NO. OF DIFFERENT HEMATOCRITS
C     N = NO. OF DIFFERENT PRESSURE AND VOL. FLOW POINTS
C   AUTHOR = NAME OF AUTHOR WHOSE DATAIS BEING USED
C     P=PRESSURE DROP IN CMS WATER/CM. OF TUBE.
C     Q = VOL. FLOW RATE IN CC./SEC.
      DIMENSION R(10),H(10,10), P(10,10,20),Q(10,10,20),PP(10,10,20),TWA
     1LL(10,10,20),EETA(10,10,20)
      READ(5,9) L,M,N,AUTHOR
C     READ THE DIFFERENT RADII
      READ(5,19)(R(I),I=1,L)
C     READ THE DIFFERENT HEMATOCRITS AT EACH RADII
      READ(5,29) ((H(I,J),J=1,M),I=1,L)
C  READ THE PRESSURE AND VOL.FLOW RATE AT DIFFERENT HEMATOCRITS FOR EACH RAD
      READ(5,39) (((P(I,J,K),K=1,N),J=1,M),I=1,L)
      READ(5,49) (((Q(I,J,K),K=1,N),J=1,M),I=1,L)
      WRITE(6,59) L,M,N
      WRITE(6,69)
      WRITE(6,309) (R(I),I=1,L)
      WRITE(6,79)
      WRITE(6,319) ((H(I,J),J=1,M),I=1,L)
      WRITE(6,89)
      WRITE(6,329) (((P(I,J,K),K=1,N),J=1,M),I=1,L)
      WRITE(6,99)
      WRITE(6,339) (((Q(I,J,K),K=1,N),J=1,M),I=1,L)
      WRITE(6,209) AUTHOR
      DO 200 I=1,L
      WRITE(6,109) R(I)
      DO 200 J=1,M
      WRITE(6,119) H(I,J)
      WRITE(6,129)
      DO 300 K=1,N
      PP(I,J,K)=P(I,J,K)*980.0
      TWALL(I,J,K)=R(I)*PP(I,J,K)/2.0
      EETA(I,J,K)=(4*Q(I,J,K))/(3.142*R(I)**3.0)
      WRITE(6,139) TWALL(I,J,K),EETA(I,J,K)
300   CONTINUE
200   CONTINUE
```

```
 9    FORMAT(3I10,A9)
19    FORMAT(5E10.0)
29    FORMAT(4F10.0)
39    FORMAT(5F10.0)
49    FORMAT(5E10.0)
59    FORMAT(2X,24HNO.OF DIFFERENT RADII,L=,I2,//,2X,30HNO.OF DIFFERENT
     1HEMATOCRITS,M=,I2,//,2X,47HNO.OF DIFFERENT PRESSURE AND VOL.FLOW P
     2OINTS,N=,I2)
69    FORMAT(//,2X,5HRADII)
79    FORMAT(//,2X,11HHEMATOCRITS)
89    FORMAT(//,2X,9HPRESSURES)
99    FORMAT(//,2X,8HVOL.FLOW)
109   FORMAT(//,2X,7HRADIUS=,E12.4,2X,3HCMS)
119   FORMAT(///,2X,11HHEMATOCRII=,F7.2,2X,7HPERCENT)
129   FORMAT(//,2X,14HTW DYNES/SQ.CM, 10X,16H(4Q/PR3) PER SEC,/)
139   FORMAT(2X,F12.4,15X,F12.4)
209   FORMAT(////,2X,7HDATA OF,2X,A9,//)
309   FORMAT(10(2X,E12.4))
319   FORMAT(10(2X,F7.2))
329   FORMAT(10(2X,F7.2))
339   FORMAT(5(2X,E12.4))
      END
```

A.2.2 Program No. 2

This Program evaluates the shear rate at the wall and prints out the shear rate-shear stress relationship, assuming no slip at the wall.

The shear rate at the wall is evaluated from the equation:

$$\left(-\frac{dV_z}{dr}\right)_w = \frac{3}{4}\frac{4Q}{\pi r_o^3} + \frac{\tau_w}{4}\frac{d(4Q/\pi r_o^3)}{d\tau_w} \qquad (20)$$

with the usual notation.

This program is capable of evaluating the shear rate for a maximum of 10 radii, 10 hematocrits and 20 values of shear stress (similar to Program No. 1). It also has an additional feature in that it incorporates a subroutine called LESQ. This is a least-squares subroutine which evaluates the co-efficients of a number of polynomials up to a maximum order 6. It may be used to fit a polynomial to the shear stress-shear rate relationship if desired. The control number LS may be used to include the subroutine into the Main Program if a least squares fit is desired, or to exclude it, if not.

Notation Used in the Program

R = radius in cms.

H = hematocrit in per cent

L = no. of different radii

M = no. of different hematocrits

N = no. of different T and E points

T = shear stress at the wall

E = $4Q/\pi R^3$ with the usual notation

AUTHOR = name of author whose data is being used

LS = control number for least squares fit. If fit desired, put LS = 2; if not, leave blank.

VV = vertical segment of slope of $4Q/\pi R^3$ vs. $\tau_w$ plot at each point

HH = horizontal segment of slope of $4Q/\ R^3$ vs. $_w$ plot at each point

S = slope at each point = VV/HH

SHRATE = $(-dV_z/dr)_w$ = shear rate at the wall

N = no. of points to be fitted to the polynomial

MPOLY = highest degree of polynomial desired ($\leq 6$)

```
C     PROGRAM NUMBER 2
C     STRESS-SHEAR RATE RELATIONSHIP WITH NO SLIP AT THE WALL
C     DATA FROM 4Q/PR3 VS.TW CURVES USING PROGRAM NO. 1
C     R=RADIUS IN CMS.
C     H=HEMATOCRIT IN PER CENT
C     T=SHEAR STRESS AT THE WALL
C     E=4Q/PR3
C     VV=VERTICAL SEGMENT OF SLOPE OF 4Q/PR3 VS.TW AT EACH POINT
C     HH=HORIZONT SEGMENT OF SLOPE OF 4Q/PR3 VS.TW AT EACH POINT
C     L = NO. OF DIFFERENT RADII
C     M = NO. OF DIFFERENT HEMATOCRITS
C     N = NO. OF DIFFERENT T AND E POINTS
C   AUTHOR = NAME OF AUTHOR WHOSE DATAIS BEING USED
C     LS=CONTROL NO.FOR LEAST SQUARES FIT.IF FIT DESIRED PUT LS=2,IF NOT
C     LEAVE BLANK
      DIMENSION R(10),H(10,10), T(10,10,20),E(10,10,20),VV(10,10,20),HH(
     110,10,20),S(10,10,20),SHRATE(10,10,20),X(20),Y(20),A(40),B(10),ERR
     10R(20),TW(20)
      READ(5,9) L,M,N,LS,AUTHOR
C     READ THE DIFFERENT RADII
      READ(5,19)(R(I),I=1,L)
C     READ THE DIFFERENT HEMATOCRITS AT EACH RADII
      READ(5,29) ((H(I,J),J=1,M),I=1,L)
      READ(5,39) (((T(I,J,K),K=1,N),J=1,M),I=1,L)
      READ(5,49) (((E(I,J,K),K=1,N),J=1,M),I=1,L)
      READ(5,129) (((VV(I,J,K),K=1,N),J=1,M),I=1,L)
      READ(5,129) (((HH(I,J,K),K=1,N),J=1,M),I=1,L)
      WRITE(6,59) L,M,N
      WRITE(6,69)
      WRITE(6,309) (R(I),I=1,L)
      WRITE(6,79)
      WRITE(6,319) ((H(I,J),J=1,M),I=1,L)
      WRITE(6,89)
      WRITE(6,329) (((T(I,J,K),K=1,N),J=1,M),I=1,L)
      WRITE(6,99)
      WRITE(6,339) (((E(I,J,K),K=1,N),J=1,M),I=1,L)
      WRITE(6,139)
      WRITE(6,149) (((VV(I,J,K),K=1,N),J=1,M),I=1,L)
      WRITE(6,159)
      WRITE(6,149) (((HH(I,J,K),K=1,N),J=1,M),I=1,L)
      WRITE(6,209) AUTHOR
```

```
      DO 100 I=1,L
      WRITE(6,109) R(I)
      DO 100 J=1,M
      WRITE(6,119) H(I,J)
      WRITE(6,169)
      DO 100 K=1,N
      S(I,J,K)=VV(I,J,K)/HH(I,J,K)
      SHRATE(I,J,K)=0.75*E(I,J,K)+0.25*T(I,J,K)*S(I,J,K)
      WRITE(6,179)T(I,J,K),SHRATE(I,J,K)
  100 CONTINUE
      IF(LS.LE.1) GO TO 11
C     TO FIND A LEAST SQUARES FIT OF TW AND SHEAR RATE
      II=I
      JJ=J
      KK=K
      LL=L
      MM=M
      NN=N
C     N=NO.OF POINTS TO BE FITTED
C     MPOLY=HIGHEST DEGREE OF POLYNOMIAL DESIRED - LESSEQ TO 6
      READ(5,409) N,MPOLY
      WRITE(6,419)
      DO 300 M=1,MPOLY
      WRITE(6,429) M
      DO 300 II=1,LL
      WRITE(6,109) R(II)
      DO 300 JJ=1,MM
      WRITE(6,119) H(II,JJ)
      DO 400 KK=1,NN
      I=KK
      X(I)=T(II,JJ,KK)
      Y(I)=SHRATE(II,JJ,KK)
  400 CONTINUE
      CALL LESQ(A,B,X,Y,M,N)
      M1=M+1
      WRITE(6,439)
      WRITE(6,449) (B(L),L=1,M1)
      WRITE(6,459)
      DO 300 I= 1,NN
      SUMB=0
      DO 500 J=1,M1
      L=M1+1-J
      SUMA=SUMB*X(I)
      SUMC=SUMA
      SUMB=SUMC+B(L)
```

```
500  CONTINUE
     TW(I)=SUMB
     ERROR(I)=(TW(I)-Y(I))*100.0/Y(I)
     WRITE(6,469) X(I),Y(I),TW(I),ERROR(I)
300  CONTINUE
9    FORMAT(4I10,A9)
19   FORMAT(5E10.0)
29   FORMAT(4F10.0)
39   FORMAT(5F10.0)
49   FORMAT(5F10.0)
59   FORMAT(2X,24HNO.OF DIFFERENT RADII,L=,I2,//,2X,30HNO.OF DIFFERENT
    1HEMATOCRITS,M=,I2,//,2X,33HNO.OF DIFFERENT T AND E POINTS,N=,I2)
69   FORMAT(//,2X,5HRADII)
79   FORMAT(//,2X,11HHEMATOCRITS)
89   FORMAT(//,2X,1HT,/)
99   FORMAT(//,2X,1HE,/)
109  FORMAT(//,2X,7HRADIUS=,E12.4,2X,3HCMS)
119  FORMAT(///,2X,11HHEMATOCRIT=,F7.2,2X,7HPERCENT)
129  FORMAT(5F10.0)
139  FORMAT(//,2X,20HVERTICAL SEGMENTS,VV)
149  FORMAT(5(2X,F7.3))
159  FORMAT(//,2X,22HHORIZONTAL SEGMENTS,HH)
169  FORMAT(//,2X,14HTW DYNES/SQ.CM,10X,26HSHEAR RATE AT WALL PER SEC,/
    1)
179  FORMAT(2X,F12.4,15X,F12.4)
189  FORMAT(5(F10.6,5X))
209  FORMAT(////,2X,7HDATA OF,2X,A9,//)
309  FORMAT(10(2X,E12.4))
319  FORMAT(10(2X,F7.2))
329  FORMAT(5(2X,F7.4))
339  FORMAT(5(2X,F9.4))
409  FORMAT(2I10)
419  FORMAT(////,2X,17HLEAST SQUARES FIT,/)
429  FORMAT(//,2X,21HDEGREE OF POLYNOMIAL=,I3)
439  FORMAT(//,2X,4HA(0),11X,4HA(1),11X,4HA(2),11X,4HA(3),11X,4HA(4),11
    1X,4HA(5),11X,4HA(6))
449  FORMAT(7(F7.4,8X))
459  FORMAT(//,2X,14HTW DYNES/SQ.CM,13X,26HSHEAR RATE AT WALL PER SEC,1
    18X,33HSHEAR RATE AT WALL (LESQ) PER SEC,17X,13HERROR PERCENT)
469  FORMAT(2X,2(F12.4,25X),E12.4,20X,F12.4)
11   STOP
     END
```

A.2.3 Program No. 3

This program evaluates the parameter A at a series of points ( 5) using the equation shown below:

$$A = \frac{-\left[\ln\left\{1 + \frac{\mu\dot{\gamma}}{(\tau_{yap} - \tau_y)} - \frac{(\tau - \tau_y)}{(\tau_{yap} - \tau_y)}\right\}\right]}{\tau - \tau_y} \qquad (32)$$

It then incorporates each value of A and its average value into the equation shown below to evaluate the values of $\dot{\gamma}_w$, and then compares each value of $\dot{\gamma}_w$ with that obtained using the Weissenberg, Rabinowitch and Mooney equation (20) (See Program 2), as fed into the computer.

$$\dot{\gamma} = \frac{1}{\mu}\left[(\tau - \tau_y) - (\tau_{yap} - \tau_y)\left[1 - \exp\left\{-A(\tau - \tau_y)\right\}\right]\right] \qquad (31)$$

As with the previous two programs, this one is also capable of computing the necessary values of A and $\tau_w$ for a maximum of 10 radii, 10 hematocrits (for each radius), and 20 values of shear stresses and shear rates as obtained by using Programs 1 and 2.

Notation Used in the Program

R = radius in cms.

H = hematocrit in per cent

L = no. of different radii

M = no. of different hematocrits

N = no. of different $\tilde{\tau}_w$ and $(-dV_z/dr)$ points

T = shear stress at the wall

SHRATE = $(-dV_z/dr)_w$ = shear rate at the wall as obtained from Program No. 2 (i.e., equation (20)

NN = no. of $\tilde{\tau}_w$ and $(-dV_z/dr)_w$ points along the non-linear segment of the basic shear diagram

FI = slope of the straight line section of the basic shear diagram

TY = yield stress in dynes/sq.cm. as obtained from the basic shear diagram

TYAP = apparant yield stress in dynes/sq.cm. as obtained from the basic shear diagram

GAMMA = shear rate as determined from the model

DIFF = difference between SHRATE and GAMMA

ERROR = error per cent between SHRATE and GAMMA

```
C     PROGRAM NUMBER 3
C     TO VERIFY THE VALIDITY OF A MODEL FOR BLOOD.
C     R=RADIUS IN CMS.
C     H=HEMATOCRIT IN PER CENT
C     T=SHEAR STRESS AT THE WALL
C     L = NO. OF DIFFERENT RADII
C     M = NO. OF DIFFERENT HEMATOCRITS
C     N = NO. OF DIFFERENT T AND SHRATE POINTS
C     NN=NO.OF T AND SHRATE POINTS ALONG THE CURVE
C   AUTHOR = NAME OF AUTHOR WHOSE DATAIS BEING USED
C     FI=SLOPE OF GAMMA-DOT VS.TW STRAIGHT LINE SECTION
C     TY=YIELD STRESS DYNES/SQ.CM.
C     TYAP=APPARANT YIELD STRESS
      DIMENSION R(10),H(10,10),T(10,10,20),SHRATE(10,10,20),FI(10,10),TY
     1AP(10,10),A(10,10,20),GAMMA(10,10,20),ERROR(10,10,20),TY(10,10),AA
     2VG(10,10),DIFF(10,10,20),ERRAVG(10,10)
      READ(5,9) L,M,N,NN,AUTHOR
C     READ THE DIFFERENT RADII
      READ(5,19)(R(I),I=1,L)
C     READ THE DIFFERENT HEMATOCRITS AT EACH RADII
      READ(5,29) ((H(I,J),J=1,M),I=1,L)
      READ(5,49) ((FI(I,J),J=1,M),I=1,L)
      READ(5,49) ((TY(I,J),J=1,M),I=1,L)
      READ(5,49) ((TYAP(I,J),J=1,M),I=1,L)
      READ(5,39) (((T(I,J,K),K=1,N),J=1,M),I=1,L)
      READ(5,39) (((SHRATE(I,J,K),K=1,N),J=1,M),I=1,L)
      WRITE(6,59) L,M,N
      WRITE(6,69)
      WRITE(6,79)  (R(I),I=1,L)
      WRITE(6,89)
      WRITE(6,99)  ((H(I,J),J=1,M),I=1,L)
      WRITE(6,149)
      WRITE(6,159)((FI(I,J),J=1,M),I=1,L)
      WRITE(6,169)
      WRITE(6,159)((TY(I,J),J=1,M),I=1,L)
      WRITE(6,179)
      WRITE(6,159)((TYAP(I,J),J=1,M),I=1,L)
      WRITE(6,319)
      WRITE(6,329) (((T(I,J,K),K=1,N),J=1,M),I=1,L)
      WRITE(6,129)
      WRITE(6,139) (((SHRATE(I,J,K),K=1,N),J=1,M),I=1,L)
      DO 100 I=1,L
      WRITE(6,109) R(I)
      DO 100 J=1,M
      WRITE(6,119) H(I,J)
      WRITE(6,189)
```

```
      DO 200 K=1,NN
      B=SHRATE(I,J,K)/(FI(I,J)*(TYAP(I,J)-TY(I,J)))
      C=(T(I,J,K)-TY(I,J))/(TYAP(I,J)-TY(I,J))
      D=1.0+B-C
      E=T(I,J,K)-TY(I,J)
      IF(D.LE.0.0) GO TO 1
      A(I,J,K)=-(ALOG(D))/E
1     WRITE(6,199) T(I,J,K),A(I,J,K)
200   CONTINUE
      SUMA=0.0
      DO 300 K=1,NN
      SUMB=SUMA+A(I,J,K)
      SUMA=SUMB
300   CONTINUE
      WRITE(6,239) SUMA
      AAVG(I,J)=SUMA/NN
      WRITE(6,249) AAVG(I,J)
100   CONTINUE
      NJRD=NN
3     DO 500 I=1,L
      WRITE(6,109)  R(I)
      DO 500 J=1,M
      WRITE(6,119) H(I,J)
      IF(KK.EQ.0.0) GO TO 4
      DO 500 KK=1,NJRD
4     WRITE(6,209)A(I,J,KK)
      WRITE(6,219)
      DO 700 K=1,N
      O=T(I,J,K)-TY(I,J)
      P=A(I,J,KK)*O
      Q=EXP(-P)
      S=1.0-Q
      U=(TYAP(I,J)-TY(I,J))*S
      V=T(I,J,K)-TY(I,J)
      W=V-U
      GAMMA(I,J,K)=FI(I,J)*W
      DIFF(I,J,K)=GAMMA(I,J,K)-SHRATE(I,J,K)
      ERROR(I,J,K)=((GAMMA(I,J,K)-SHRATE(I,J,K))*100.0)/SHRATE(I,J,K)
      WRITE(6,229) T(I,J,K),SHRATE(I,J,K),GAMMA(I,J,K),DIFF(I,J,K),ERROR
     1(I,J,K)
700   CONTINUE
      SUMC=0.0
      DO 800 K=1,N
      SUMD=SUMC+ERROR(I,J,K)
      SUMC=SUMD
800   CONTINUE
      WRITE(6,339) SUMC
      ERRAVG(I,J)=SUMC/N
```

```
      WRITE(6,349) ERRAVG(I,J)
500   CONTINUE
      IF(NJRD.EQ.1) GO TO 5
      KK=1
      DO 600 I=1,L
      DO 600 J=1,M
      A(I,J,KK)=AAVG(I,J)
600   CONTINUE
      NJRD=1
      GO TO 3
9     FORMAT(4I10,A9)
19    FORMAT(5E10.0)
29    FORMAT(4F10.0)
39    FORMAT(5F10.0)
49    FORMAT(4F10.0)
59    FORMAT(2X,24HNO.OF DIFFERENT RADII,L=,I2,//,2X,30HNO.OF DIFFERENT
     1HEMATOCRITS,M=,I2,//,2X,38HNO.OF DIFFERENT T AND SHRATE POINTS,N=,
     2I2)
69    FORMAT(//,2X,5HRADII)
79    FORMAT(10(2X,E12.4))
89    FORMAT(//,2X,11HHEMATOCRITS)
 99   FORMAT(10(2X,F7.2))
109   FORMAT(//,2X,7HRADIUS=,E12.4,2X,3HCMS)
119   FORMAT(///,2X,11HHEMATOCRIT=,F7.2,2X,7HPERCENT)
129   FORMAT(//,2X,11HSHEAR RATES)
139   FORMAT(10(2X,F9.4))
149   FORMAT(//,2X,2HF1,/)
159   FORMAT (5(2X,F9.4))
169   FORMAT(//,2X,2HTY,/)
179   FORMAT(//,2X,4HTYAP,/)
189   FORMAT(////,2X,15HTW DYNES/SQ.CM.,15X,10HEXPONENT A,//)
199   FORMAT(2X,F12.4,15X,F12.4)
209   FORMAT(////,2X,11HEXPONENT A=F12.4)
219   FORMAT(//,2X,15HTW DYNES/SQ.CM.,10X,18HSHEAR RATE PER SEC,5X,32HSH
     1EAR RATE (THEORETICAL) PER SEC,5X,10HDIFFERENCE,15X,13HERROR PERCE
     2NT,//)
229   FORMAT(2X,4(F12.4,15X),F10.4)
239   FORMAT(//,2X,17HEXPONENT A TOTAL=F12.4)
249   FORMAT(//,2X,25HEXPONENT A AVERAGE VALUE=F12.4)
319   FORMAT(//,2X,1HT,/)
329   FORMAT(10(2X,F7.4))
339   FORMAT(//,98X,12HTOTAL ERROR=,F10.4)
349   FORMAT(//,95X,15HAVERAGE ERROR=,F10.4)
5     STOP
      END
```

## APPENDIX III

### A.3 GLOSSARY OF MEDICAL TERMS

**Agglutination** — A phenomenon consisting of the collection into clumps of the cells distributed in a fluid. It is believed to be caused by specific substances called agglutinins, the molecules of which become attached to the cells.

**Albumin** — A protein found in nearly every animal and in many vegetable tissues, and characterized by being soluble in water and coagulable by heat. It contains carbon, hydrogen, nitrogen oxygen and sulpher, but its exact composition has not been determined, although the formula for crystallized albumin has been given as $C_{720}H_{1134}N_{218}S_5O_{248}$.

**Alveolus** — A general term used in anatomical nomenclature to designate a small sac-like dilation.

**Arteriole** — A very small artery.

**Artery** — A vessel comveying blood from the heart. It is composed of three coats; an outer one consisting of connective tissue and elastic fibres; an inner one lined with endothelium and containing collagenous and elastic fibres; and a middle coat composed of elastic and muscular fibres.

**Endothelium** — The layer of epithelial cells that lines the cavities of the heart and of the blood and lymph vessels and the serous cavities of the body, originating from the mesoderm.

**Epithelium** — A tissue composed of contiguous cells with a minimum of intercellular substance.

**Erythrocyte** — One of the elements found in peripheral blood. Normally in the human, the mature form is a non-nucleated yellowish, circular biconcave disc, adapted, by virtue of its configuration and its hemoglobin content, to transport oxygen.

**Fibrin** — A whitish insoluble protein formed from fibrinogen by the action of thrombin (fibrin ferment), as in the clotting of blood. Fibrin forms the essential portion of the blood clot.

| | |
|---|---|
| Fibrinogen | A plasma protein of high molecular weight that is converted to fibrin through the action of thrombin. |
| Ghost Cell | One which appears only as a shadowy outline. |
| Globulin | A class of proteins characterized by being insoluble in water, but soluble in saline solutions. |
| Granulocyte | Any cell containing granules. |
| Haemoglobin | The oxygen-carrying-pigment of the erythrocytes formed by the developing erythrocyte in bone marrow. |
| Hematocrit | The volume percentage of erythrocytes in whole blood. Originally applied to the apparatus or procedure used in its determination, but later used to designate the result of the determination. |
| Hemolysis | The liberation of haemoglobin. Hemolysis consists of the separation of the haemoglobin from the corpuscles and its appearance in the fluid in which the corpuscles are suspended. It may be caused by hemolysins, by chemicals, by freezing, or heating, or by distilled water. |

| | |
|---|---|
| Heparin | A mucopolysaccharide acid occurring in the various tissues, but most abundantly in the liver. In pharmacy, a mixture of active principles obtained from the livers or lungs of domestic animals; injected intravenously it renders the blood incoagulable, most probably by interfering with the formation of intrinsic thrombo plastin and the action of thrombin. |
| Heparinize | To treat with heparin, in order to increase the clotting time of blood. |
| Leukocyte | Any colourless amoeboid cell mass, applied especially to one of the formed elements of the blood, consisting of a colourless granular mass of protoplasm, having amoeboid movements and varying in size between 0.005 and 0.015 mm. in diameter. |
| Lumen | The cavity or channel within a tube or tubular organ. |
| Lymph | A transparent slightly yellow liquid of alkaline reaction found in the lymphatic vessels. |

| | |
|---|---|
| Mesoderm | The middle layer of the three primary germ layers of the embryo, lying between the ectoderm and the entoderm. |
| Plasma | The fluid portion of blood in which the corpuscles are suspended. |
| Platelet | A circular or oval disk, 2-3 in diameter, found in the blood of all mammals, which is concerned in the coagulation of the blood and in concentration of the clot and hence in thrombosis. They average about 250,000 per cu.mm. of blood. |
| Precapillary | A vessel lacking complete coats, intermediate between an arteriole and a true capillary. |
| Pulmonary | Pertaining to the lungs. |
| Solution. A.C.D. | Abreviation for anticoagulant acid citrate dextrose solution used to prevent coagulation of blood in preparation of plasma or whole blood for indirect transfusions |
| Ringers | A clear colourless liquid with a mild saline taste, containing in each 100 ml., 820-900 mg. of sodium chloride, 25-35 mg. of potassium chloride and 30-36 mg. of calcium chloride prepared with recently boiled purified water. |

| | |
|---|---|
| Saline | A solution of sodium chloride in purified water. |
| Serum | Plasma from which the fibrinogen has been separated in the process of clotting. |
| Sphincter | A ring-like band of muscle fibres that constricts a passage or closes a natural orifice. |
| Thrombocyte | A blood platelet |
| Vena | A vessel that conveys blood to or towards the heart. |
| Venous | Of or pertaining to the veins. |
| Venous Capillary | Minute channels proximate to the venules which carry venous blood. |
| Venule | Any one of the small vessels that collect blood from the capillary plexuses and join to form veins. |